Some studies of the reactions of carbon nucleophiles with aromatic nitro compounds

Gaynor Louise Duffield

SOME STUDIES OF THE REACTIONS OF CARBON NUCLEOPHILES WITH AROMATIC NITRO-COMPOUNDS

by

Gaynor Louise Duffield BSc (Dunelm)

Trevelyan College

A thesis submitted for the degree of Doctor of Philosophy in the Department of Chemistry, University of Durham

1996.

Some studies of the reactions of carbon nucleophiles with aromatic nitro-compounds

Gaynor Louise Duffield

A thesis submitted for the degree of Doctor of Philosophy in the Department of Chemistry, University of Durham, 1996.

Abstract

Some reactions of aromatic nitro-compounds with carbon nucleophiles have been investigated. The techniques used include NMR spectroscopy, UV-visible spectroscopy and stopped-flow spectrophotometry.

The initial rapid reactions of carbanions derived from ring-substituted phenylacetonitriles with 1,3,5-trinitrobenzene yield σ-adducts. Carbanions were generated from the phenylacetonitriles by reaction with sodium methoxide in methanol. Values of the equilibrium constants for the deprotonation reaction were determined spectrophotometrically. Rate constants for the σ-adduct forming reactions were measured in methanol using the stopped-flow method. With increasing carbanion reactivity rate constants for the C-C bond forming reaction increase to a limit of *circa* 10^9 dm^3 mol^{-1} s^{-1}, close to the diffusion limit. Data were also obtained for reaction of the carbanions with 4-nitrobenzofuroxan and with 4-nitrobenzofurazan.

An interesting slower reaction was observed in the reaction of carbanions with 1,3,5-TNB, 4-nitrobenzofuroxan and 4-nitrobenzofurazan. This yields coloured products and the nature of the process has been investigated.

Attempts have been made to isolate the σ-adducts formed from carbanions. The adduct formed from 1,3,5-trinitrobenzene and phenylacetonitrile in the presence of triethylamine has been produced in crystalline form. NMR measurements *in situ* have indicated the formation of adducts from 4-nitrobenzofuroxan and from 4-nitrobenzofurazan with deuterated nitromethane in the presence of triethylamine.

The reactions of the TNB-phenylacetonitrile adduct with oxidising agents have been investigated. The reagents used include chlorine and triphenylmethyl bromide. These studies show that protonation of the σ-adduct to yield a nitronic acid may compete with oxidation. A detailed study was made of the protonation equilibrium using perchloric acid in acetonitrile-water mixtures. Initial protonation was followed by a slower irreversible decomposition reaction where rate constants have been measured.

Declaration

The material in this thesis is the result of research undertaken in the Department of Chemistry, University of Durham between October 1993 and October 1996. It is the original work of the author except where acknowledged by reference and has not been submitted for any other degree.

Statement of Copyright

Acknowledgements

I would like to thank my supervisor Dr M.R.Crampton for his invaluable guidance, friendship and support, throughout my time in Durham.

I would also like to thank my colleagues Simon, Ian, Helen and Andy and Colin for maintenance and repair of spectroscopic and computing equipment.

Finally I would like to thank Zeneca for funding this work and Dr J.H. Atherton at Zeneca for his advice and use of equipment at Zeneca.

To my family and David,
who made it all possible.

Table of Contents

Table of Figures

Chapter 1

Introduction

1. Nucleophilic and electrophilic aromatic substitution

Substitution reactions involving aromatic compounds occur with three types of reagent, namely nucleophiles, electrophiles, and free radicals. Here only electrophilic and nucleophilic substitution will be discussed.

1.1 Electrophilic aromatic substitution

Electrophilic aromatic substitution is the most widely studied of these reactions. Replacement of a ring hydrogen is a common reaction due to the excellent leaving group ability of the proton, H^+.The general equation for electrophilic aromatic substitution is shown in equation 1.1.

$$\mathbf{Ar\text{-}X + Y \text{ or } Y\text{-}Z \rightarrow Ar\text{-}Y + X \text{ or } X\text{-}Z} \qquad \text{equation 1.1}$$

Y may or may not have a formal positive charge as neutral species can also behave as electrophiles.

Due to the excellent leaving group ability of H^+ the widest range of reactions are when X=H and Y≠H. Reactions of this type include nitration, sulfonation, halogenation and Friedel-Crafts reactions. Electrophiles thus include both those with a positive charge, NO_2^+, ArN_2^+, Hg^{2+}, and also neutral covalent species, Cl_2, SO_2, Br_2.Typical reactions are shown in scheme 1.1.

Scheme 1.1

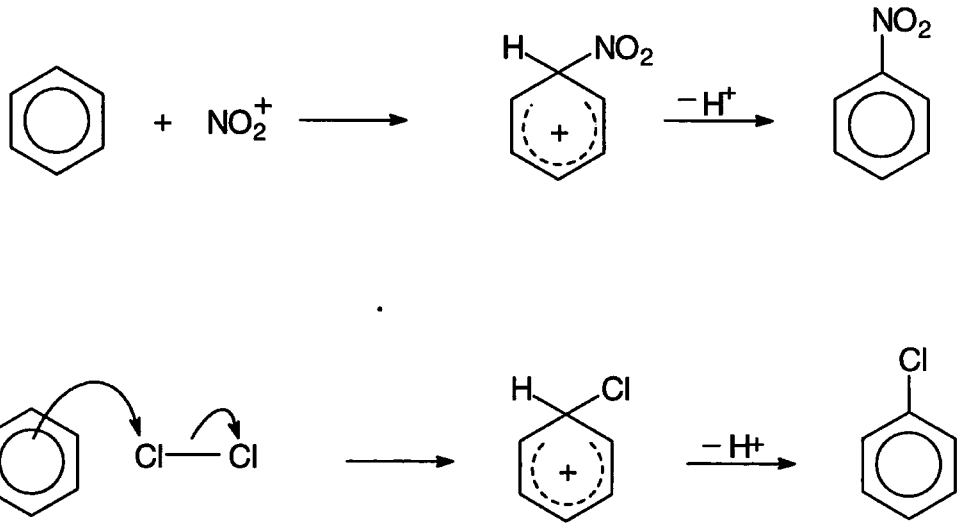

There are also numerous electrophilic aromatic substitution reactions where the group replaced is not hydrogen, and where the electrophile is not H^+.Some of the many possibilities are shown in table 1.1.[1]

Table 1.1

Ar-X	**Y or Y-Z**
ArMgCl	NOCl
ArLi	R_3SiX
ArHgCl	I_2, NOCl, $SO_3(H_2O)$
$ArB(OH)_2$	$HgCl_2/H_2O$, HNO_3, $Hal_2/H2O$
ArR	$R'COCl/AlCl_3$, ArN_2^+, HNO_3, Hal_2
$ArSiR_3$	HNO_3, $Hg(OAc)_2$, RCOCl, Hal_2
$ArSO_3H$	Cl_2/H_2O, HNO_3, ArN_2^+

1.2 Nucleophilic aromatic substitution

The general equation for nucleophilic aromatic substitution is shown in scheme 1.2.

Scheme 1.2

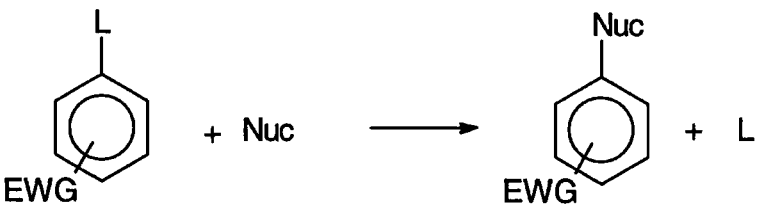

The nucleophile may bear a negative charge or be neutral, L is a good leaving group, and EWG is one or many electron withdrawing groups which are very important to this reaction. The electron withdrawing group , usually one or more nitro groups, activates the ring to attack by the nucleophile and also stabilises the intermediate cyclohexadienyl anion.

The most common pathway for the S_NAr reaction is addition-elimination with addition of the nucleophile at the position bearing the leaving group. Loss of the leaving group from the σ^L-adduct then gives a neutral species, as shown in scheme 1.3.

Scheme 1.3

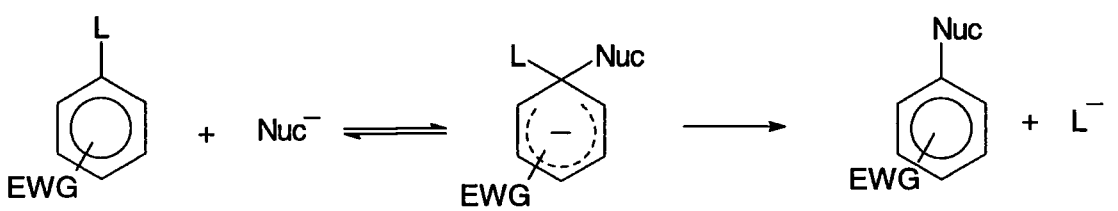

There are many examples of this type of reaction, as there are for substitution of hydrogen in electrophilic aromatic substitution. Scheme 1.4 shows the reaction of 1-chloro-2,4,6-trinitrobenzene (picryl chloride) with hydroxide ion to yield picric acid.[2]

Scheme 1.4

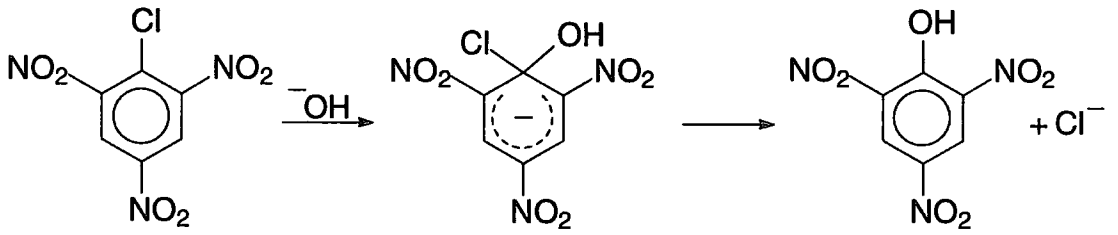

There is also a second possible reaction pathway, which involves addition of the nucleophile to a carbon bearing hydrogen to form a σ^H-adduct. However this σ^H-adduct cannot then convert to the analogous neutral species as in the case of the σ^L-adduct, since displacement of hydrogen is only possible through loss of the H^- anion which is unstable. The high bond energy of the C-H bond also contributes to making this an unlikely subsequent reaction, scheme 1.5.

Scheme 1.5

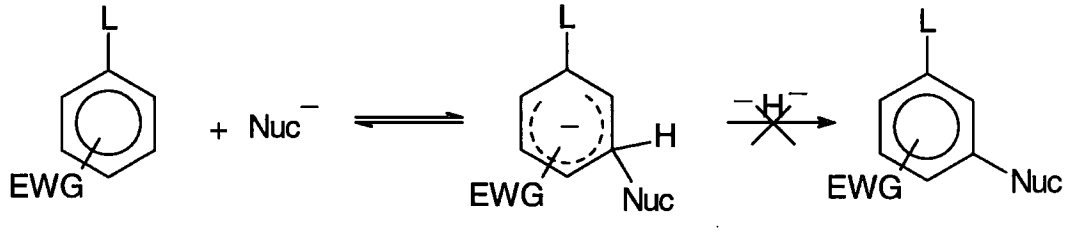

There are a few examples of reactions proceeding via σ^H-adducts but these are not general processes.

Thus replacement of hydrogen via electrophilic aromatic substitution is an easy and very common reaction and many examples are known. However to replace hydrogen via nucleophilic aromatic substitution is not an easy reaction, most nucleophilic aromatic substitutions occur with an anion e.g. Cl^-, Br^- as the leaving group There are however many possibilities of direct or indirect transformation of σ^H-adducts into stable species.

An alternative mechanism for nucleophilic aromatic substitution has now been shown to occur involving a single transition state. It has been shown that in the reaction of 2-(4-nitrophenoxy)-4,6-dimethoxy-1,3,5-triazine with various substituted phenolate ions that

there is no curvature in the Brönsted plot of $logk_{obs}$ versus pK_a of the substituted phenoxides.[3] This provides good evidence that there is no change in the rate determining step, scheme 1.6.

Scheme 1.6

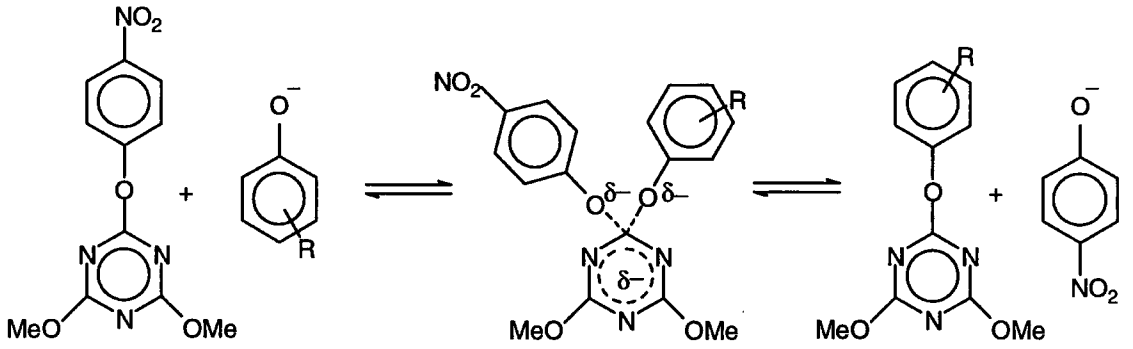

A stepwise process would involve a change in rate determining step where $\delta pK=0$ thus such linearity indicates the existence of a single transition state consistent with a concerted process.

The geometry of the transition state is likely to be similar to that of a Meisenheimer complex but with longer forming and breaking bonds.

1.3 Nucleophilic Aromatic Substitution of Hydrogen

Although replacement of a ring hydrogen is not a general reaction there are now several examples of this type. As shown in scheme 1.7 reaction of a π-deficient arene with a nucleophile may yield an intermediate which is converted to the substituted product.

Scheme 1.7

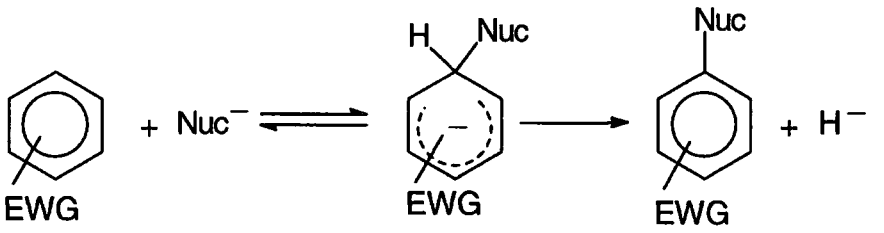

Several of these reactions involve arenes activated by a nitro group and carbon nucleophiles. Nucleophilic substitution of hydrogen reactions of this type are usually considered to proceed via the two-step addition elimination-reaction mechanism and are designated S_NAr^H. However the reactions may be more complicated than in scheme 1.7 and may involve formation of charge-transfer complexes, ion radical salts and other elementary steps.

Depending on how effectively the nitro groups delocalize the negative charge, a very stable σ-adduct may be formed and the reaction will terminate after the addition stage. Further aromatization to the final aromatic product may occur with the aid of added oxidants or an auto-aromatization process.

The cyanide anion plays an important part in the S_NAr^H. For example derivatives of 1,3-DNB react with the cyanide anion in alcoholic solution to give 6-alkoxy-2-nitrobenzonitriles, scheme 1.8.[4] A possible explanation for this is that the initially formed σ-adducts are oxidised by excess dinitrobenzene to give dinitrobenzonitriles which then react with the alkoxide anion, from the alcoholysis of CN^-, via an S_NAr reaction of a

nitro group. The reaction also occurs for 1,3,5-TNB, 1-chloro-2,4-dinitrobenzene, and 1-amino-2,4-DNB, scheme 1.8.

Scheme 1.8

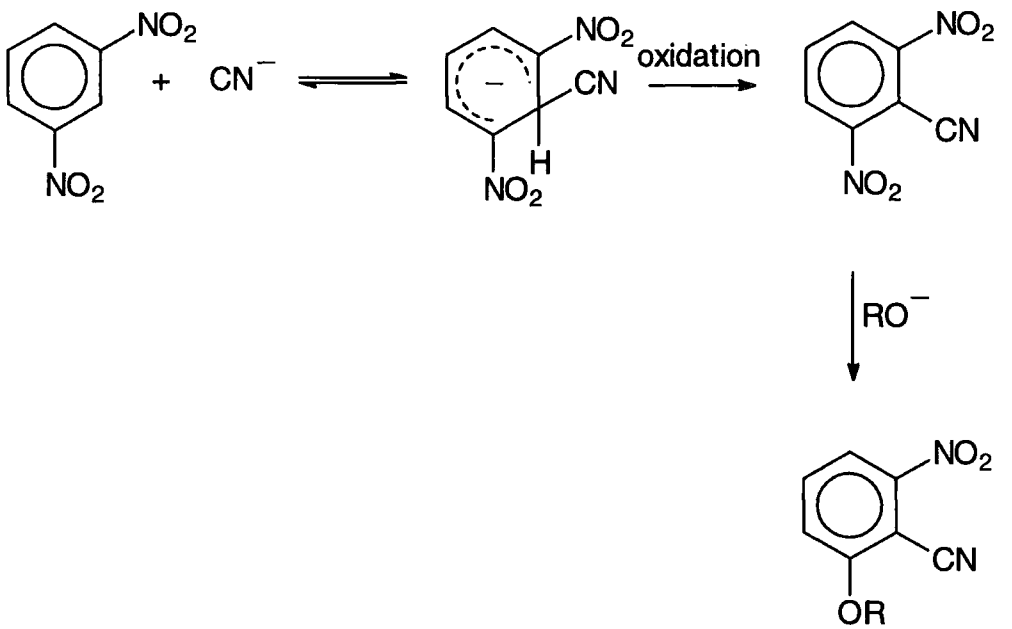

The formation of ortho-cyano phenols has been observed in dipolar aprotic solvents such as DMSO. A detailed study of the reactions of a series of nitroaromatics with an electron withdrawing group at the 2- or 4- positions has been made.[5]

Scheme 1.9

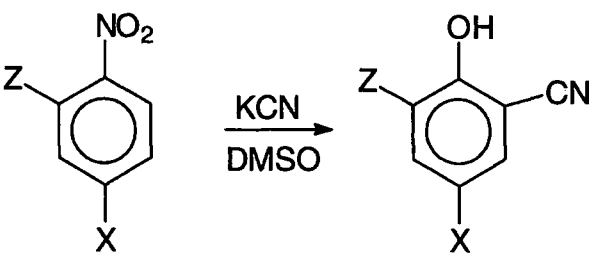

i) Z=H X=CN
ii) Z=CN X=H

The reaction is accompanied by evolution of nitrous acid and a Nef-type process is proposed involving isomerization of the ortho-cyano adduct into a spirocyclohexadienyl oxaziridine oxide followed by loss of a hyponitrite anion.

Scheme 1.10

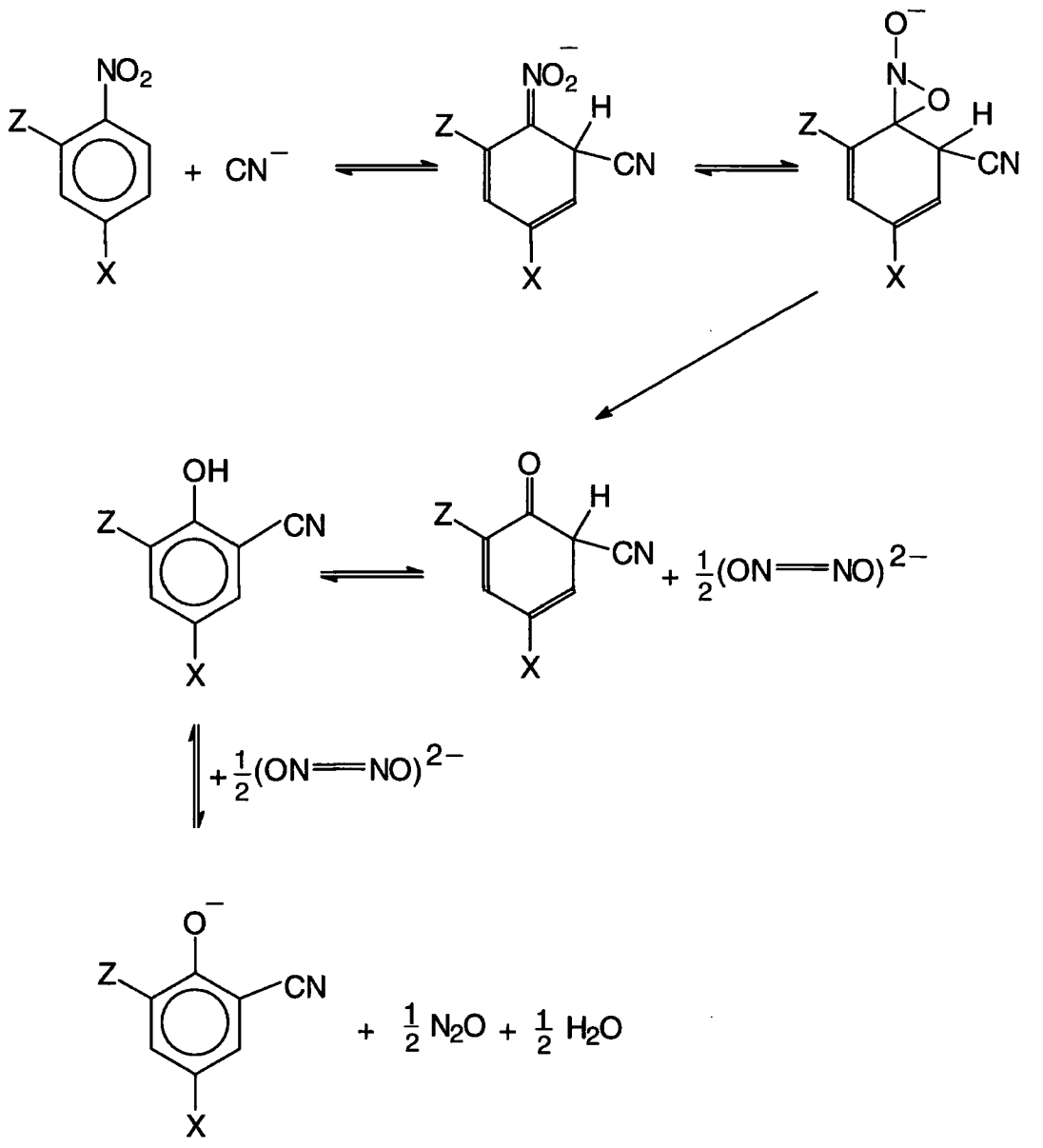

A mechanism involving radicals which was proposed for the reaction of 9-nitroanthracene with cyanide is unlikely here as no EPR signal is observed. The presence of the phenoxide ion product is indicated by isolation of the methyl ether on treatment of the reaction mixture with methyl sulfate in the absence of added base.

Reaction of 4-chloronitrobenzene with activated methylene compounds in the presence of a strong base (potassium t-butoxide in t-butylamine or potassium amide in liquid ammonia) at low temperature results in the formation of 2-substituted 4-

chloronitrobenzenes with no substitution of the chlorine atom.[6] This is a typical example of S_NAr^H reactions of nitroarenes.

4-Chloronitrobenzene will also react with substituted phenylacetonitriles using potassium hydroxide as a base in methanol.[7] It is proposed that after initial formation of the σ^H-adduct spontaneous oxidation occurs to produce a 3-aryl-5-anthranil derivative, scheme 1.11. However the intermediate (**2**) which is considered to exist as the potassium salt is not isolable as it undergoes further reaction.

Scheme 1.11

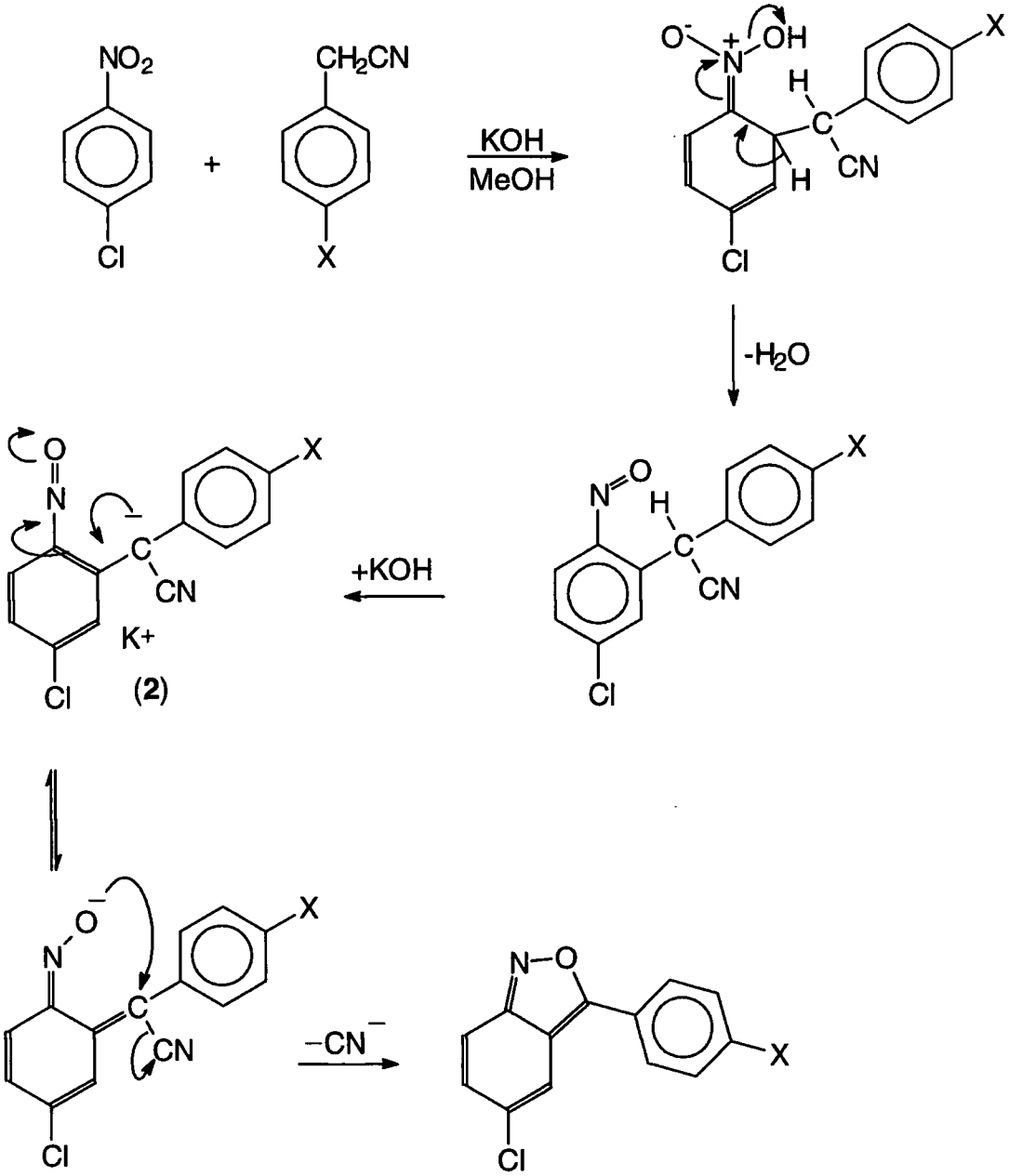

Phenoxide ions may react with nitroaromatics either as oxygen or carbon nucleophiles. As shown in scheme 1.12 the reactions with phenoxide ion of 1,3-dinitrobenzene or 1,3,5-trinitrobenzene in the presence of sodium hydroxide in DMSO may yield biphenyl derivatives. This may be regarded as formal displacement of the hydrogen atom on the aromatic ring by the carbon atom of the phenolate.[8]

Scheme 1.12

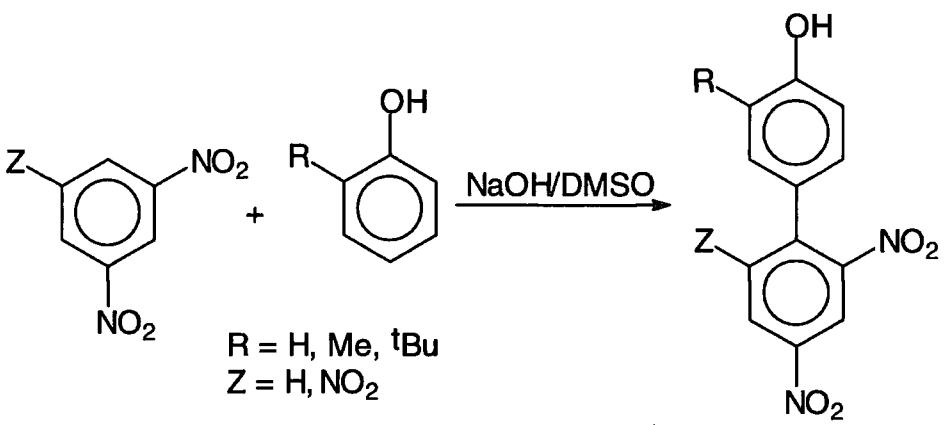

1,4-Dinitrobenzene, 1,2,4- and 1,3,5-trinitrobenzene, which are highly electrophilic nitroarenes, undergo substitution of hydrogen when reacted with poorly nucleophilic phenyl and methyl radicals.[9] Such radicals are produced from the corresponding carboxylic acids, so that heating 1,2,4-TNB with benzoic acid and ammonium persulfate in the presence of silver nitrate produces 2,4,5-trinitrodiphenyl in 40% yield, scheme 1.13.

Scheme 1.13

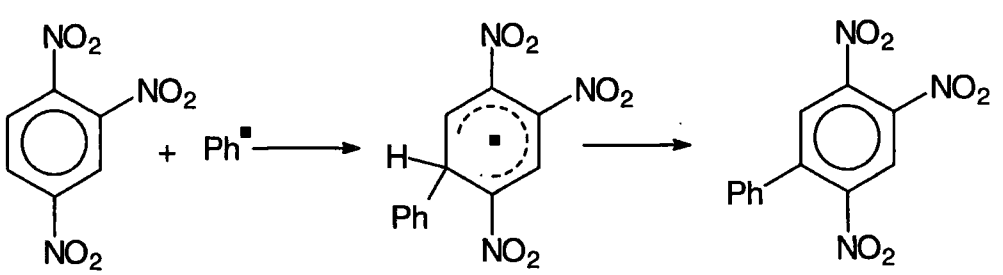

Reaction of 1,2,4-TNB with the more nucleophilic 1-adamantyl radical does not result in hydrogen displacement, instead adamantyl- denitration products are formed.

Another reaction involving radicals is the amination of nitrobenzene with benzamide anion, involving direct formation of an aromatic amide bond, the mechanism shown in scheme 1.14 has been proposed.[10]

Scheme 1.14

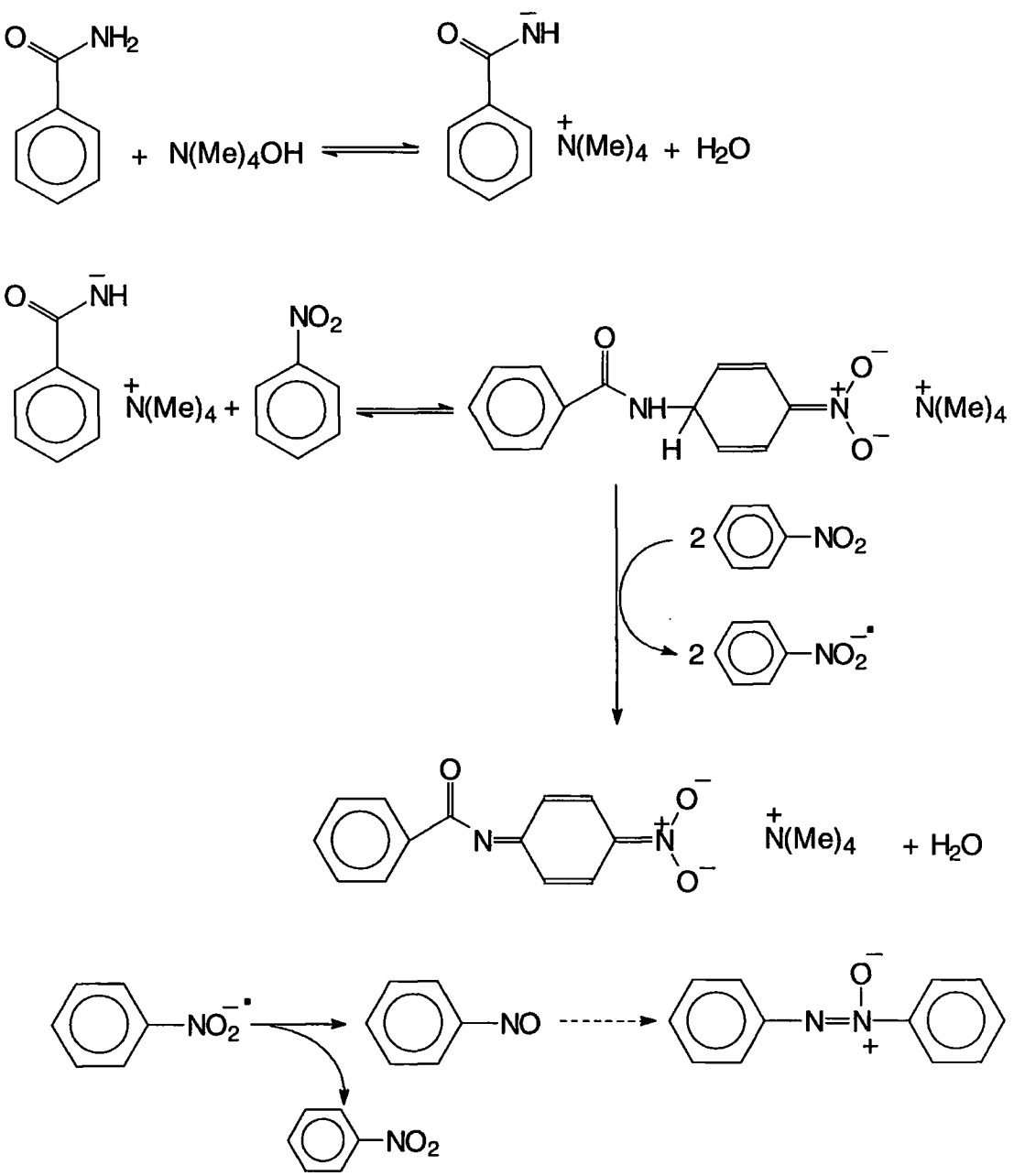

Organometallic compounds react with nitroaromatics to form adducts which may be oxidised *in situ*. Nitrobenzene reacts with such organometallics at the *ortho*- and *para*-positions to give nitronate adducts in a 2:1 ratio. In reactions of *para*-Z-substituted nitrobenzenes addition takes place exclusively at the *ortho*-position, scheme 1.15. Due to effective delocalization of the negative charge and a partial covalent bond formation, these nitronate adducts are fairly stable. They may however be decomposed by the action of mineral acid or by oxidation. Initially bromine and DDQ were used as the oxidants, however better yields have recently been obtained using an alkaline acetone-water solution of $KMnO_4$.[11]

Scheme 1.15

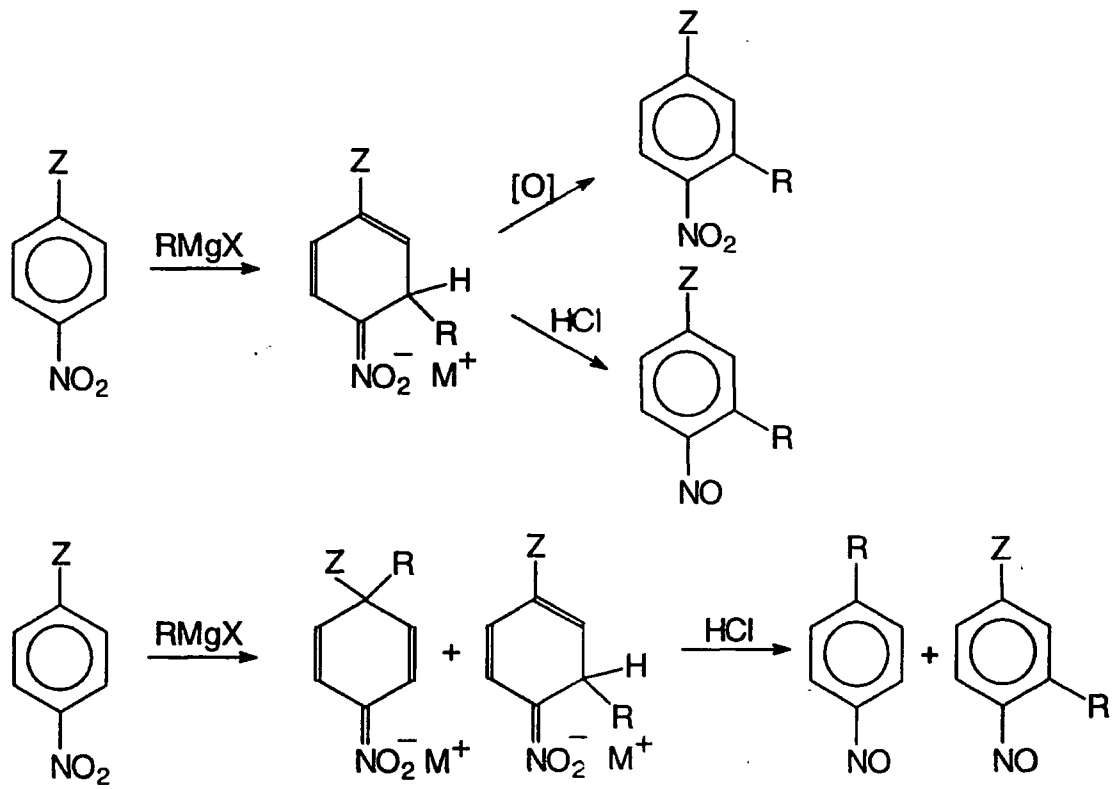

An important feature of this reaction is that nitroaromatics bearing electron withdrawing groups, usually susceptible to attack by organometallics, undergo alkylation intact. Some of the many possibilities are shown in table 1.2.[12, 13]

Table 1.2

Z	RMgX	Yield/%
H	CH_3Li	2-nitrotoluene 32
		4-nitrotoluene 20
C_2H_5	CH_3MgX	52
Cl	CH_3MgX	56
Cl	$C_6H_5CH_2CH_2MgX$	36
I	CH_3MgX	74
OCH_3	CH_3MgX	56
OCH_3	$C_6H_5CH_2CH_2MgX$	62
$COCH_3$	CH_3MgX	51
CO_2CH_3	CH_3MgX	72
CN	CH_3MgX	70

Although these rearomatisation processes use an external agent to achieve the substitution of hydrogen, it is relevant to mention them here.

Addition of a strong acid, such as HCl, to the σ-adduct formed from reaction of the nitroarene with RMgX produces a nitronic acid. This subsequently undergoes acid-catalysed elimination of water to give a nitroso derivative.[11]

Scheme 1.16

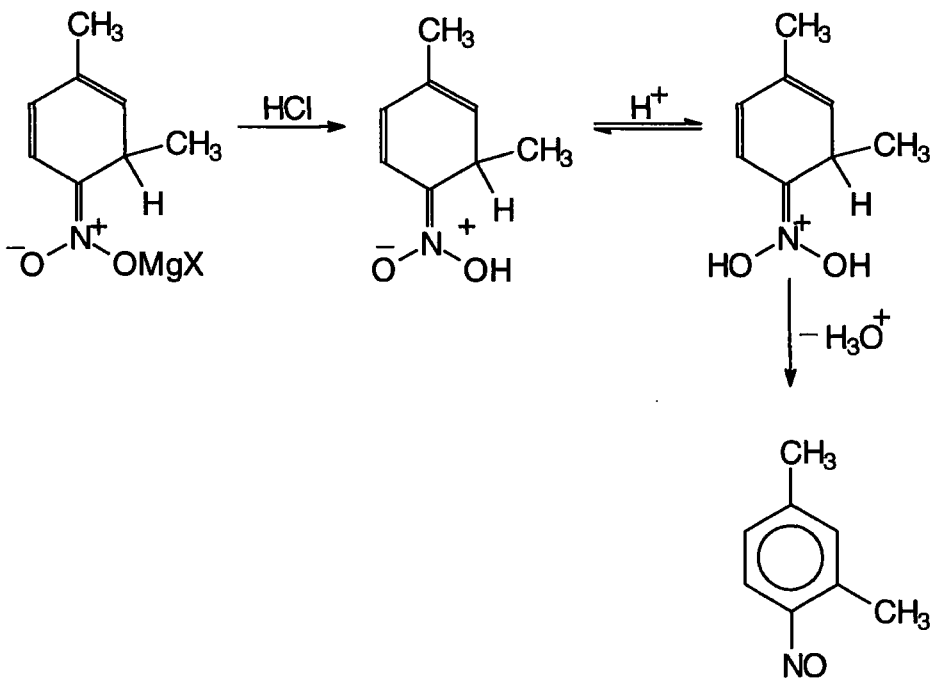

Competition for protonation at a carbon atom rather than at oxygen is the key to the second process which uses the alkaline acetone-water solution. Protonation at a carbon atom results in formation of dihydro compounds, which on refluxing in methanol solution eliminate HNO_2 to form alkyl derivatives, scheme 1.17.[14]

Scheme 1.17

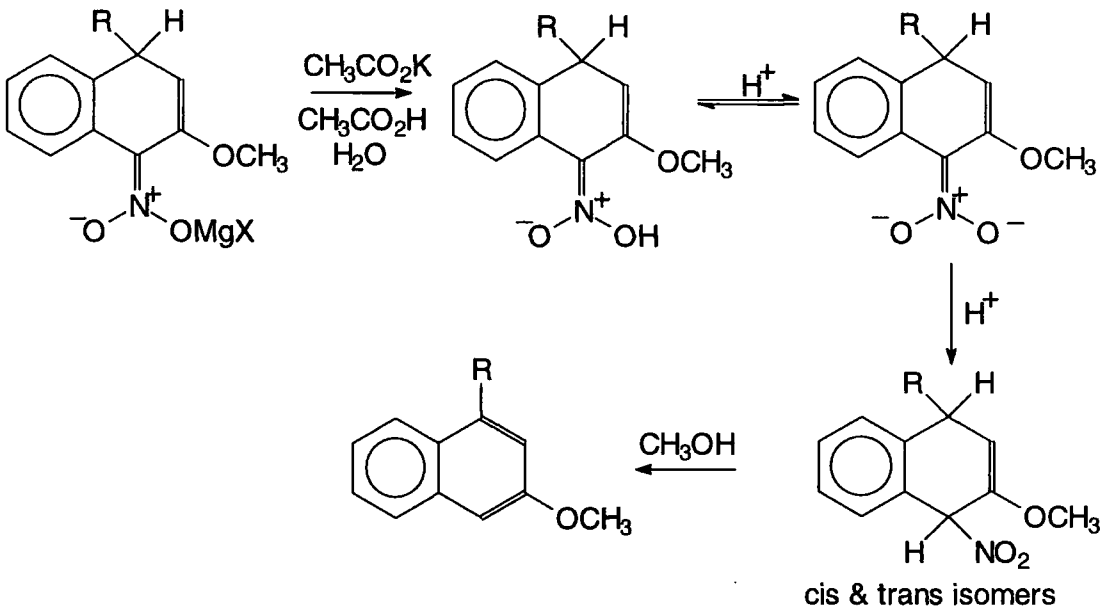

Fluorine assisted addition of silyl enol ethers to aromatic nitro compounds produces adducts which are oxidised, *in situ,* on addition of a stoichiometric amount of oxidant, e.g. bromine in cyclohexane or DDQ in THF, scheme 1.18.[15] The regiochemistry is controlled by the size of the silicon reagent, with less hindered silyl enol ethers both ortho and para substitution occurs, but para substitution is dominant when bulky silyl reagents, trimethylsilyl ketene acetal, are used.

Scheme 1.18

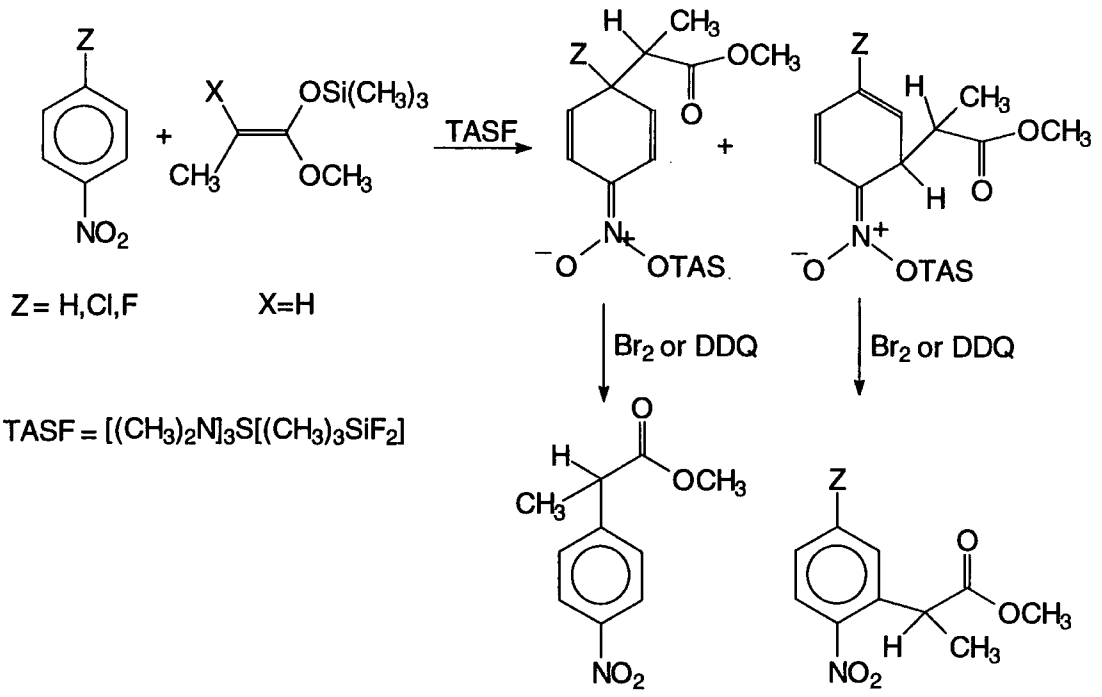

The mechanism of the oxidation step involves bromination of the initial σ-adduct and rearomatisation through loss of HBr.[16]

Scheme 1.19

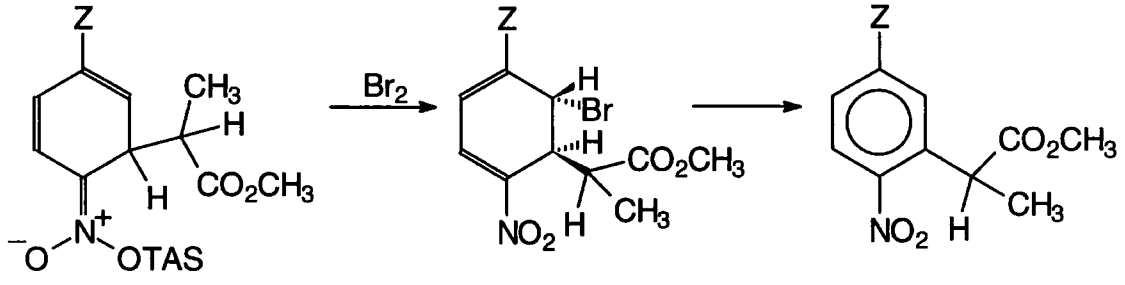

Interestingly, if 4-fluoro- or 4-chloronitrobenzene are used, only the ortho substituted product is formed with no S_NAr displacement of Cl or F to give the para product.[15]

1.4 Vicarious nucleophilic substitution of hydrogen (VS_NAr^H)

In this type of reaction, introduced by Makosza in the late 1970s, the loss of hydrogen from the sp^3 hybridised carbon in the σ-adduct intermediate, is accompanied by loss of a good leaving group from the nucleophile, scheme 1.20.

Scheme 1.20

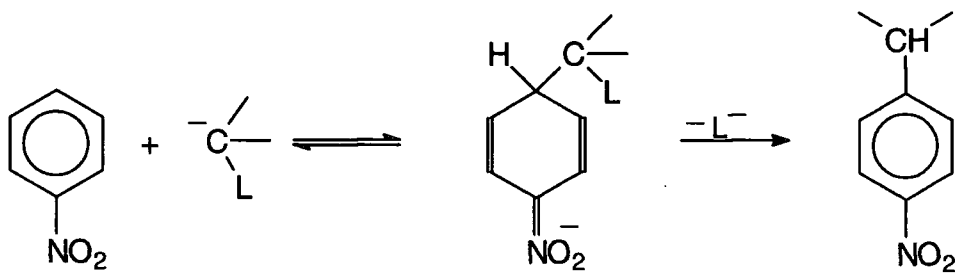

Makosza has shown that the mechanism for loss of the hydrogen from the initially formed σ-adduct involves a base catalysed β-elimination rather than a hydride shift, scheme 1.21.

Scheme 1.21

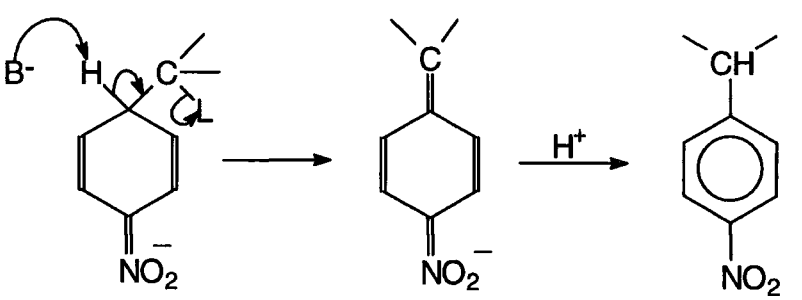

Most VS_NAr^H reactions involve addition of carbanions to nitroarenes and these have been widely studied. It has been shown that in nitroarenes possessing a good leaving group, e.g. Cl, Br, I, which would be susceptible to S_NAr processes, VS_NAr^H may occur preferentially. Thus 4-X-substituted nitrobenzenes undergo VS_NAr^H to produce substitution of the ortho-hydrogen atom. However for L=F, NO_2 both pathways operate and both products are formed, scheme 1.22.[17]

Scheme 1.22

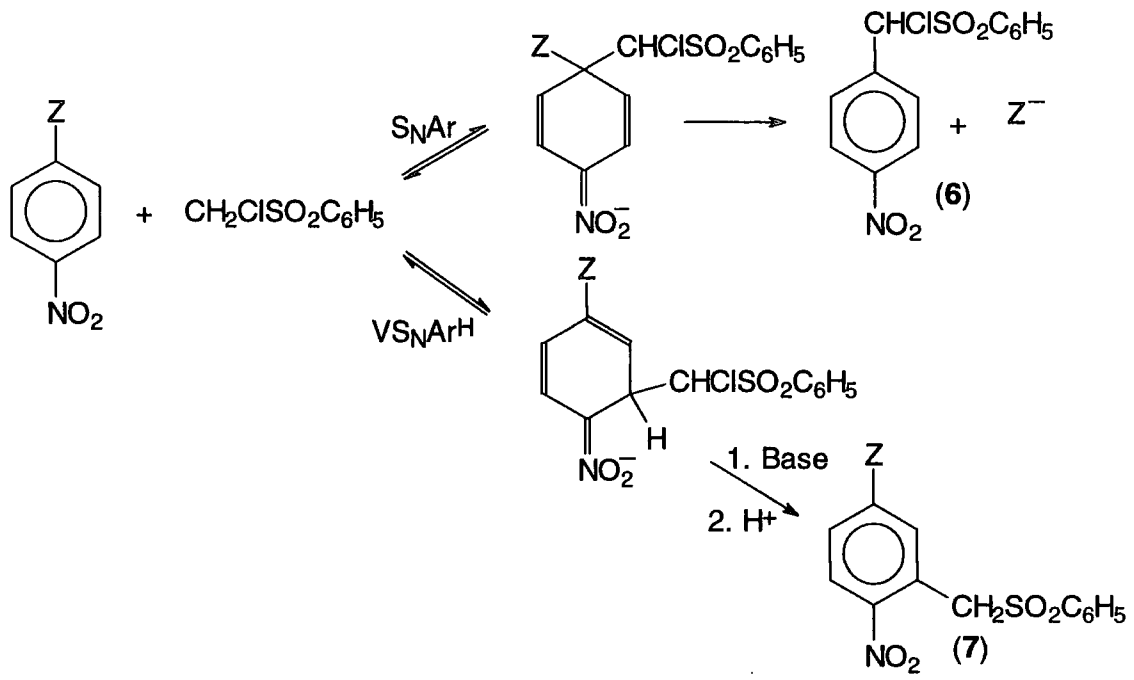

Table 1.3 [18]

Z	Yield (7)/%
Cl	69
Br	61
I	74
F	18*
NO_2	13*
CN	52

* (**6**) is also formed.

A carbanion which has a good leaving group attached may undergo self-condensation with its C-H acid precursor in basic media, thus for VS_NAr^H only carbanions which do not readily undergo this process can be used. The carbanions have the general formula $LYCR^-$, where L is a leaving group and Y is an electron delocalising substituent to stabilise the carbanion.Hence by careful combination of L, Y, and R, a large range of carbanions which undergo VS_NAr^H can be designed. Some of the possibilities are shown in table 1.4.

Table 1.4

L	Cl, Br, CH_3O, C_6H_5O, CH_3S, C_6H_5S, $(CH_3)_2NC(S)S$
Y	$C_6H_5SO_2$, C_6H_5SO, CN C_6H_5S, Cl, $P(O)(OCH_3)_2$
R	H, alkyl, aryl, C_6H_5S, Cl

1.4.1 Copper mediated VS_NAr^H

This novel mechanistic approach was inspired by the cross coupling of iodoarenes with 1,3-DNB and 1,3,5-TNB in quinoline in the presence of copper or copper (I) oxide to produce biphenyls.[18] The process has recently been advanced by a modification using copper t-butoxide and dimethoxyethane as a solvent which has considerably improved the yields.[19]

Reaction of 1,3-DNB with 4-iodophenol has been rationalized as a copper (I) promoted S_N^H process involving formation of a zwitterionic intermediate which then eliminates HI to give the product, scheme 1.23.[19] This is considered a more acceptable mechanism than one involving 2,6-dinitrophenyl copper but the mechanisms still need some clarification.

Scheme 1.23

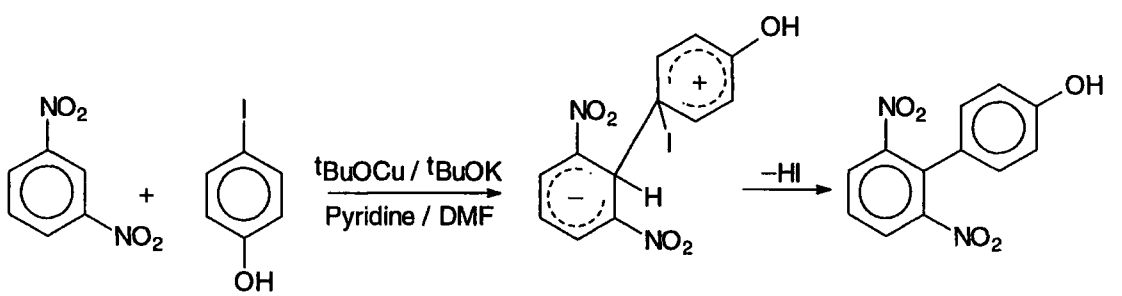

Strong argument that the reaction is copper mediated comes from studies with α-bromo and α-iodo carbanions generated from typical vicarious reagents, which are able to cause copper mediated displacement of hydrogen in 1,3-DNB.[19]

1.5 Formation of σ-complexes

Addition of bases to trinitroaromatic compounds produces intensely coloured species, the formation of which can be reversed by acid. Colour formation may be followed by slow nucleophilic substitution. Early workers in this field including Lobry de Bruyn and van Leent found that in favourable cases highly coloured solids could be isolated. It was proposed that the structure of such compounds was the quinonoid structure, scheme 1.24, and the first evidence that this was the case was provided by Meisenheimer.

Scheme 1.24

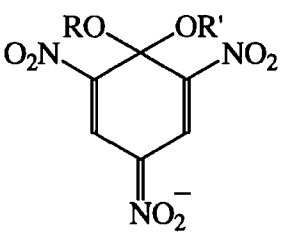

Addition of potassium methoxide to 2,4,6-trinitrophenetole and potassium ethoxide to 2,4,6-trinitroanisole produced identical compounds which on acidification produced a mixture of methyl and ethyl picrates.[20] This also produced strong evidence for the S_NAr mechanism of nucleophilic aromatic substitution. The structure of these adducts has now been confirmed by NMR and crystallographic methods. Thus salts containing cyclohexadienate ions are known as Meisenheimer complexes.

Most reactions of nitroaromatic compounds to form σ-complexes occur with oxygen or nitrogen nucleophiles, however reactions with carbon nucleophiles have also been reported.For the purposes of this thesis there is particular interest in the reaction of carbanionic nucleophiles with nitroaromatics, especially 4-nitrobenzofuroxan (4-NBF), 4-nitrobenzofurazan (4-NBZ), and 1,3,5-trinitrobenzene (1,3,5-TNB).

There are a number of examples of the reaction of 1,3,5-TNB with carbon nucleophiles, particularly carbanions, all carried out with methanol as the solvent and with the stable σ -complexes formed by attack of the nucleophile at an unsubstituted carbon atom.[21,22,23] The reaction of 1,3,5-TNB with the malononitrile anion is shown below, scheme 1.25.

Scheme 1.25

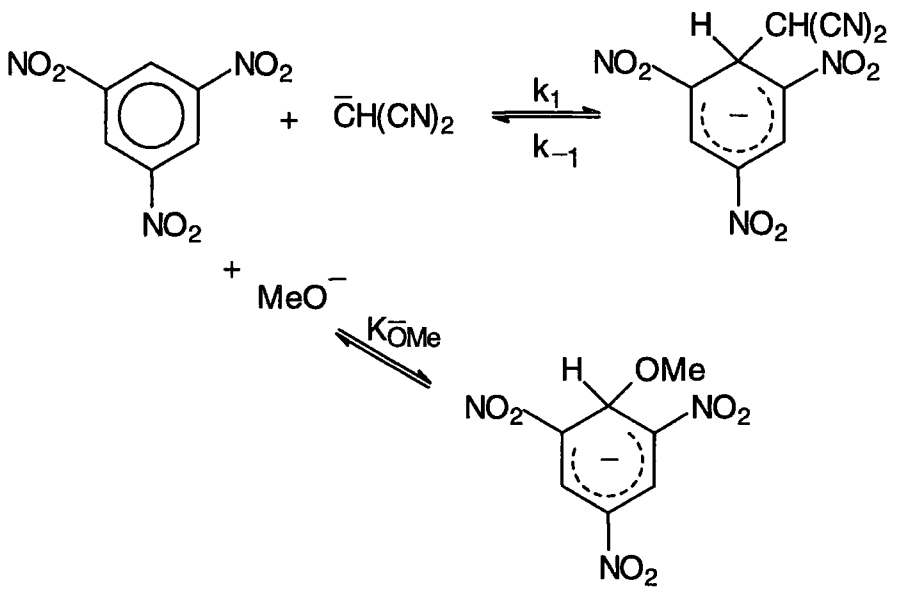

As can be seen above 1,3,5-TNB will also react with the methoxide anion in a competitive reaction to that of the carbanion, and this must be taken into account when considering the kinetics of these systems.

Table 1.5 shows other carbon nucleophiles which react in the same way to form σ-complexes.

Table 1.5 [21,22,23]

Nucleophile	k_1/dm^3 mol^{-1} s^{-1}	k_{-1}/ s^{-1}	K_1/ dm^3 mol^{-1}	pK_a
$(CH_3)_2CNO_2^-$	0.36	0.09	4	13.50
$CH(CN)_2^-$	3.0×10^5	6500	40	14.14
$CH_3CHNO_2^-$	34	0.09	380	14.20
$CH_3COCHCO_2CH_3^-$	5500	420	11.7	14.29
$CNCHCO_2CH_3^-$	1.3×10^5	62	1660	15.18
$CH_2NO_2^-$	800	0.011	7×10^4	15.60
$C_2H_5C(CN)_2^-$			33	15.60
$CH(CO_2CH_3)_2^-$	2.5×10^5	20.5	1.22×10^4	17.22
CN^-	16	0.08	200	13.30

All these carbanions have been found to give σ-adducts with 1,3,5-TNB. The value of the equilibrium constants show a general correlation with basicity as measured by pK_a values. However there is some evidence that steric interactions lower values of

equilibrium constants.For example the value of K_1 for the ethylmalononitrile anion is lower than would be expected from its pK_a value. The nucleophilic reactivities, in terms of rate constants k_1, are helpfully discussed in terms of their intrinsic reactivities (see section 4).

4-NBF and 4-NBZ are 10π electron heteroaromatic ring systems which have a high tendency towards σ-complex formation with nucleophiles due to the low aromaticity of the benzofuroxan/furazan ring systems.

As a result of this, together with the electron withdrawing effect of the furoxan/furazan rings, only mononitro activation is needed to ensure high σ-complex stability. However the corresponding dinitro compounds do exist and react similarly.

This makes 4-NBF and 4-NBZ ideal for reaction with carbanions, however as most reactions are carried out in methanolic solution there is again a problem of complexation with the methoxide anion.[23] Data are given in scheme 1.26 for reaction with furazan and furoxan at 25°C in methanol.[23]

Scheme 1.26

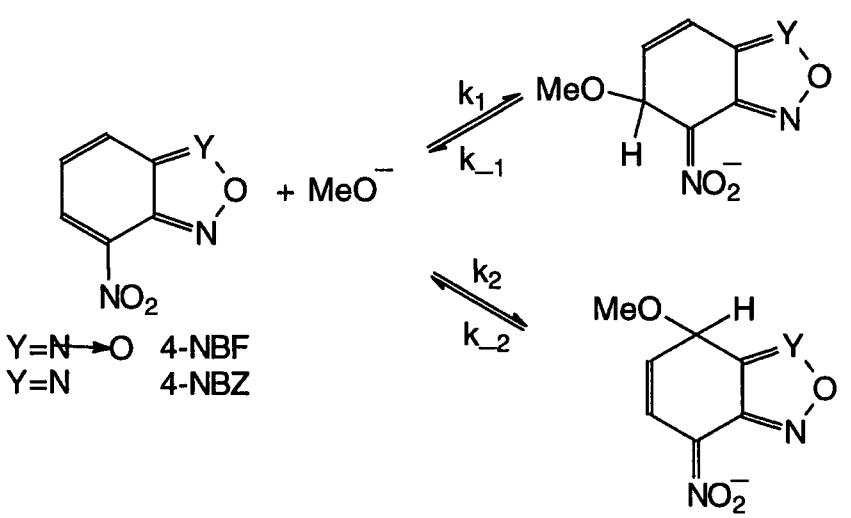

	4-NBF	4-NBZ
k_1/dm^3 mol^{-1} s^{-1}	1950	1200
k_{-1}/s^{-1}	4.6	8.5
k_2/l mol^{-1} s^{-1}	28.5	6.0
k_{-2}/s^{-1}	3.4×10^{-3}	2.0×10^{-3}

Addition at the 5-position is the result of kinetic control whereas addition at the 7-position is the result of thermodynamic control.
The 4,6-dinitro derivatives are sufficiently good electrophiles to react with methanol in the absence of base to give methoxy adducts and liberate protons.

As seen above, isomeric addition can occur at structurally different unsubstituted positions of a nitroaromatic, this original kinetic finding has been confirmed by NMR studies. NMR spectroscopy allows the position of nucleophilic attack in σ-adduct formation to be readily defined due to the change from sp^2 to sp^3 hybridization at the carbon atom undergoing substitution. This produces a pronounced shift to high field of the resonance due to the atom at this carbon. With 4,6-dinitrobenzofuroxan, interesting stereoisomerism occurs due to the chirality of the tetrahedral ring carbon C-7. In the acetone and nitromethane complexes the geminal protons are diastereotopic and appear as the AB of an ABX system.[24]

Scheme 1.27

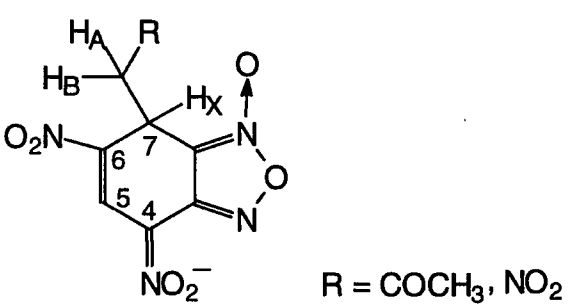

Introducing a second chiral centre at C-7 results in the formation of two diastereoisomeric complexes and such adducts have been identified for the cyclopentanone adducts of 4,6-DNBF, scheme 1.28.

Scheme 1.28

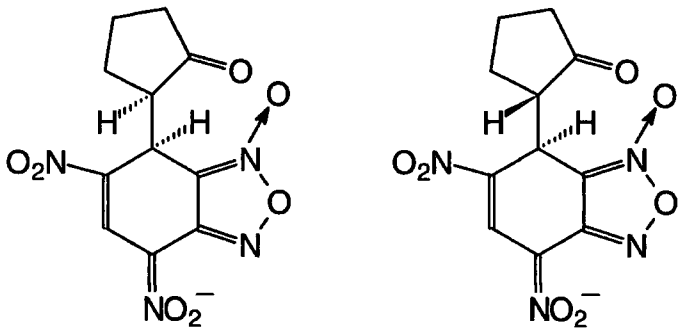

An interesting sequence of reactions occurs in DMSO on addition of 2,4-pentanedione to DNBF. Initially the ketonic σ-complex with nonequivalent methyl groups is observed but this undergoes slow and partial conversion to the enolic form, scheme 1.29. Complete equilibration at 32°C produces a 30:70 ratio of ketonic : enolic forms and the presence of two broad singlets for the methyl resonances of the enolic form provide evidence of fast equilibration between the two enolic tautomeric forms.[24]

Scheme 1.29

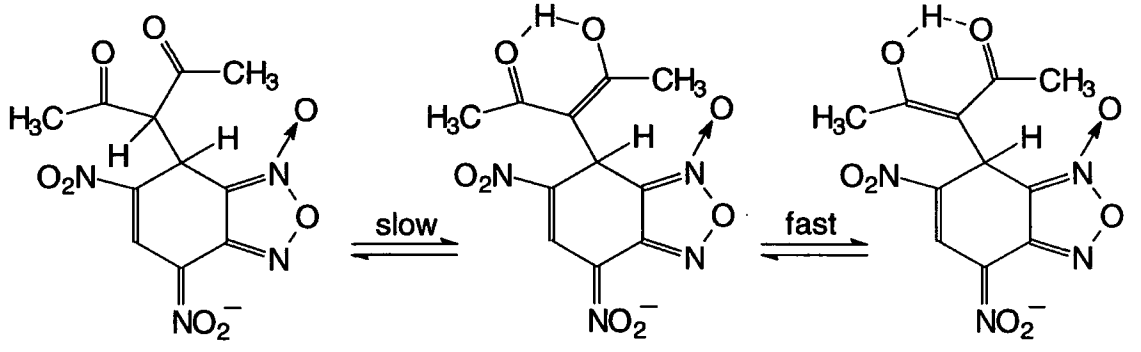

Competitive attack at substituted and unsubstituted positions of 4-NBF and 4-NBZ has also been confirmed by NMR. The substituted methoxy isomer has been observed prior to conversion to the 7-adduct, scheme 1.30.[25,26]

Scheme 1.30

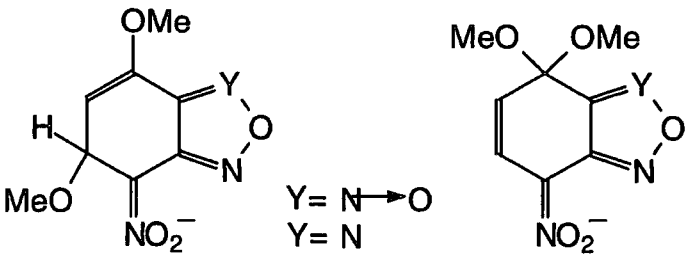

There are no reported reactions of kinetic studies of carbanions with these two compounds, however this report presents reactions of phenylacetonitrile anions with 4-NBF and 4-NBZ.

1.6 Proton transfer and carbon basicities

The rates of chemical reactions are influenced by both the thermodynamic driving force and also a kinetic parameter, often called the "intrinsic barrier".

In order to obtain a measure of relative reactivity, systems with the same equilibrium constant should be compared. However the situation becomes even simpler if the thermodynamic driving force is removed, that is $\Delta G°=0$ and consequently K=1, and absolute intrinsic rate constants k_0 are measured.In practice k_0 is obtained from extrapolation of a plot of logk versus logK, where k is the rate constant and K is the equilibrium constant for the reaction, as shown in figure 1.1.

Figure 1.1

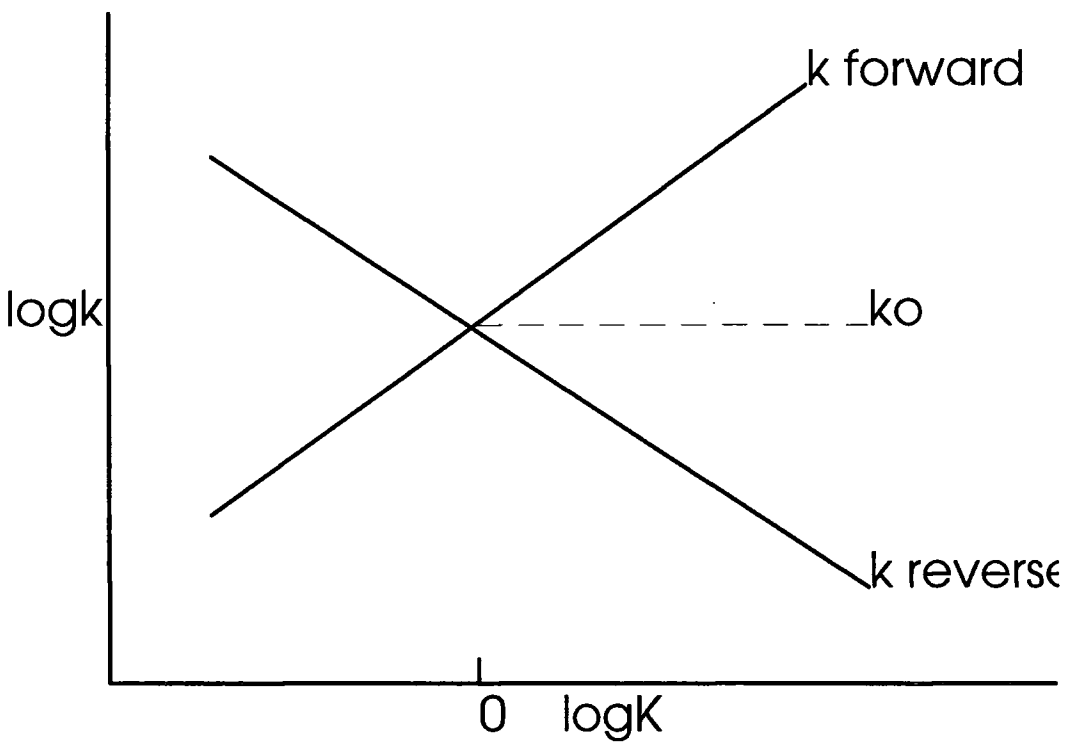

Many values of intrinsic rate constants have been measured especially for proton transfer reactions, some of the values for carbon acids relevant to this project are shown below.[27]

	$\log k_0$[a]	$\Delta G°$/kcal mole^{-1}
$RCH(CN)_2$	7.0	7.9
$4\text{-}NO_2C_6H_4CH_2CN$	3.1	13.1
$2,4\text{-}(NO_2)_2C_6H_3CH_2CN$	3.0	13.3

a All values in aqueous solution.

(For "normal" acids, i.e those in which there is fast proton dissociation, $\log k_0 \approx 9.5\text{-}10.0$ and $\Delta G° = 3.8\text{-}4.5$ kcal $mole^{-1}$).

Intrinsic barriers are thus much larger than for "normal" acids and this can be explained by consideration of three factors.

Firstly, carbon acids and bases are poor hydrogen bond acceptors and donors and thus they may not enter into the hydrogen bonded network of the solvent and a proton jump mechanism may not operate. This is also the most probable reason for direct proton transfers at carbon, i.e. there is no solvent bridge in the transition state.

Secondly there is a marked difference in structure between the carbon acids and their conjugate bases, and the structural and electronic reorganisation significantly influences the intrinsic barrier.However for nitrile compounds there is a great deal of evidence that the negative charge in the conjugate base is not strongly delocalised. Thus it is more like a true carbanion and much less structural reorganisation is involved resulting in intrinsic reactivities of the same order of magnitude as those for proton transfer between oxygen and nitrogen.

The third factor which has an important effect upon $\Delta G°$ is the solvent reorganisation which occurs during the reaction.There are two types of this, one concerning the the desolvation of the reactants in order for there to be close enough approach for the reaction to occur.The other involves changes in the orientation of solvent molecules, thus affecting dipole-dipole interactions and breaking and formation of solvent-solvent and solvent-solute hydrogen bonds.In the case of nitriles dipole-dipole interactions are most likely dominant.

Intrinsic rate constants for proton transfer in cyano-carbon acids are thus much greater than those of other carbon acids but are significantly lower than those for HCN and simple N and O acids.There is also no approach to the diffusion limit of the rate constants as for the normal acids, indeed it has been shown that the protonation of the malononitrile anion is not a diffusion controlled process.

Comparisons may be drawn between the intrinsic reactivities for proton transfer, and for reaction with nitro-aromatic compounds, of cyano-carbon acids. Using malononitrile as an example, it can be seen that there is a similar amount of structural and electronic

reorganisation during both reactions, and that the geometry at the carbon atom of the carbon base and the σ-adduct is similar, scheme 1.31.

Scheme 1.31

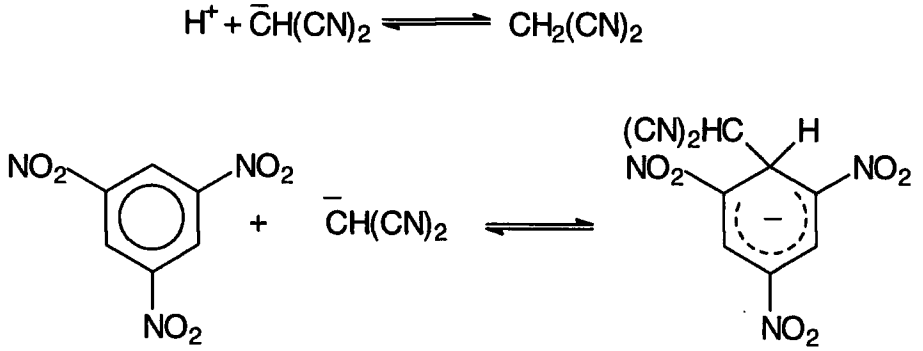

Since both reactions involve the malononitrile anion the amount of delocalisation on both carbanions is identical.Further in both the parent malononitrile and the σ-adduct the negative charge may be considered to have been neutralised, in the case of the σ-adduct the charge is almost neutralised due to the high electrophilicity of 1,3,5-TNB and the extensive delocalisation in the σ-adduct. However σ-adduct formation with 1,3,5-TNB involves extensive delocalisation in the aromatic ring and in the nitro groups. This will be accompanied by solvation changes. This extra electronic and solvent re-organisation results in an intrinsic reactivity lower than that observed for simple protonation of the malononitrile anion.

	$\log k_0$	
Proton transfer	7.00	in water [27]
Reaction with nitroaromatics	4.40	in methanol [22]

1.7 The diffusion limit of bimolecular reactions

The maximum rate at which bimolecular reactions can occur is of interest. When limitations due to mixing (macroscopic diffusion limit) are eliminated, the maximum rate of a bimolecular reaction is equal to the rate of encounter of the two molecules. These are diffusion-controlled reactions. The approximate magnitude of rate constants for such reactions may be deduced from a simplified theoretical model for the diffusion process.

It is assumed that the reacting molecules may be treated as spheres undergoing normal Brownian motion in a viscous fluid which react when they approach to a distance r_{AB}. Neglecting inter-molecular forces, it may be shown that the second order rate constant for two reacting species A and B is given by

$$k_2 = 400\pi r_{AB} L(D_A + D_B) \qquad \text{equation 1.2}$$

where L is the Avagadro number, D_A and D_B are diffusion coefficients of A and B in m^2 s^{-1} and r_{AB} is in m.

Using the Stokes-Einstein relationship for species *i* gives a useful approximation

$$D_i = \frac{k_B T}{6\pi\eta r_i}$$

where D_i is the diffusion coefficient, r_i is the radius, η is the solvent viscosity and k_B is the Boltzmann constant.

Substituting this into equation 1.2

$$k_2 = \frac{2000 L k_B T}{3\eta}\left(2 + \frac{r_A}{r_B} + \frac{r_B}{r_A}\right)$$

For molecules of a similar size, $r_A \approx r_B$, the rate constant is approximately independent of the species involved, thus

$$k_2 = \frac{8000 L k_B T}{3\eta} = \frac{8000 RT}{3\eta}$$

Values calculated from this equation at 25°C give 3×10^9 dm^3 mol^{-1} s^{-1} for dimethyl sulfoxide, a fairly viscous solvent and 7.4×10^9 dm^3 mol^{-1} s^{-1} for water, a less viscous solvent. Of particular interest for the work in this thesis is the value for methanol, 1.2×10^{10} dm^3 mol^{-1} s^{-1}.

Chapter 2

Reactions of nitroarenes with carbanions, kinetic and equilibrium studies.

Proton transfers involving carbon acids are often slower than those involving normal acids where the dissociating proton is bound to oxygen or nitrogen. However among carbon acids there are large variations in reactivity. Factors[28] which are believed to be responsible for this behaviour include:- i) the poor hydrogen bonding ability of carbon acids and carbanions, ii) the need for structural reorganisation in forming resonance stabilised carbanions, and iii) the need for solvent reorganisation accompanying reaction. There is evidence that carbon acids activated by cyano groups may approach normal behaviour. The cyano group is thought to stabilise negative charge mainly by inductive effects rather than resonance effects[29]. Thus rate constants for the thermodynamically favourable proton transfers involving cyano activated carbon acids may approach a value of 10^{10} dm^3 mol^{-1} s^{-1}. Values of intrinsic rate constants for the thermoneutral reactions are several orders of magnitude lower.

Some studies have been reported of the kinetics of σ-adduct formation from aromatic nitro-compounds and carbanions[30,31]. In this work kinetic and equilibrium results have been obtained for reactions of carbanions derived from phenylacetonitriles with 1,3,5-trinitrobenzene, 4-nitrobenzofuroxan, 4-nitrobenzofurazan and 1,3-dinitrobenzene. Variation in the basicities of the carbanions was achieved by varying the nature of the substituent , R, in the aromatic ring of the carbon acids. Some measurements were made with the carbanions derived from malononitrile and from some nitroalkanes. The aims were to measure rate constants for reactions of the carbanions with the aromatic nitro-compounds and, if possible, to determine intrinsic reactivities for these reaction types. It was necessary in the course of the work to determine equilibrium constants for deprotonation of the carbon acids by base.

2.1 Reactions with 1,3,5-trinitrobenzene

Several solvent systems were initially investigated for this reaction including sodium ethoxide in ethanol, sodium methoxide in methanol/DMSO mixtures and sodium methoxide in methanol. The latter medium was chosen for detailed study, one reason being that acidity functions are well defined here.

Kinetic measurements were made at 25°C by mixing solutions containing 1,3,5-TNB and substituted phenylacetonitrile and sodium methoxide. The results provide evidence for the reactions shown in schemes 2.1 and 2.2.

Scheme 2.1

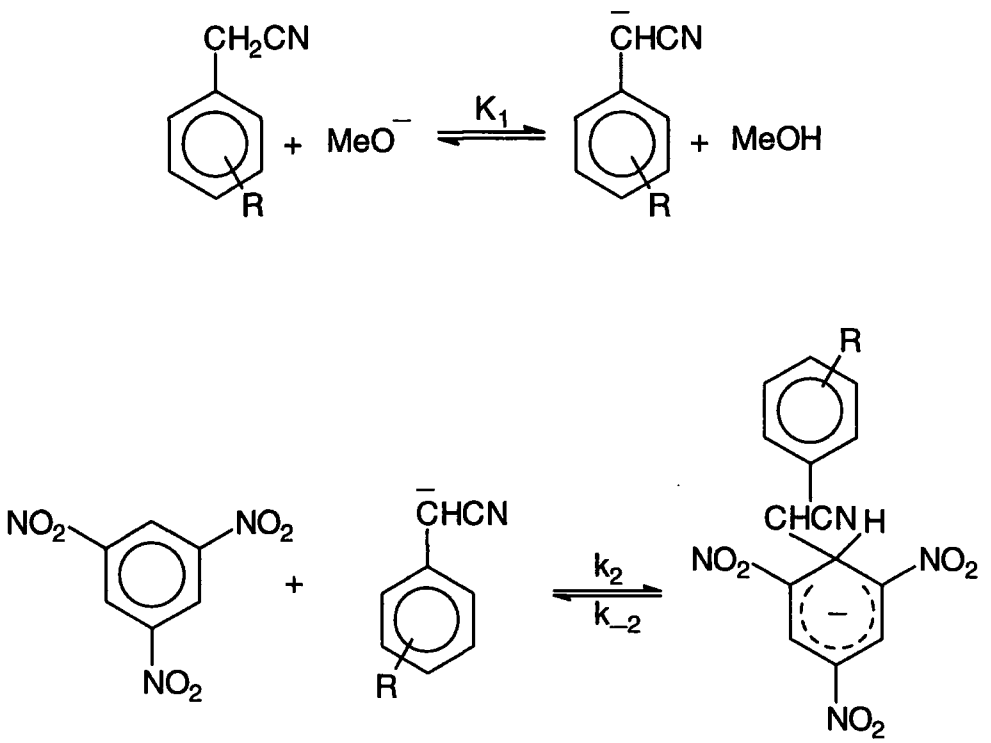

Scheme 2.2

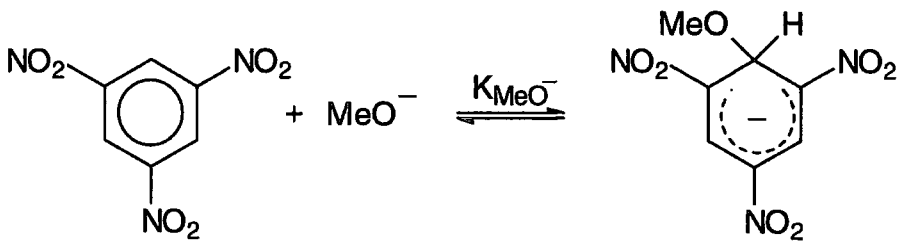

The equilibration of 1,3,5-TNB with methoxide is known to be a rapid process[46] on the stopped flow time-scale with an equilibrium constant , K_{OMe}, of 17 dm^3 mol^{-1}. The major process observed was formation of the σ-adducts with $lambda_{max}$ at 450nm and 520-540nm (shoulder).

Measurements were made with the concentrations of phenylacetonitrile and sodium methoxide much greater than that of 1,3,5-TNB and ionic strength was maintained at 0.01 mol dm^{-3} using sodium chloride as the added electrolyte. Under these conditions reactions were accurately first order and rate constants were independent of the concentration of 1,3,5-TNB in the range 1×10^{-5} to 1×10^{-4} mol dm^{-3}. This indicates that carbanion formation is rapid and the formation of σ-adducts is rate determining. The rate expression for this system is derived as follows.

$$[TNB]+[C_6H_5CHCN.TNB^-]+[TNB.OMe^-]=\text{constant}$$

$$\text{Since } K_{OMe^-}=\frac{[TNB.OMe^-]}{[TNB][MeO^-]}$$

$$[TNB][1+K_{MeO^-}[MeO^-]]+[C_6H_5CHCN.TNB^-]=\text{constant}$$

Differentiating

$$\frac{d[TNB]}{dt}[1+K_{MeO^-}[MeO^-]]+\frac{d[C_6H_5CHCN.TNB^-]}{dt}=0$$

$$\frac{d[TNB]}{dt}\left[1+K_{MeO^-}\,[MeO^-]\right]+k_2[C_6H_5CHCN^-][TNB]$$
$$-k_{-2}[C_6H_5CHCN.TNB^-]=0$$

Hence

$$\frac{d[TNB]}{dt}\left[1+K_{MeO^-}\,[MeO^-]\right]+k_2[C_6H_5CHCN^-][TNB] \qquad \text{equation 2.1}$$
$$-k_{-2}\left[\text{constant}-\left[[TNB]\left[1+K_{MeO^-}\,[MeO^-]\right]\right]\right]=0$$

At equilibrium $\frac{d[TNB]}{dt}=0$

$$k_2[C_6H_5CHCN^-][TNB]_{eq}$$
$$-k_{-2}\left[\text{constant}-[TNB]_{eq}\left[1+K_{MeO^-}\,[MeO^-]\right]\right]=0 \qquad \text{equation 2.2}$$

Subtracting equation 2.2 from equation 2.1

$$\frac{d[TNB]}{dt}\left[1+K_{MeO^-}\,[MeO^-]\right]+k_2[C_6H_5CHCN^-]([TNB]-[TNB]_{eq})$$
$$+k_{-2}\left[1+K_{MeO^-}\,[MeO^-]\right]([TNB]-[TNB]_{eq})=0$$

But $k_{obs}=-\frac{d[TNB]}{dt}\frac{1}{([TNB]-[TNB]_{eq})}$

$$-k_{obs}\left[1+K_{MeO}\cdot[MeO^-]\right]+k_2[C_6H_5CHCN^-]+k_{-2}\left[1+K_{MeO}\cdot[MeO^-]\right]=0$$

$$k_{obs}=\frac{k_2[C_6H_5CHCN^-]}{1+K_{MeO}\cdot[MeO^-]}+k_{-2}$$

But $K_1 \equiv \frac{[C_6H_5CHCN^-]}{[C_6H_5CH_2CN][MeO^-]}$

Thus $k_{obs} = K_1 k_2 \frac{[C_6H_5CH_2CN]}{1 + K_{MeO} \cdot [MeO^-]} [MeO^-] + k_{-2}$

A typical absorbance against time plot is shown in figure 2.1 and results are shown in tables 2.1 to 2.7.

Figure 2.1

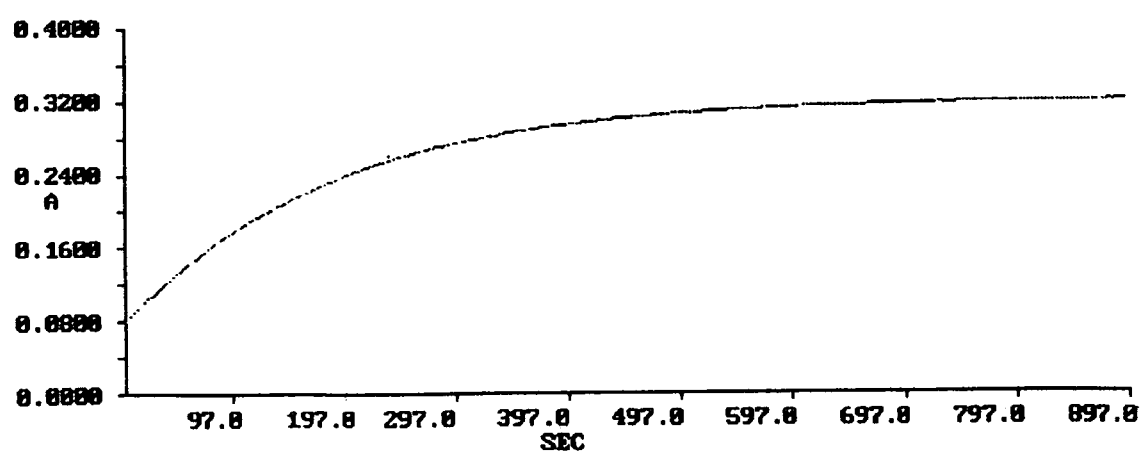

Absorbance versus time plot for reaction of 1,3,5-TNB, 4-$ClC_6H_4CH_2CN$ and NaOMe at 450nm.

Table 2.1

$[C_6F_5CH_2CN]$/ mol dm^{-3}	[TNB]/mol dm^{-3}	[NaOMe]/mol dm^{-3}	Average k_{obs}/s^{-1} at 425nm
0.0005	6×10^{-5}	0.01	19.56
0.00125	6×10^{-5}	0.01	21.08
0.0025	6×10^{-5}	0.01	23.96
0.0050	6×10^{-5}	0.01	30.40
0.0075	6×10^{-5}	0.01	35.17
0.0025	6×10^{-5}	0.005	21.07
0.0050	6×10^{-5}	0.005	24.05
0.0075	6×10^{-5}	0.005	26.80
0.0085	6×10^{-5}	0.005	28.62
0.0100	6×10^{-5}	0.005	30.21

Table 2.2

$[4\text{-}CNC_6H_4CH_2CN]$/ mol dm^{-3}	[TNB]/mol dm^{-3}	[NaOMe]/mol dm^{-3}	Average k_{obs}/s^{-1} at 450nm
0.0005	5×10^{-5}	0.01	5.118
0.0010	5×10^{-5}	0.01	6.333
0.0015	5×10^{-5}	0.01	7.453
0.0020	5×10^{-5}	0.01	8.539
0.0025	5×10^{-5}	0.01	9.566
0.0005	5×10^{-5}	0.005	4.680
0.0010	5×10^{-5}	0.005	4.988
0.0015	5×10^{-5}	0.005	5.414
0.0020	5×10^{-5}	0.005	6.381
0.0025	5×10^{-5}	0.005	6.776

Table 2.3

[4-$NO_2C_6H_4CH_2CN$] /mol dm^{-3}	[TNB]/mol dm^{-3}	[NaOMe]/mol dm^{-3}	Average k_{obs}/s^{-1} at 453nm
0.0005	4×10^{-5}	0.01	18.49
0.00125	4×10^{-5}	0.01	23.48
0.0025	4×10^{-5}	0.01	35.63
0.0050	4×10^{-5}	0.01	54.82
0.0075	4×10^{-5}	0.01	78.24
0.0005	4×10^{-5}	0.005	18.09
0.00125	4×10^{-5}	0.005	22.21
0.0025	4×10^{-5}	0.005	26.91
0.0050	4×10^{-5}	0.005	37.66
0.0075	4×10^{-5}	0.005	49.42

Table 2.4

[4-$CF_3C_6H_4CH_2CN$] /mol dm^{-3}	[TNB]/mol dm^{-3}	[NaOMe]/mol dm^{-3}	Average k_{obs}/s^{-1} at 447nm
0.0005	5×10^{-5}	0.01	15.42×10^{-2}
0.0010	5×10^{-5}	0.01	18.13×10^{-2}
0.0015	5×10^{-5}	0 01	21.09×10^{-2}
0.0020	5×10^{-5}	0.01	24.14×10^{-2}
0.0025	5×10^{-5}	0.01	27.48×10^{-2}
0.0005	5×10^{-5}	0.005	14.68×10^{-2}
0.0010	5×10^{-5}	0.005	16.58×10^{-2}
0.0015	5×10^{-5}	0.005	18.82×10^{-2}
0.0020	5×10^{-5}	0.005	21.17×10^{-2}
0.0025	5×10^{-5}	0.005	23.21×10^{-2}

Table 2.5

[3-$CF_3C_6H_4CH_2CN$] /mol dm^{-3}	[TNB]/mol dm^{-3}	[NaOMe]/mol dm^{-3}	Average k_{obs}/s^{-1} at 445nm
0.0005	5×10^{-5}	0.01	22.48×10^{-3}
0.0010	5×10^{-5}	0.01	26.76×10^{-3}
0.0015	5×10^{-5}	0 01	32.93×10^{-3}
0.0020	5×10^{-5}	0.01	37.87×10^{-3}
0.0025	5×10^{-5}	0.01	42.55×10^{-3}
0.0005	5×10^{-5}	0.005	19.63×10^{-3}
0.0010	5×10^{-5}	0.005	24.81×10^{-3}
0.0015	5×10^{-5}	0.005	28.13×10^{-3}
0.0020	5×10^{-5}	0.005	31.39×10^{-3}
0.0025	5×10^{-5}	0.005	34.57×10^{-3}

Table 2.6

[3-$ClC_6H_4CH_2CN$] /mol dm^{-3}	[TNB]/mol dm^{-3}	[NaOMe]/mol dm^{-3}	Average k_{obs}/s^{-1} at 448nm
0.0005	5×10^{-5}	0.01	14.46×10^{-3}
0.0010	5×10^{-5}	0.01	16.16×10^{-3}
0.0015	5×10^{-5}	0 01	18.86×10^{-3}
0.0020	5×10^{-5}	0.01	20.77×10^{-3}
0.0025	5×10^{-5}	0.01	22.36×10^{-3}
0.0005	5×10^{-5}	0.005	10.57×10^{-3}
0.0010	5×10^{-5}	0.005	11.79×10^{-3}
0.0015	5×10^{-5}	0.005	12.07×10^{-3}
0.0020	5×10^{-5}	0.005	13.82×10^{-3}
0.0025	5×10^{-5}	0.005	14.04×10^{-3}

Table 2.7

[4-$ClC_6H_4CH_2CN$] /mol dm^{-3}	[TNB]/mol dm^{-3}	[NaOMe]/mol dm^{-3}	Average k_{obs}/s^{-1} at 450nm
0.0005	5×10^{-5}	0.01	4.924×10^{-3}
0.0010	5×10^{-5}	0.01	5.238×10^{-3}
0.0015	5×10^{-5}	0.01	5.983×10^{-3}
0.0020	5×10^{-5}	0.01	6.812×10^{-3}
0.0025	5×10^{-5}	0.01	7.859×10^{-3}
0.0005	5×10^{-5}	0.005	3.780×10^{-3}
0.0010	5×10^{-5}	0.005	4.427×10^{-3}
0.0015	5×10^{-5}	0.005	4.993×10^{-3}
0.0020	5×10^{-5}	0.005	5.337×10^{-3}
0.0025	5×10^{-5}	0.005	5.993×10^{-3}

Plots of kobs vs the concentration of phenylacetonitrile, at constant methoxide concentration, were linear and allowed the calculation of values k_2K_1 and k_{-2}. A representative plot is shown in figure 2.2 and data are collected in table 2.8.

Figure 2.2

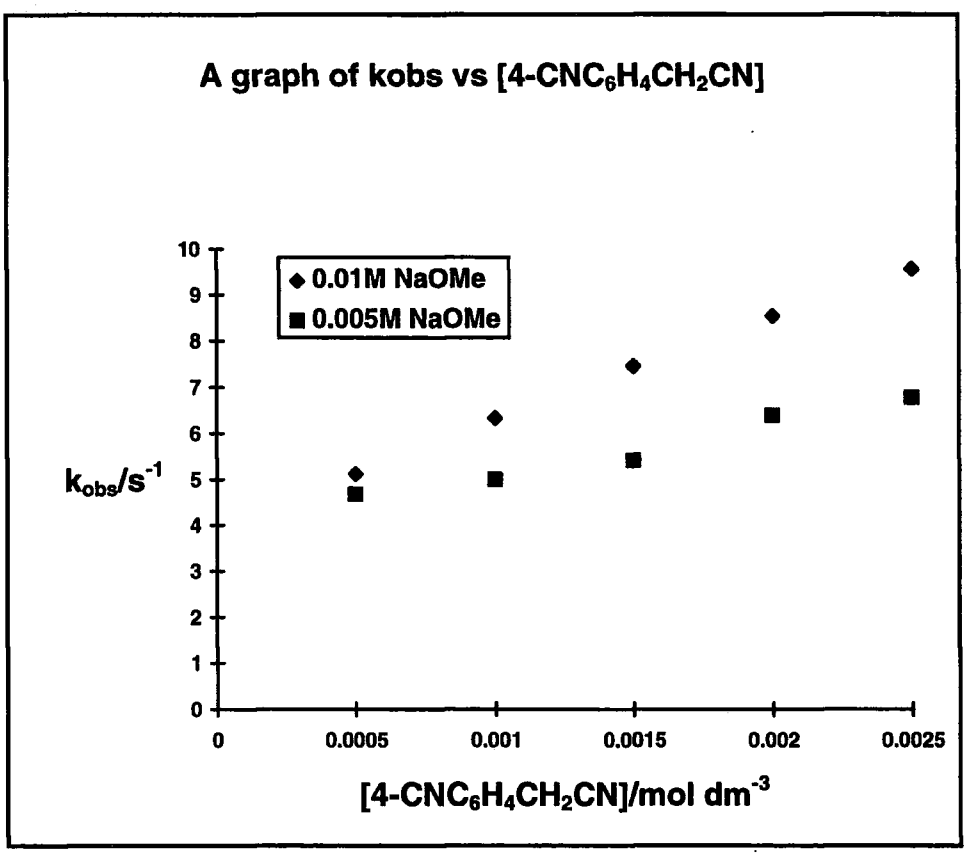

Table 2.8

Summary of results

R	k_{-2}/s^{-1}	$K_1k_2/dm^6mol^{-2}\ s^{-1}$	K_1K_2/dm^6mol^{-2}*
4-NO_2	14.90	9.87×10^5	6.51×10^4
2,3,4,5,6-F_5	18.20	2.65×10^5	1.46×10^4
4-CN	4.10	2.44×10^5	5.95×10^4
4-CF_3	1.25×10^{-1}	8.12×10^3	6.50×10^4
3-CF_3	1.68×10^{-2}	1.41×10^3	8.39×10^4
3-Cl	1.14×10^{-2}	460.00	4.04×10^4
4-Cl	2.20×10^{-3}	210.00	9.55×10^4

* Values were calculated as $K_1k_2/\ k_{-2}$

It is interesting that the values of the product K_1K_2 are insensitive to the nature of the ring substituent, R, in the phenylacetonitrile and are all close to 5×10^4 dm^6 mol^{-2}. The increases in the value of K_1 with increasing electron withdrawal of the substituent, R, are exactly balanced by corresponding decreases in the values of K_2. Since ionization involves the development of a complete unit of negative charge on the phenylacetonitrile anions, the inference is that in the reaction with 1,3,5-TNB to produce adducts the negative charge is completely transferred from the carbanion to the aromatic ring. The slight decreases in value of K_1 K_2 with *ortho*-substituted derivative 2,3,4,5,6-F_5 may represent a small unfavourable steric interaction in the corresponding sigma-adduct resulting in a decrease in value of K_2 .

In order to obtain values of the rate constant k_2, it is necessary to know the values of K_1 for reaction of the carbon acids with methoxide.

2.2 Acidities of carbon acids in methanol

Carbanions were generated from phenylacetonitriles by reaction with sodium methoxide in methanol. Values of the equilibrium constant, K_1 , were determined spectrophotometrically using the strong UV-VIS absorption of the carbanions. In all cases equilibration was rapid on the stopped-flow time scale.

For 4-nitrophenylacetonitrile ionization occurred in dilute solutions of base where the basicity of the medium is adequately expressed by the methoxide concentration as shown in equation 2.3.

$$K_1 = \frac{[RC_6H_4CHCN^-]}{[RC_6H_4CH_2CN][MeO^-]} \qquad \text{equation 2.3}$$

However for less acidic phenylacetonitriles, sufficient ionization to allow measurement of the equilibrium constant occurred only in more basic media. Here an acidity function is needed to express the basicity of the medium and it is necessary to include activity coefficients in equations describing the solution. A relation between the equilibrium constant K_1 and the H_M acidity function may be derived as follows [32].

$$BH^+ \overset{K_a}{\rightleftharpoons} B + H^+$$

$$K_a = \frac{a_{H^+} a_B}{a_{BH^+}}$$

$$K_a = \frac{a_{H^+} [B] \gamma_B}{[BH+] \gamma_{BH^+}}$$

Thus

$$\frac{K_a[BH+]}{[B]} = \frac{a_{H^+} \gamma_B}{\gamma_{BH^+}} \qquad \text{equation 2.4}$$

The quantity $\frac{a_{H^+} \gamma_B}{\gamma_{BH^+}}$ is defined as h_o, however it is more convenient to use a logarithimic scale thus a quantity H_o is defined as in equation 2.5.

$$H_o = -\log_{10} h_o = -\log_{10}\left\{\frac{K_a[BH+]}{[B]}\right\} = -\log_{10}\frac{a_H + \gamma_B}{\gamma_{BH+}} \qquad \text{equation 2.5}$$

For solutions in methanol the acidity function H_M is used, this is defined by equation 2.6, where K^M_{SH} is the ionization of a species SH in methanol and γ_i refer to methanol as the standard state.

$$H_M = -\log_{10} h_o = -\log_{10}\frac{a_H + \gamma_B}{\gamma_{BH+}} = pK^M_{SH} + \log_{10}\frac{[S^-]}{[SH]} \qquad \text{equation 2.6}$$

From equation 2.4

$$\log_{10} K_a = \log_{10}\frac{[BH+]}{[B]} - H_M \qquad \text{equation 2.7}$$

When $K_a = K_{MeOH}$ equation 2.7 becomes

$$\log_{10} K_{MeOH} = \log_{10}[MeO^-] - H_M$$

For the ionization of phenylacetonitriles in methanol

$$K_1 = \frac{[RC_6H_4CHCN^-]}{[RC_6H_4CH_2CN][MeO^-]}$$

Thus

$$\log K_1 = \log_{10}\frac{[RC_6H_4CHCN^-]}{[RC_6H_4CH_2CN]} - \log_{10} K_{MeOH} - H_M \qquad \text{equation 2.8}$$

(The value of $\log_{10} K_{MeOH}$, the autoprotolysis constant[31] for methanol is -16.92.)

Acidity functions for methanolic sodium methoxide have been reported based on the ionisation of substituted anilines and also on methoxide additions to α-cyanostilbenes. Since the latter case involves base addition they are in fact J_M scales. In all cases the ionisation involves formation of a negative charge which is delocalized into an aromatic ring, thus the H_M and J_M scales closely parallel each other. Since the reaction of methoxide with α-cyanostilbenes, R, results in the formation of carbanions which closely resemble those procuced from the ionization of phenylacetonitriles, scheme 2.3, it was decided to use the J_M data to obtain values to substitute for H_M in the final expression. J_M is defined below.

$$J_M = -\log_{10}\frac{a_H + \gamma_{ROMe}}{\gamma_R a_{MeOH}} = pK_1 K_{MeOH} + \log_{10}\frac{[ROMe^-]}{[R]}$$

Scheme 2.3

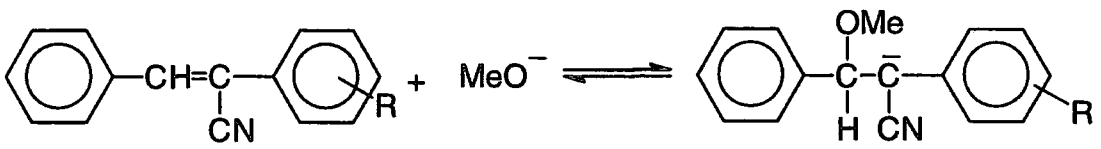

Results are shown in tables 2.9 to 2.14.

Table 2.9

4-Cyanophenylacetonitrile

[NaOMe]/mol dm^{-3}	Abs at 387nm	K[a]/dm^{3}mol^{-1}	J_M
3.50	0.84	3.35×10^{-3}	20.24
3.00	0.70	4.47×10^{-3}	19.70
2.50	0.52	6.49×10^{-3}	19.18
2.00	0.16	3.64×10^{-3}	18.66

a K is calculated as $\log_{10}\frac{A}{0.96-A}+16.92-J_M$

Table 2.10

4-Nitrophenylacetonitrile

[NaOMe]/mol dm^{-3}	Abs at 527nm	K[a]/dm^{3}mol^{-1}	J_M
0.20	0.682	0.972	16.44
0.30	1.110	1.252	16.64
0.50	1.708	1.082	17.08
0.60	1.828	1.033	17.18
0.80	2.204	1.225	17.40
1.00	2.346	1.080	17.60

a K is calculated as $\log_{10}\frac{A}{2.80-A}+16.92-J_M$

Table 2.11

2-Nitrophenylacetonitrile

[NaOMe]/mol dm^{-3}	Abs at 544nm	K^a/dm^{3}mol^{-1}	J_M
0.50	0.190	0.168	17.08
0.60	0.269	0.210	17.18
0.80	0.303	0.150	17.40
1.00	0.436	0.170	17.60

a K is calculated as $\log_{10}\frac{A}{0.972-A}+16.92-J_M$

Table 2.12

2,3,4,5,6-pentafluorophenylacetonitrile

[NaOMe]/mol dm^{-3}	Abs at 313nm	K^a/dm^{3}mol^{-1}	J_M
2.80	0.129	4.55×10^{-4}	19.50
3.00	0.208	5.18×10^{-4}	19.70
3.20	0.260	4.04×10^{-4}	19.94
3.40	0.314	3.53×10^{-4}	20.12
3.61	0.490	4.84×10^{-4}	20.34

a K is calculated as $\log_{10}\frac{A}{0.875-A}+16.92-J_M$

Table 2.13

3,5-bis(trifluoromethyl)phenylacetonitrile

[NaOMe]/mol dm^{-3}	Abs at 343nm	K^a/dm^{3}mol^{-1}	J_M
2.20	0.095	1.05×10^{-3}	18.86
2.40	0.150	1.06×10^{-3}	19.08
2.60	0.270	1.36×10^{-3}	19.28
2.80	0.358	1.21×10^{-3}	19.50
3.00	0.408	0.93×10^{-3}	19.70
3.20	0.640	1.24×10^{-3}	19.94
3.40	0.706	1.04×10^{-3}	20.12

a K is calculated as $\log_{10}\frac{A}{1.134-A}+16.92-J_M$

Table 2.14[33]

R[a]	$\log_{10}K_1$[b]	σ^-[c]	$\log_{10}K_1$[d]	$\log_{10}K_1$[e]	pK_a[f]
4-NO_2	0.04				16.9
2-NO_2	-0.76				17.7
2-CN				-2.30	19.2
4-CN	-2.35	1.02			19.3
3,5-$(CF_3)_2$	-2.90				19.8
2,3,4,5,6-F_5	-3.30				20.2
4-CF_3		0.65	-4.06	-4.22	21.0
3-CF_3		0.43	-5.08	-5.27	22.1
3-Cl		0.36	-5.40	-5.71	22.4
4-Cl		0.19	-6.19	-6.37	23.2
3-MeO		0.10	-6.60		23.5
H		0.00	-7.06		24.0
3-Me		-0.086	-7.46		24.4

a Ring substituent in phenylacetonitrile

b Direct determination in methanolic sodium methoxide

c From O. Exner, *Prog.Phys.Org.Chem*, 1973, **10**, 1 and T. Kuang-Chih, *Acta Chim.Sinica.*, 1966, **32**, 107.

d Calculated using equation 2.9.

e Calculated from measurements in methanol-mixtures containing sodium methoxide.

f $pK_a = pK_I + pK_M$.

For phenylacetonitriles less acidic than the pentafluoro derivative insufficient ionization occurred in methanolic sodium methoxide solutions to allow calculation of values of K_1 using equation 2.8. However Kroeger and Stewart[32] showed that for carbanion formation from α-cyanostilbenes a Hammett plot *versus* σ^- gave a value for ρ of 4.62. The similarity of carbanion formation from phenylacetonitriles to this process leads us to expect a similar ρ value. Here equation 2.9 was used to calculate values of K_1 for substituted phenylacetonitriles using the value for $\log_{10} K_1$ of -2.35 for the 4-cyano derivative as an anchor point.

$$\log_{10} K_1(CN) - \log_{10} K_1(R) = 4.62\,(\sigma_{CN}^- - \sigma_R^-) \qquad \text{equation 2.9}$$

For example for the 3-chloro derivative

$$-2.35 - \log_{10} K_1(Cl) = 4.62\ (1.02 - 0.36)$$

$$\therefore \log_{10} K_1(Cl) = -5.40$$

Values of $\log_{10} K_1$ are collected in table 2.14. There is good agreement with data obtained using sodium methoxide in methanol-DMSO as a basic medium[34].

The pK_a value for pentafluorophenylacetonitrile is anomalous, it is between that of the 4-cyano and 4-trifluoromethyl derivatives. This contrasts with data for phenols where the pentafluoro-derivative is more acidic even than the 4-nitro derivative[38]. However our results accord with previous work showing the variable resonance/inductive effects of the pentafluoro substituent and in particular the relatively small effect of this grouping on the acidities of carbon acids[39].

Since values of the product k_2K_1 are available (table 2.8), knowledge of the values of K_1 allows the calculation of values of k_2 . Combination of k_2 and k_{-2} values leads to values for K_2 (k_2/k_{-2}). These values are collected in table 2.15 below.

Table 2.15

R	k_2K_1/ dm^6 mol^{-2} s^{-1}	$\log_{10}k_2$	$\log_{10}K_2$
4-NO2	9.87×10^5	5.95	4.80
2,3,4,5,6-F5	2.65×10^5	8.70	7.40
4-CN	2.44×10^5	7.70	7.10
4-CF3	8.12×10^3	8.00	7.60
3-CF3	1.41×10^3	8.20	10.1
3-Cl	460	8.10	10.1
4-Cl	210	8.50	11.1

2.3 Reaction with 4-nitrobenzofuroxan

The rate constants for reaction of the more reactive phenylacetonitrile anions with 1,3,5-TNB are greater than 10^8 dm^3 mol^{-1} s^{-1}.The diffusion limit in methanol is 1×10^{10} dm^3 mol^{-1} s^{-1} [34]. It was thought to be of interest to investigate the reactions of these carbanions with a substrate which is more reactive than 1,3,5-TNB.

Two possible substrates were investigated, 4-nitrobenzofuroxan and 4,6-dinitrobenzofuroxan.

(**8**) X=NO_2 4,6-DNBF
(**9**) X=H 4-NBF

As discussed previously, problems are encountered with these substrates due to their reaction with the methoxide anion.This reaction occurs to a lesser extent with 4-NBF and thus this is the substrate chosen for this study.

The adduct formed is shown as that resulting from attack at the 5-position, scheme 2.4, as this is likely to be the most rapid process and the one to which kinetic data measured will apply. However it is probable that slow isomerization to give the adduct resulting from carbanion attack at the 7-position will occur.

Scheme 2.4

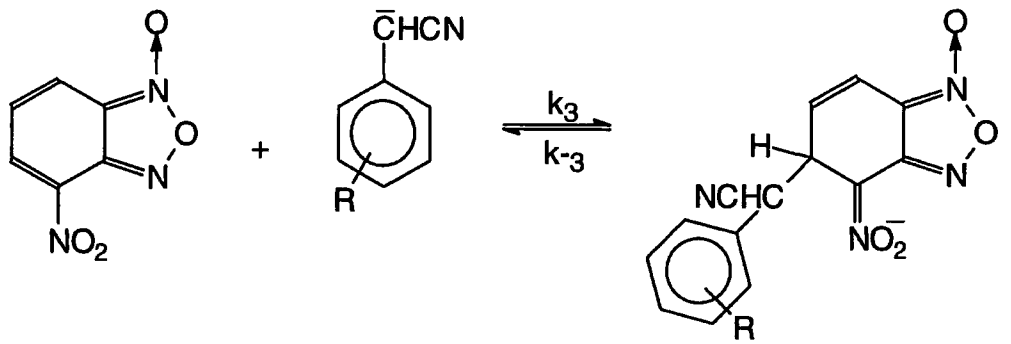

Since measurements were made in methanolic sodium methoxide there is a competitive reaction with the methoxide ions as shown in scheme 2.5.

Scheme 2.5

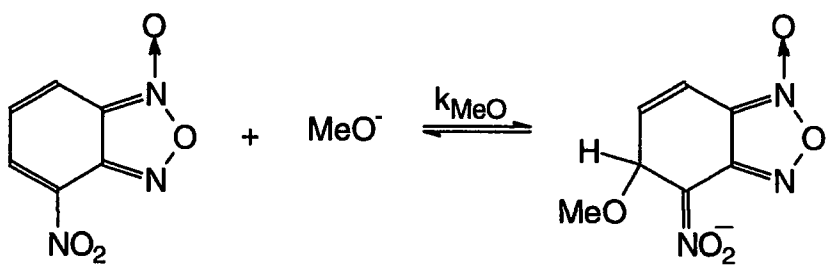

It is known from ^{1}H NMR measurements that reaction of 4-NBF with methoxide alone results in rapid formation of the 5-methoxy adduct followed by slower isomerization to the 7-methoxy adduct. UV measurements have shown that 4-NBF has an absorption maximum at 403nm while the methoxy-adducts both absorb at 340nm. Kinetic studies give a value of 1950 $dm^3\ mol^{-1}\ s^{-1}$ for the rate constant for attack at the 5-position[23] and this was confirmed by experiment.

It was found that working at constant sodium methoxide concentration increases in the concentration of phenylacetonitrile resulted in increases in the value of the first order rate constant. These were measured both as decreases in absorbance at 403nm (fading of substrate) and increases in absorbance at 340nm (formation of adduct). Results are shown in tables 2.16 to 2.20.

Table 2.16

[4-$NO_2C_6H_4CH_2CN$]/ mol dm^{-3}	[NaOMe]/ mol dm^{-3}	Average k_{obs}/s^{-1} at 340nm
1×10^{-4}	3×10^{-3}	11.82
2×10^{-4}	"	22.05
3×10^{-4}	"	31.45
4×10^{-4}	"	40.65
1×10^{-4}	5×10^{-3}	22.87
2×10^{-4}	"	36.49
3×10^{-4}	"	53.17
4×10^{-4}	"	66.48
1×10^{-4}	7×10^{-3}	33.67
2×10^{-4}	"	51.81
3×10^{-4}	"	73.89
4×10^{-4}	"	91.52

[4-$NO_2C_6H_4CH_2CN$]/ mol dm^{-3}	[NaOMe]/ mol dm^{-3}	Average k_{obs}/s^{-1} at 404nm
1×10^{-4}	3×10^{-3}	12.07
2×10^{-4}	"	21.97
3×10^{-4}	"	30.76
4×10^{-4}	"	41.98
1×10^{-4}	5×10^{-3}	22.79
2×10^{-4}	"	37.18
3×10^{-4}	"	51.49
4×10^{-4}	"	67.07
1×10^{-4}	7×10^{-3}	32.90
2×10^{-4}	"	52.22
3×10^{-4}	"	74.15
4×10^{-4}	"	91.04

[4-NBF]=2×10^{-5}M

Table 2.17

[2-$NO_2C_6H_4CH_2CN$]/ mol dm^{-3}	[NaOMe]/ mol dm^{-3}	Average k_{obs}/s^{-1} at 340nm
1×10^{-4}	3×10^{-3}	9.597
2×10^{-4}	"	11.20
3×10^{-4}	"	13.27
4×10^{-4}	"	15.38
1×10^{-4}	5×10^{-3}	14.58
2×10^{-4}	"	19.30
3×10^{-4}	"	24.37
4×10^{-4}	"	28.37
1×10^{-4}	7×10^{-3}	19.64
2×10^{-4}	"	26.61
3×10^{-4}	"	32.12
4×10^{-4}	"	38.73

[2-$NO_2C_6H_4CH_2CN$]/ mol dm^{-3}	[NaOMe]/ mol dm^{-3}	Average k_{obs}/s^{-1} at 404nm
1×10^{-4}	3×10^{-3}	9.272
2×10^{-4}	"	11.19
3×10^{-4}	"	13.54
4×10^{-4}	"	15.26
1×10^{-4}	5×10^{-3}	14.41
2×10^{-4}	"	19.76
3×10^{-4}	"	23.83
4×10^{-4}	"	27.53
1×10^{-4}	7×10^{-3}	19.64
2×10^{-4}	"	26.46
3×10^{-4}	"	31.53
4×10^{-4}	"	38.87

[4-NBF]=2×10^{-5}M

Table 2.18

[4-$CNC_6H_4CH_2CN$]/ mol dm^{-3}	[NaOMe]/ mol dm^{-3}	Average k_{obs}/s^{-1} at 340nm
0.005	3×10^{-3}	11.78
0.010	"	19.79
0.015	"	28.19
0.020	"	39.63
0.005	5×10^{-3}	21.46
0.010	"	34.60
0.015	"	45.58
0.020	"	58.11
0.005	7×10^{-3}	33.95
0.010	"	49.47
0.015	"	68.12
0.020	"	96.46

[4-$CNC_6H_4CH_2CN$]/ mol dm^{-3}	[NaOMe]/ mol dm^{-3}	Average k_{obs}/s^{-1} at 404nm
0.005	3×10^{-3}	12.59
0.010	"	21.15
0.015	"	31.57
0.020	"	44.77
0.005	5×10^{-3}	22.14
0.010	"	35.53
0.015	"	58.78
0.020	"	78.89
0.005	7×10^{-3}	34.61
0.010	"	48.86
0.015	"	101.6
0.020	"	N/A

[4-NBF]=2×10^{-5}M

Table 2.19

[3,5-$(CF_3)_2C_6H_3CH_2CN$]/ mol dm^{-3}	[NaOMe]/ mol dm^{-3}	Average k_{obs}/s^{-1} at 340nm
0.025	5×10^{-3}	36.70
0.035		48.60
0.050		65.42
0.065		78.07
0.025	7×10^{-3}	50.63
0.035		68.98
0.050		90.68
0.065		118.2

[3,5-$(CF_3)_2C_6H_3CH_2CN$]/ mol dm^{-3}	[NaOMe]/ mol dm^{-3}	Average k_{obs}/s^{-1} at 404nm
0.025	5×10^{-3}	36.59
0.035		51.36
0.050		63.69
0.065		79.22
0.025	7×10^{-3}	50.26
0.035		68.64
0.050		92.25
0.065		118.5

[4-NBF]=2×10^{-5}M

Table 2.20

[2,3,4,5,6-$C_6F_5CH_2CN$]/ mol dm^{-3}	[NaOMe]/ mol dm^{-3}	Average k_{obs}/s^{-1} at 340nm
0.015	3×10^{-3}	18.53
0.025	"	26.19
0.035	"	34.15
0.050	"	45.36
0.015	5×10^{-3}	29.90
0.025	"	46.04
0.035	"	58.92
0.050	"	76.53
0.015	7×10^{-3}	43.26
0.025	"	60.63
0.035	"	79.32
0.050	"	104.1

[2,3,4,5,6-$C_6F_5CH_2CN$]/ mol dm^{-3}	[NaOMe]/ mol dm^{-3}	Average k_{obs}/s^{-1} at 404nm
0.015	3×10^{-3}	18.35
0.025	"	25.45
0.035	"	33.01
0.050	"	43.70
0.015	5×10^{-3}	30.11
0.025	"	45.71
0.035	"	58.20
0.050	"	76.63
0.015	7×10^{-3}	41.99
0.025	"	60.15
0.035	"	78.41
0.050	"	106.5

[4-NBF]=2×10^{-5} M

A summary of the results is shown in table 2.21.

Table 2.21

R	$K_1/dm^3\ mol^{-1}$	$k_3/dm^3\ mol^{-1}s^{-1}$
4-NO_2	1.107	3.02×10^7
2-NO_2	0.175	5.32×10^7
4-CN	4.49×10^{-3}	1.21×10^8
3,5-$(CF_3)_2$	1.13×10^{-3}	1.92×10^8
2,3,4,5,6-F_5	4.43×10^{-4}	6.03×10^8
$CH_2(CN)_2$	600	5.55×10^4

It was found that under the experimental conditions used equilibrium constants for adduct formation are high. Hence in the equilibration process the forward terms dominate the rate expression at the expense of the reverse terms. It was found that experimental data fitted equation 2.10.

$$k_{obs} = k_{OMe}[MeO^-] + k_3K_1[MeO^-]\ [RC_6H_4CH_2CN] \qquad \text{equation 2.10}$$

Figure 2.3

Graph of k_{obs} *versus* [4-$NO_2C_6H_4CH_2CN$]at 340nm

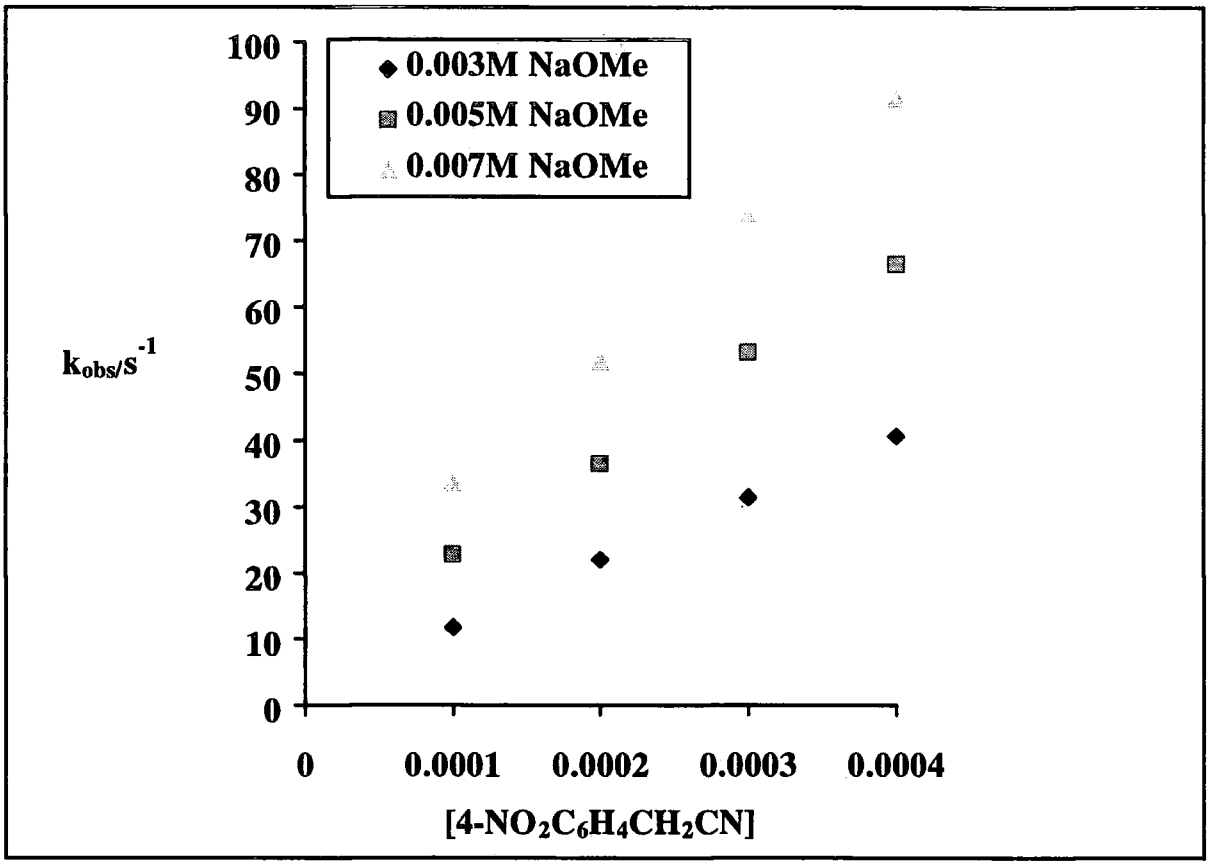

This plot, figure 2.3, of k_{obs} *versus* the concentration of phenylacetonitrile gave the product k_3K_1 as the slope and k_{OMe} [MeO^-] as the intercept. Since values of K_1 are known, values of k_3 may be calculated, these are shown in table 2.21.

Addition of phenylacetonitriles less acidic than the pentafluoro derivative caused no enhancement of k_{obs} above that observed in the presence of methoxide alone. For phenylacetonitriles where $K_1 < 10^{-4}$ dm^3 mol^{-1} the condition $k_{OMe} > k_3K_1[RC_6H_4CH_2CN]$ will apply so that the final term in equation 2.10 becomes immeasurably small. It is expected that adducts formed from 4-NBF with all the phenylacetonitrile carbanions will have greater thermodynamic stabilities than the methoxide adducts. However since the UV spectra of the two types of adduct are similar, conversion of the initially formed

methoxide adducts to the more stable carbanionic adducts is not observable under this system.

Data were also obtained for the reaction of the malononitrile carbanion with 4-NBF. Malononitrile is known to be considerably more acidic than the phenylacetonitriles with a value for K_1 of 600 dm^3 mol^{-1} [23]. Results are shown in table 2.22 and lead to a value for k_3 of 5.55×10^4 dm^3 mol^{-1} s^{-1}. The lower basicity of the malononitrile carbanion leads to a lower rate constant for attack on 4-NBF.

Table 2.22

$[CH_2(CN)_2]$/ mol dm^{-3}	[NaOMe]/ mol dm^{-3}	Average k_{obs}/s^{-1} at 340nm
2×10^{-4}	3×10^{-3}	30.23
3×10^{-4}	"	49.60
4×10^{-4}	"	66.69
5×10^{-4}	"	82.37
1×10^{-4}	5×10^{-3}	20.49
2×10^{-4}	"	39.77
3×10^{-4}	"	55.87
4×10^{-4}	"	72.80
1×10^{-4}	7×10^{-3}	29.03
2×10^{-4}	"	44.52
3×10^{-4}	"	63.09
4×10^{-4}	"	82.78

$[CH_2(CN)_2]$/ mol dm^{-3}	[NaOMe]/ mol dm^{-3}	Average k_{obs}/s^{-1} at 404nm
2×10^{-4}	3×10^{-3}	33.88
3×10^{-4}	"	49.45
4×10^{-4}	"	66.34
5×10^{-4}	"	82.45
1×10^{-4}	5×10^{-3}	20.49
2×10^{-4}	"	40.07
3×10^{-4}	"	55.61
4×10^{-4}	"	70.15
1×10^{-4}	7×10^{-3}	28.85
2×10^{-4}	"	44.00
3×10^{-4}	"	63.91
4×10^{-4}	"	82.78

[4-NBF]=2×10^{-5}M

2.4 Reaction with 4-nitrobenzofurazan

A slow reaction of the malononitrile anion with 4-nitrobenzofuroxan (4-NBF) produced a purple coloured adduct, which over time intensified and produced a marked change in the absorbance spectrum, (this will be discussed in more detail later). To examine if this reaction is peculiar to 4-NBF or if it occurs with related compounds, reactions with 4-nitrobenzofurazan (4-NBZ) have been studied. The kinetic data from this reaction can also be compared to data already collected for trends in behaviour of the phenylacetonitriles.

4-NBZ reacts with carbanions in the same way as 4-NBF, scheme 2.6.

Scheme 2.6

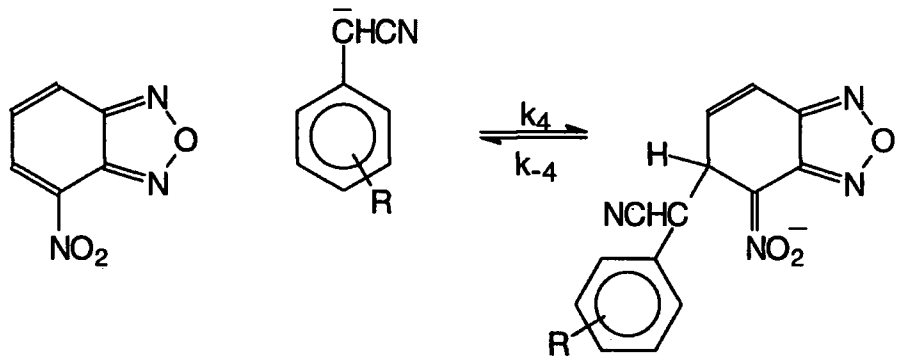

From spectrophotometric measurements both the methoxide and carbanion σ-adducts absorb at 330nm giving an increase in absorbance as the reaction proceeds, (the 4-NBZ itself absorbs at 320nm). As with 4-NBF the results are compatible with the equilibrium to give the adduct proceeding virtually to completion.Hence the forward reaction dominates the rate expression.

There is some interference from the reaction of 4-NBZ with methoxide ions in these reactions as with 4-NBF. It is known that the rate constant k_{MeO^-} has the value $1200dm^3\ mol^{-1}\ s^{-1}$.

The first order rate constant is given by

$$k_{obs} = k_{OMe}[MeO^-] + k_4[RC_6H_4CHCN^-] \qquad \text{equation 2.11}$$

Substituting for K_1, the equilibrium constant for $RC_6H_4CH_2CN$ with methoxide,

$$k_{obs} = k_{OMe}[MeO^-] + K_1\, k_4[RC_6H_4CH_2CN][MeO^-] \qquad \text{equation 2.12}$$

Experimental results are reported in tables 2.23 to 2.27 k_{obs} and are the average of at least ten values and were measured at 25°C using a Hi-Tech stopped-flow spectrophotometer. All concentrations are given after mixing. Graphs were plotted of k_{obs} versus the concentration of substituted phenylacetonitrile at constant methoxide concentration and as required by equation 2.12 these were linear with a positive intercept. The values of the slopes and intercepts were directly proportional to the methoxide concentration and thus calculation of k_4 was possible. These results are collected in table 2.28.

Table 2.23

$[CH_2(CN)_2]$ /mol dm^{-3}	[NaOMe] / mol dm^{-3}	Average k_{obs} /s^{-1} at 330nm
2×10^{-4}	3×10^{-3}	28.51
3×10^{-4}	"	38.95
4×10^{-4}	"	49.99
5×10^{-4}	"	58.19
2×10^{-4}	5×10^{-3}	30.10
3×10^{-4}	"	44.70
4×10^{-4}	"	54.55
5×10^{-4}	"	67.67
2×10^{-4}	7×10^{-3}	35.30
3×10^{-4}	"	48.21
4×10^{-4}	"	59.55
5×10^{-4}	"	71.24

[4-NBZ] = 2×10^{-5}M

Table 2.24

$[4\text{-}NO_2C_6H_4CH_2CN]$ /mol dm^{-3}	[NaOMe] / mol dm^{-3}	Average k_{obs} /s^{-1} at 330nm
2×10^{-4}	5×10^{-3}	20.62
3×10^{-4}	"	26.98
4×10^{-4}	"	34.81
5×10^{-4}	"	38.16
2×10^{-4}	7×10^{-3}	26.80
3×10^{-4}	"	36.14
4×10^{-4}	"	47.18
5×10^{-4}	"	53.00
2×10^{-4}	9×10^{-3}	41.34
3×10^{-4}	"	54.39
4×10^{-4}	"	67.06
5×10^{-4}	"	79.89

[4-NBZ] = 2×10^{-5}M

Table 2.25

$[C_6F_5CH_2CN]$ /mol dm^{-3}	[NaOMe] /mol dm^{-3}	Average k_{obs} /s^{-1} at 330nm
0.010	5×10^{-3}	19.23
0.015	"	23.06
0.020	"	27.65
0.025	"	31.29
0.010	7×10^{-3}	25.36
0.015	"	32.22
0.020	"	38.36
0.025	"	44.46
0.010	9×10^{-3}	33.90
0.015	"	43.31
0.020	"	52.15
0.030	"	60.25

[4-NBZ] = 2×10^{-5}M

Table 2.26

$[3,5-(CF_3)_2C_6H_4CH_2CN]$ /mol dm^{-3}	[NaOMe] /mol dm^{-3}	Average k_{obs} /s^{-1} at 330nm
0.025	5×10^{-3}	29.13
0.035	"	37.02
0.045	"	45.65
0.055	"	52.89
0.025	7×10^{-3}	39.52
0.035	"	52.67
0.045	"	61.77
0.055	"	72.82
0.025	9×10^{-3}	55.90
0.035	"	70.05
0.045	"	84.42
0.055	"	101.7

[4-NBZ] = 2×10^{-5}M

Table 2.27

[2-$NO_2C_6H_4CH_2CN$] /mol dm^{-3}	[NaOMe] /mol dm^{-3}	Average k_{obs} /s^{-1} at 330nm
2×10^{-4}	5×10^{-3}	12.97
3×10^{-4}	"	14.73
4×10^{-4}	"	18.37
5×10^{-4}	"	19.72
2×10^{-4}	7×10^{-3}	18.85
3×10^{-4}	"	20.03
4×10^{-4}	"	24.42
5×10^{-4}	"	26.30
2×10^{-4}	9×10^{-3}	26.80
3×10^{-4}	"	30.08
4×10^{-4}	"	34.79
5×10^{-4}	"	38.90

[4-NBZ] = 2×10^{-5}M

Table 2.28

R	K_1/dm^3 mol^{-1}	k_4/dm^3 mol^{-1} s^{-1}
4-NO_2	1.107	1.26×10^7
2-NO_2	0.175	2.38×10^7
3,5-$(CF_3)_2$	1.13×10^{-3}	1.48×10^8
2,3,4,5,6-F_5	4.43×10^{-4}	4.08×10^8
$CH_2(CN)_2$	600	1.87×10^5

It can be seen that as the ability of the substituent to stabilise the anion increases, the value of the rate constant k_4 decreases. This also occurs for 4-NBF and in fact the values obtained here are very similar to those for 4-NBF. Unfortunately, values of k_{-4} are too small to allow measurement.

2.5 Discussion

It is known[35] that rate constants for the carbon-carbon bond forming reaction between acetate enolate anions and quinolinium and acridinium cations have values in the range 10^5-4×10^7 dm^3 mol^{-1} s^{-1}. A value of 9×10^5 dm^3 mol^{-1} s^{-1} [36]has been reported for the carbon-carbon bond forming reaction of the neutral nucleophile 3,4-diaminothiophene with 4,6-dinitrobenzofuroxan. The values obtained in this study are even higher. Figure 2.4 shows a logarithmic plot of rate constants for the forward and reverse reactions for σ-adduct formation from 1,3,5-TNB versus the equilibrium constants K_2. Also in figure 2.4 are values of k_3 and k_4 for reaction of the phenylacetonitrile anions with 4-NBF and 4-NBZ respectively. Unfortunately it was not possible to measure values of the reverse rate constants here so values are plotted versus the corresponding K_2 values as abscissa.

Figure 2.4

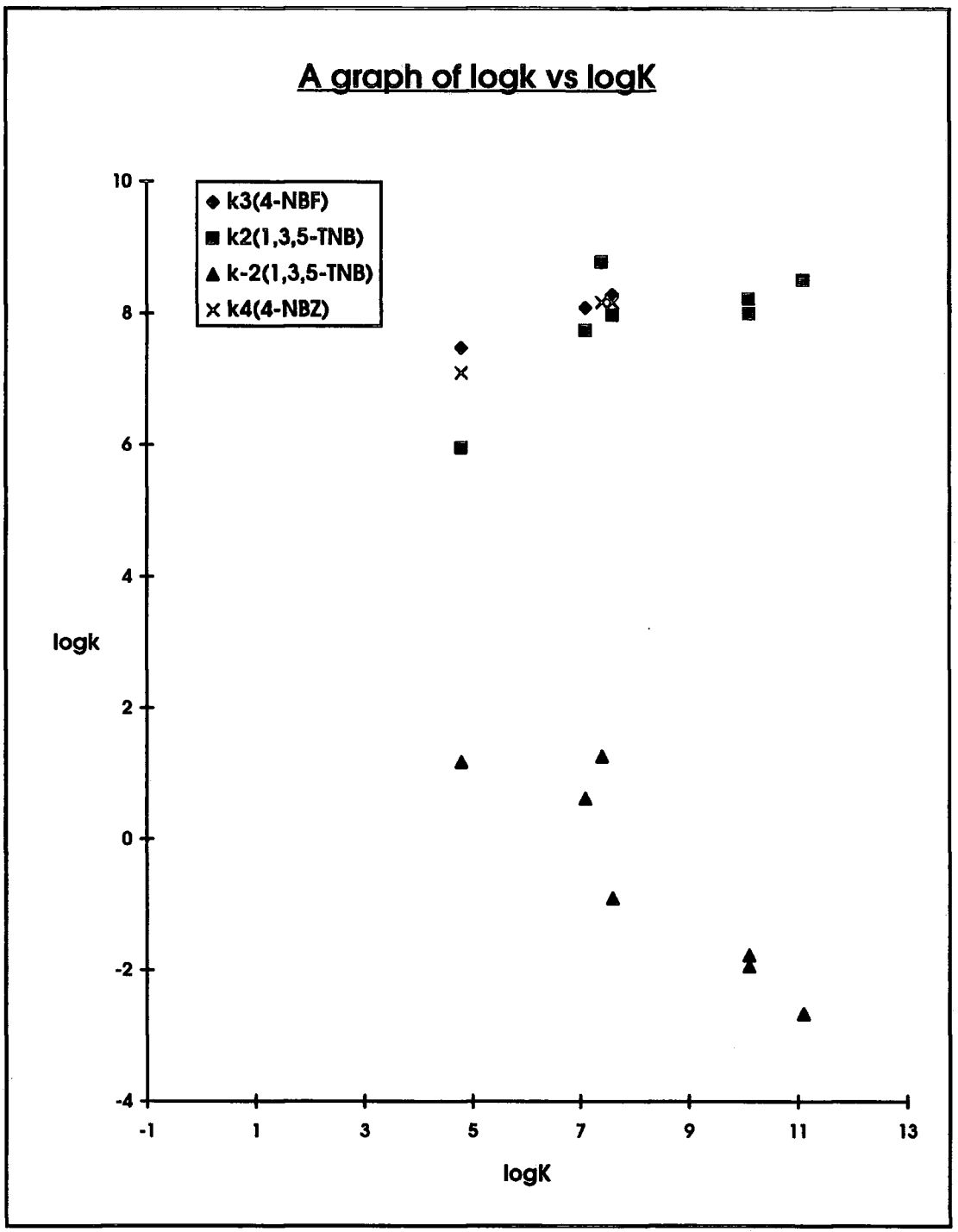

With increasing reactivity of the phenylacetonitrile anions values of the forward rate constant for reaction with 1,3,5-TNB approach a limit of 10^9 dm^3 mol^{-1} s^{-1} which indicates extremely rapid reaction but is slower than that expected for diffusion controlled reactions in methanol ($10^{10}dm^3$ mol^{-1} s^{-1}). Adducts formed by nucleophilic

attack on 4-NBF and 4-NBZ are known to be more stable than those formed by 1,3,5-TNB and correspondingly it was found that forward rate constants were larger for adduct formation with these nitroaromatics. However the rate constants approach a similar limit to those for 1,3,5-TNB.

The high reactivities of the phenylacetonitrile anions may reflect activation by the α-cyano group. Thus there is evidence that the cyano-group activates mainly by inductive effects rather than resonance effects so that in nitrile anions the negative charge is not strongly delocalized.

Intrinsic rate constants have been estimated for these reactions since it has been argued that low intrinsic rate constants are associated with lack of synchronisation between bond formation and the solvent and electronic reorganisation accompanying reaction, the PNS effect. By extrapolation of the plot in figure 4 it is possible to estimate a value for the intrinsic rate constant for the carbon-carbon bond forming reaction between phenylacetonitriles and 1,3,5-TNB. A value for $\log k_0$ of 2.5±0.5 is obtained.

Values of intrinsic rate constants for σ-adduct formation may be compared with those for proton transfer, table 2.29.

Table 2.29

	$\log k_0$	
	σ-adduct formation	Proton transfer[38]
$CH(CN_2)^-$	4.40[22]	7.00
$CH(CN)Ph^-$	2.50	4.00
$CH_2NO_2^-$	-0.74[22]	0.70

The carbanion order is the same in both types of reaction, reflecting variations in the PNS effect in the carbanions, however the values for σ-adduct formation are lower than those for proton transfer. This most likely reflects an additional PNS effect associated with the transfer of negative charge to the TNB ring to give delocalized anions. This is exemplified in reactions of the nitromethane carbanion. The low intrinsic reactivity for the proton transfer equilibrium may be associated with non-synchronisation of proton-proton transfer with the electronic and solvent reorganisation required in the carbanion.

In the σ-adduct forming reaction there are two PNS effects. One, as before, associated with electronic and solvent reorganisation in the carbanion due to the relocation of the negative charge from the oxygen to the carbon. However now there is a further PNS effect associated with electronic and solvent reorganisation in the trinitrobenzene ring, scheme 2.7.

Scheme 2.7

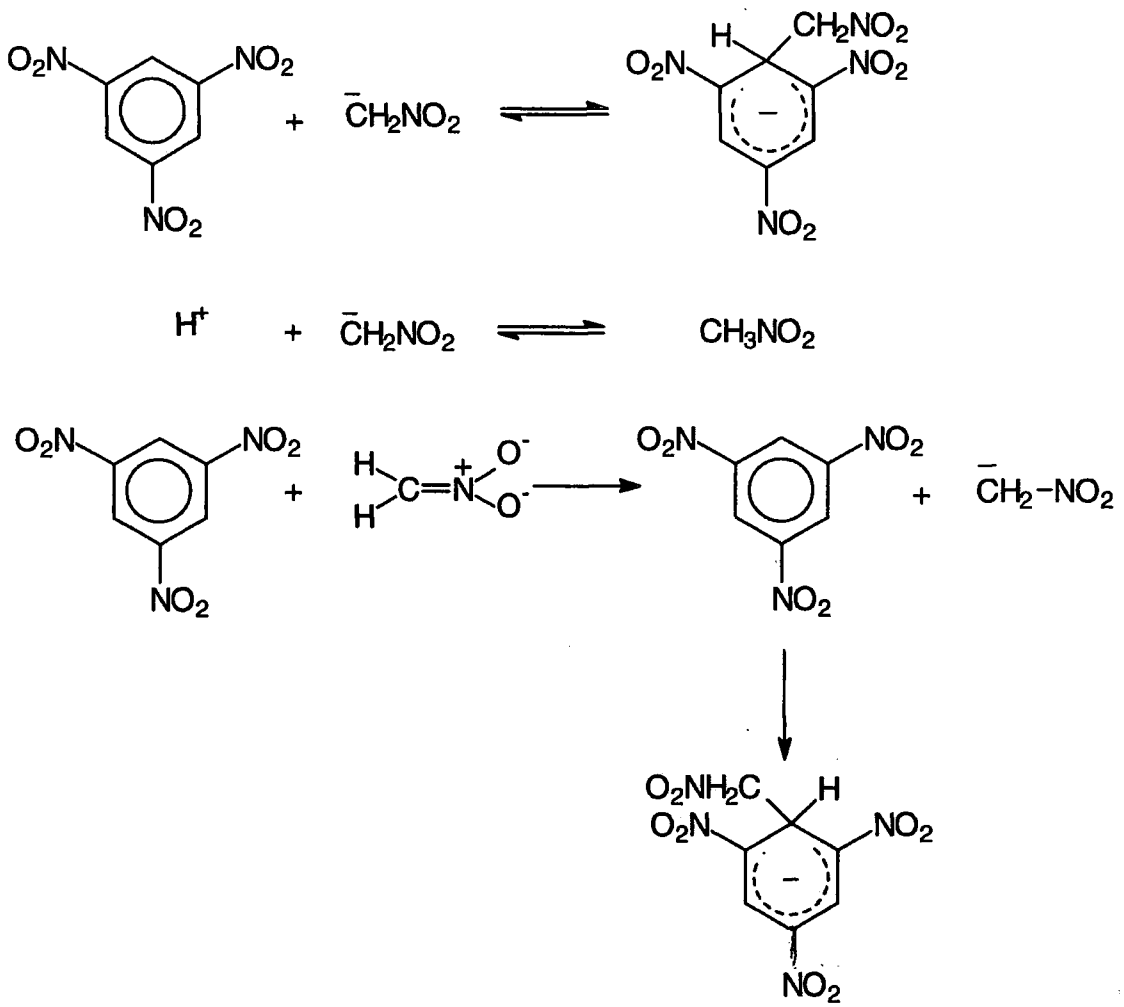

2.6 Reactions of carbanions with 1,3-dinitrobenzene

For the purpose of industrial applications of this project it is pertinent to consider less substituted nitroaromatics than those already studied. Thus reactions involving 1,3-dinitrobenzene, (1,3-DNB) have been investigated.

Theoretically, the reaction should proceed as in the case of the other nitroaromatics studied, producing a σ-complex with a competing methoxide reaction, as shown in scheme 2.8.

Scheme 2.8

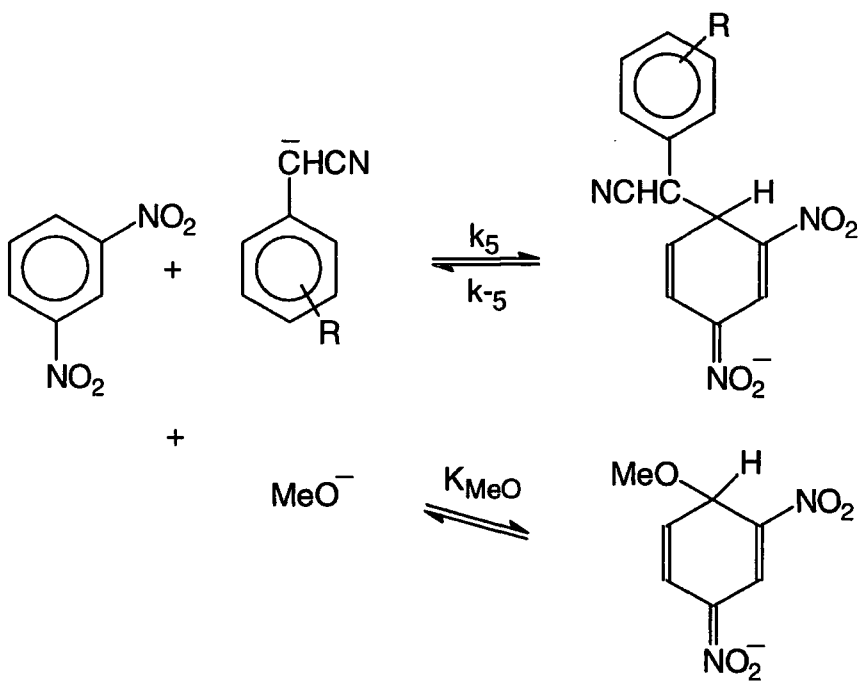

Thus $$k_{obs} = \frac{k_5[RC_6H_4CHCN^-]}{1 + K_{MeO^-}[MeO^-]} + k_{-5}$$

However, $$K_1 = \frac{[RC_6H_4CHCN^-]}{[MeO^-][RC_6H_4CH_2CN]}$$

Thus $$k_{obs} = \frac{k_5[RC_6H_4CH_2CN][MeO^-]}{1 + K_{MeO^-}[MeO^-]} + k_{-5}$$

Reactions involving phenylacetonitrile did not yield significant amounts of the σ-adduct. A test reaction using 1,3-DNB, NaOMe and $CH_2(CN)_2$ with 50/50 DMSO/MeOH (v/v) as a solvent was investigated, but this was unsuccessful. Various solvent compositions were then considered with more sucess as shown in table 2.30.

Table 2.30

[1,3-DNB]/ mol dm^{-3}	$[CH_2(CN)_2]$/ mol dm^{-3}	[NaOMe]/ mol dm^{-3}	%DMSO/ %MeOH, v/v	λ_{max}
1×10^{-4}	0.10	0.10	50/50	450nm
1×10^{-4}	0.10	0.10	70/30	545nm
1×10^{-4}	0.10	0.10	80/20	544nm
1×10^{-4}	0.10	0.10	90/10	545nm
1×10^{-4}	0.00	0.10	50/50	518nm
1×10^{-4}	0.00	0.10	70/30	518nm
1×10^{-4}	0.00	0.10	80/20	518nm
1×10^{-4}	0.00	0.10	90/10	518nm

Reaction of 1,3-DNB with methoxide alone in DMSO-methanol mixtures gives the methoxy adduct with λ_{max} 518nm. The presence of malononitrile gives, in solutions with greater than 70% DMSO, a purple species with λ_{max} 545nm. This is taken to be the adduct with the malononitrile anion. Kinetics were investigated using stopped-flow spectrophotometry.

Experimental results are reported in tables 2.31 and 2.32. Each k_{obs} is the average of at least ten values and was measured at 25°C using a Hi-Tech stopped-flow spectrophotometer. All concentrations are given after mixing.

Table 2.31

The solvent is 80/20 DMSO/MeOH, [1,3-DNB] = 5×10^{-6} mol dm^{-3}.

$[CH_2(CN)_2]$/ mol dm^{-3}	[NaOMe]/ mol dm^{-3}	k_{obs}/s^{-1} at 550nm
4.0×10^{-3}	0.20	1.299
6.0×10^{-3}	"	1.692
7.5×10^{-3}	"	1.790
8.0×10^{-3}	"	1.913
1.0×10^{-2}	"	2.171
4.0×10^{-3}	0.30	1.715
7.5×10^{-3}	"	2.240
8.0×10^{-3}	"	2.945
1.0×10^{-2}	"	3.074
4.0×10^{-3}	0.40	0.960
6.0×10^{-3}	"	1.733
7.5×10^{-3}	"	2.089
1.0×10^{-2}	"	2.940

Table 2.32

The solvent is 90/10 DMSO/MeOH, [1,3-DNB] = 1×10^{-5} mol dm^{-3}.

$[CH_2(CN)_2]$/ mol dm^{-3}	[NaOMe]/ mol dm^{-3}	k_{obs}/s^{-1} at 550nm
4.0×10^{-3}	0.05	0.088
6.0×10^{-3}	"	0.123
8.0×10^{-3}	"	0.213
1.0×10^{-2}	"	0.304
4.0×10^{-3}	0.10	0.038
6.0×10^{-3}	"	0.092
8.0×10^{-3}	"	0.110
1.0×10^{-2}	"	0.213

In order to elucidate rate constants k_5 and k_{-5}, it is necessary to calculate the value of the equilibrium constant for reaction of 1,3-DNB with sodium methoxide in the various solvent systems. Measurements were made using a UV-VIS spectrophotometer at 523nm, which is close to λ_{max} for the methoxy σ-adduct of 1,3-DNB. Results are shown in tables 2.33 and 2.34.

Table 2.33

The solvent is 80/20 DMSO/MeOH.

[NaOMe]/ mol dm^{-3}	[1,3-DNB]/ mol dm^{-3}	Abs at 523nm	K/ dm^3 mol^{-1}
0.10	1×10^{-4}	0.560	1.63
0.15	"	1.283	3.15
0.20	"	1.608	3.37
0.30	"	1.877	2.95
0.40	"	2.018	2.55
0.50	"	2.176	2.39
0.88	"	$3.995=Abs_{\infty}$	—

K is calculated as $\frac{Abs}{Abs_{\infty} - Abs} \times \frac{1}{[NaOMe]}$

Average K = 2.88 dm^3 mol^{-1}.

Table 2.34

The solvent is 90/10 DMSO/MeOH.

[NaOMe]/ mol dm^{-3}	[1,3-DNB]/ mol dm^{-3}	Abs at 523nm	K/ dm^3 mol^{-1}
0.015	1×10^{-4}	0.551	66.9
0.025	"	0.686	66.3
0.035	"	0.778	69.0
0.050	"	0.855	69.7
0.500	"	$1.10=Abs_{\infty}$	—

K is calculated as $\frac{Abs}{Abs_{\infty} - Abs} \times \frac{1}{[NaOMe]}$

Average K = 68.0 dm^3 mol^{-1}.

Plots are shown of k_{obs} *versus* malononitrile concentration at constant methoxide concentration may now be made. The results for 80/20 DMSO/MeOH do not give very good straight line graphs, figure 2.5, however results for 90/10 DMSO/MeOH are good, as shown in figure 2.6.

Figure 2.5

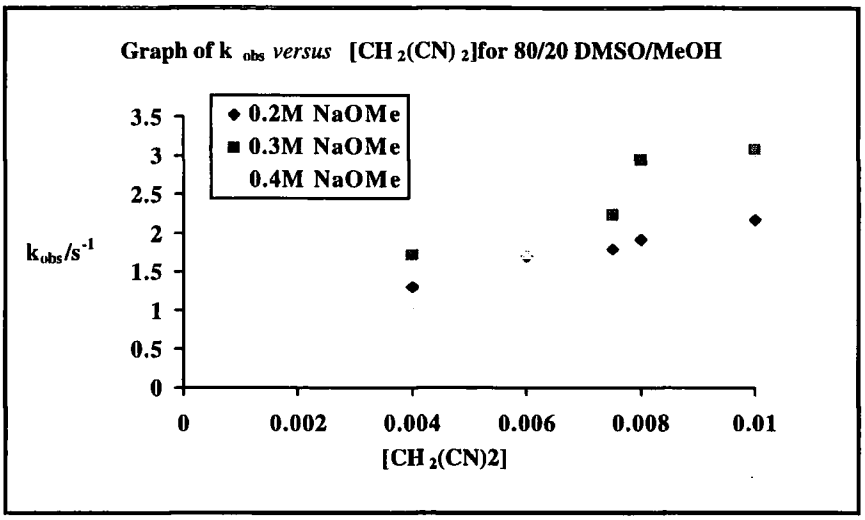

Figure 2.6

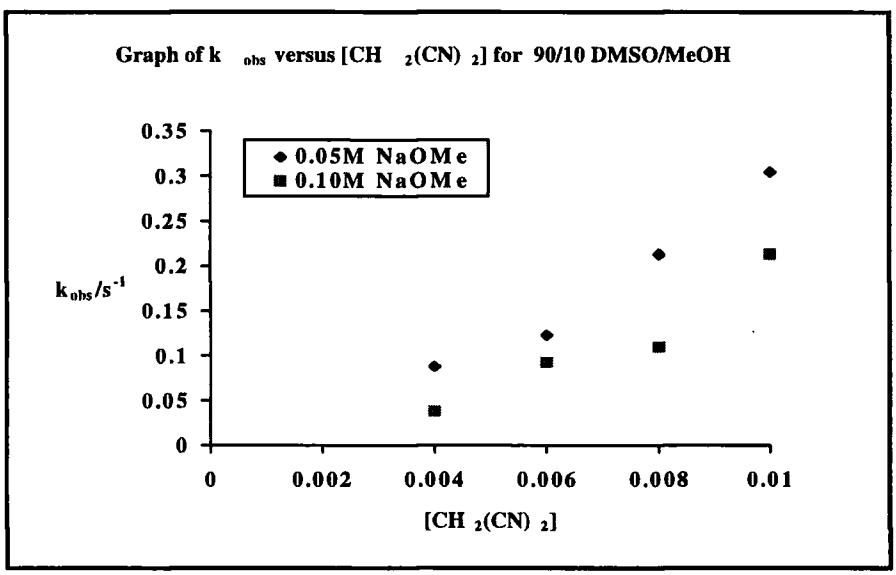

80/20 DMSO/MeOH

[NaOMe]/mol dm^{-3}	k_5K_1/dm^3 mol^{-1} s^{-1}	k_{-5}/s^{-1}
0.20	1040	0.80
0.30	1400	0.80
0.40	1210	0.70

90/10 DMSO/MeOH

[NaOMe]/mol dm^{-3}	k_5K_1/dm^3 mol^{-1} s^{-1}	k_{-5}/s^{-1}
0.05	2.16×10^3	n/a
0.10	1.40×10^3	n/a

The slopes of these plots have the value $\frac{k_5K_1[MeO^-]}{1+K[MeO^-]}$. Since the values of K have been determined at 80% and 90% DMSO, the values of k_5K_1 may be calculated. The intercepts yield values of k_{-5}. At 80% DMSO the value obtained is 0.80 s^{-1} while at 90% DMSO this value has decreased to a value close to zero.

$$CH_2(CN)_2 + MeO^- \underset{}{\overset{K_1}{\rightleftharpoons}} CH(CN)_2^- + MeOH$$

Values of k_5K_1 increase with increasing DMSO content of the solvent, while values of k_{-5} decrease. Hence the value of K_5K_1 ($\equiv k_5K_1/ k_{-5}$) will increase with increasing proportion of DMSO. It is known that DMSO will poorly solvate small and less poorly solvate large polarisable anions while methanol will solvate small localised anions, such as methoxide. Thus values of both K_5 and K_1 might be expected to increase with DMSO content.

2.7 Reactions of nitroalkanes with 1,3-dinitrobenzene

Nitroalkane anions react with 1,3,5-TNB to produce σ-adducts and therefore it was hoped that they would also undergo reaction with 1,3-DNB, as shown in scheme 2.9.

Scheme 2.9

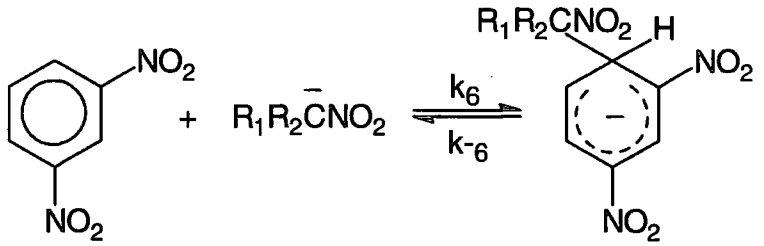

Spectra were therefore taken, using a u.v.-vis spectrophotometer, to obtain the λ_{max} values for three nitroalkanes with methanol as the solvent.The results are shown in table 2.35.

Table 2.35

$R_1R_2CHNO_2$	$[R_1R_2CHNO_2]$/ mol dm^{-3}	[NaOMe]/ mol dm^{-3}	[1,3-DNB]/ mol dm^{-3}	λ_{max}/nm
CH_3NO_2	0.010	—	—	275
	0.010	5×10^{-3}	2×10^{-3}	no reaction
	0.001	5×10^{-3}	2×10^{-3}	no reaction
$CH_3CH_2NO_2$	0.010	—	—	275
	0.010	5×10^{-3}	2×10^{-3}	no reaction
	0.001	5×10^{-3}	2×10^{-3}	no reaction
$1\text{-}CH_3(CH_2)_2NO_2$	0.010	—	—	276
	0.010	5×10^{-3}	2×10^{-3}	no reaction
	0.001	5×10^{-3}	2×10^{-3}	no reaction

No reaction occurs with 1,3-DNB, however reaction does occur with 1,3,5-TNB and also with 4,6-dinitrobenzofuroxan, therefore the reaction of nitroalkanes with 4-NBF,

scheme 2.10, was investigated. Results were obtained on a u.v.-vis spectrophotometer with methanol as the solvent and are shown in table 2.36.

Scheme 2.10

Table 2.36

$R_1R_2CHNO_2$	$[R_1R_2CHNO_2]$/ mol dm^{-3}	[NaOMe]/ mol dm^{-3}	[4-NBF]/ mol dm^{-3}	λ_{max}/ nm
CH_3NO_2	0.01	5×10^{-3}	1×10^{-4}	337
	0.10	"	"	336
$CH_3CH_2NO_2$	0.01	"	"	332
	0.10	"	"	325
1-$CH_3(CH_2)_2NO_2$	0.01	"	"	338
	0.10	"	"	333

Reaction does occur with nitroalkane anions and 4-NBF. The uv absorption spectra show a shift from 403nm, the value for 4-NBF to a wavelength of *circa* 330nm consistent with σ-adduct formation. Stopped flow investigation of this reaction was not possible, however various NMR studies of this system were made and will be reported later in this thesis.

Chapter 3

The slow reaction of 4-NBF and 4-NBZ with carbanions

3.1 Kinetic and spectroscopic studies

The reaction of 4-NBF and 4-NBZ with carbanions from malononitrile and from phenylacetonitriles resulted in rapid σ-adduct formation. Results were reported in chapter 2. The absorption maxima of the σ-adducts were at 330-340nm. In view of literature data it seems possible that the initial reaction involves attack at the 5-position. However equilibration with the adducts formed at the 7-position seems likely. Thus the initial fast reactions can be represented by scheme 3.1. It is likely that the uv spectra of the 5-adducts and 7-adducts will be similar. Here their equilibration will not be detectable by spectrophotometry.

Scheme 3.1

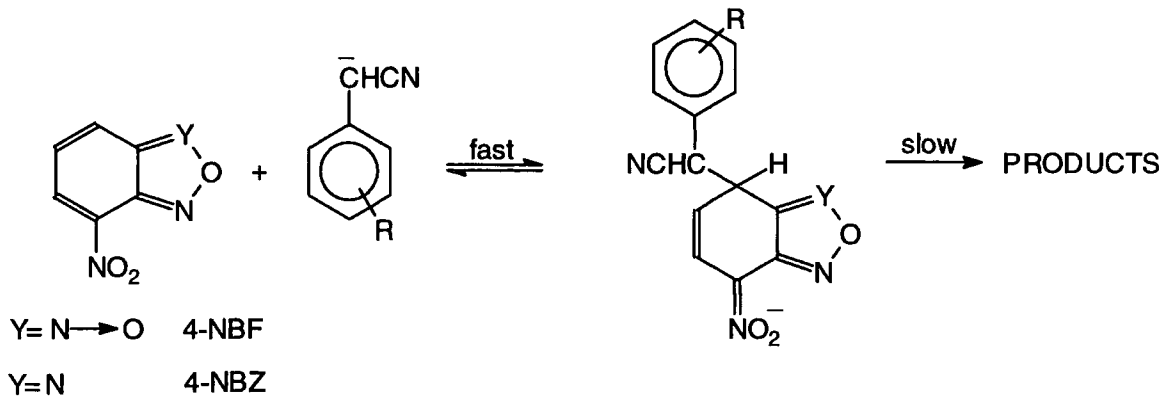

Y= N→O 4-NBF

Y=N 4-NBZ

However further dramatic spectral changes were observed on a slow time scale. These generally resulted in the formation of species absorbing internally in the visible region. Spectra are shown in figures 3.1 and 3.2 and absorption maxima are recorded in table 3.1.

Table 3.1

RCH2CN	λ_{max} 4-NBF	λ_{max} 4-NBZ
$CH_2(CN)_2$	579nm	573nm
$C_6F_5CH_2CN$	403nm	313nm
$4\text{-}NO_2C_6H_4CH_2CN$	525nm	527nm
$2\text{-}NO_2C_6H_4CH_2CN$	416nm	-

Figure 3.1

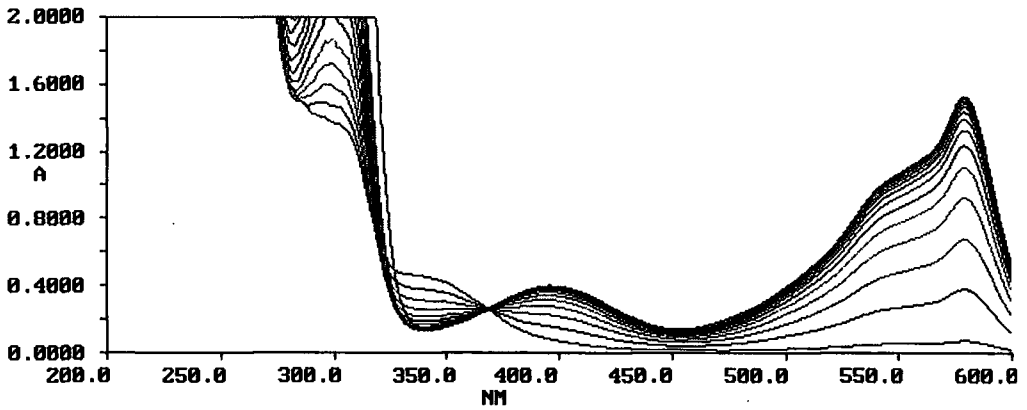

Slow reaction of $CH_2(CN)_2$, 4-NBF and NaOMe, showing formation of an absorbance maximum at 579nm over 30 minutes.

Figure 3.2

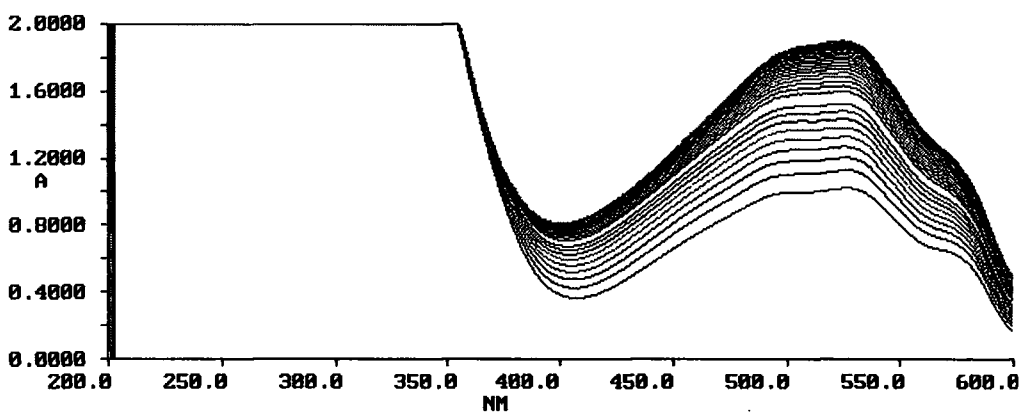

Slow reaction of $4\text{-}NO_2C_6H_4CH_2CN$, 4-NBZ and NaOMe, showing formation of an absorbance maximum at 527nm over 30 minutes.

In order to investigate this further, the rate constants of the reactions were calculated under varying concentrations of methoxide ion and carbanion. Measurements were made at 25°C using a u.v.-vis spectrophotometer.

Results are shown in tables 3.2 to 3.8 and a typical trace is shown in figure 3.3.

Table 3.2

[4-NBF]/ mol dm^{-3}	[NaOMe]/ mol dm^{-3}	$[CH_2(CN)_2]$/ mol dm^{-3}	kobs/s^{-1} at 519nm
4×10^{-5}	4×10^{-3}	0.04	9.80×10^{-3}
"	3×10^{-3}	0.04	9.80×10^{-3}
"	2×10^{-3}	0.04	11.3×10^{-3}
"	1×10^{-3}	0.04	9.60×10^{-3}
"	4×10^{-3}	0.03	11.8×10^{-3}
"	4×10^{-3}	0.02	11.8×10^{-3}
"	4×10^{-3}	0.01	12.0×10^{-3}
4×10^{-5} a	1×10^{-3}	0.01	6.70×10^{-3}
3×10^{-5} a	1×10^{-3}	0.01	6.22×10^{-3}
2×10^{-5} a	1×10^{-3}	0.01	6.37×10^{-3}
1×10^{-5} a	1×10^{-3}	0.01	6.51×10^{-3}

a Measurements made on a separate occasion

Table 3.3

[4-NBF]/ mol dm^{-3}	[NaOMe]/ mol dm^{-3}	[4-$NO_2C_6H_4CH_2CN$]/ mol dm^{-3}	kobs/s^{-1} at 525nm
4×10^{-5}	4×10^{-3}	8×10^{-3}	2.62×10^{-3}
"	3×10^{-3}	8×10^{-3}	2.75×10^{-3}
"	2×10^{-3}	8×10^{-3}	2.97×10^{-3}
"	1×10^{-3}	8×10^{-3}	2.83×10^{-3}
"	4×10^{-3}	6×10^{-3}	2.74×10^{-3}
"	4×10^{-3}	4×10^{-3}	3.01×10^{-3}
"	4×10^{-3}	2×10^{-3}	3.45×10^{-3}
"	1×10^{-3}	8×10^{-3}	2.09×10^{-3}
3×10^{-5}	1×10^{-3}	8×10^{-3}	-
2×10^{-5}	1×10^{-3}	8×10^{-3}	1.97×10^{-3}
1×10^{-5}	1×10^{-3}	8×10^{-3}	2.05×10^{-3}

Table 3.4

[4-NBF]/ mol dm^{-3}	[NaOMe]/ mol dm^{-3}	[2-$NO_2C_6H_4CH_2CN$]/ mol dm^{-3}	kobs/s^{-1} 416nm
4×10^{-5}	4×10^{-3}	8×10^{-3}	2.53×10^{-3}
"	3×10^{-3}	8×10^{-3}	3.42×10^{-3}
"	2×10^{-3}	8×10^{-3}	3.15×10^{-3}
"	1×10^{-3}	8×10^{-3}	2.54×10^{-3}
"	4×10^{-3}	6×10^{-3}	2.75×10^{-3}
"	4×10^{-3}	4×10^{-3}	2.41×10^{-3}
"	4×10^{-3}	2×10^{-3}	2.25×10^{-3}

Table 3.5

[4-NBF]/ mol dm^{-3}	[NaOMe]/ mol dm^{-3}	$[C_6F_5CH_2CN]$/ mol dm^{-3}	kobs/s^{-1} at 403nm
4×10^{-5}	4×10^{-3}	8×10^{-3}	1.58×10^{-3}
"	3×10^{-3}	8×10^{-3}	1.30×10^{-3}
"	2×10^{-3}	8×10^{-3}	1.22×10^{-3}
"	1×10^{-3}	8×10^{-3}	1.64×10^{-3}
"	4×10^{-3}	6×10^{-3}	1.58×10^{-3}
"	4×10^{-3}	4×10^{-3}	1.35×10^{-3}
"	4×10^{-3}	2×10^{-3}	1.53×10^{-3}
"	1×10^{-3}	8×10^{-3}	8.60×10^{-4}
3	1×10^{-3}	8×10^{-3}	8.48×10^{-4}
2	1×10^{-3}	8×10^{-3}	8.24×10^{-4}
1	1×10^{-3}	8×10^{-3}	8.15×10^{-4}

Table 3.6

[4-NBZ]/ mol dm^{-3}	[NaOMe]/ mol dm^{-3}	$[CH_2(CN)_2]$/ mol dm^{-3}	kobs/s^{-1} at 573nm
4×10^{-5}	4×10^{-3}	0.04	3.15×10^{-3}
"	3×10^{-3}	0.04	3.41×10^{-3}
"	2×10^{-3}	0.04	3.63×10^{-3}
"	1×10^{-3}	0.04	3.96×10^{-3}
"	4×10^{-3}	0.03	3.00×10^{-3}
"	4×10^{-3}	0.02	3.58×10^{-3}
"	4×10^{-3}	0.01	3.26×10^{-3}

Table 3.7

[4-NBZ]/ mol dm^{-3}	[NaOMe]/ mol dm^{-3}	[4-$NO_2C_6H_4CH_2CN$]/ mol dm^{-3}	kobs/s^{-1} at 527nm
4×10^{-5}	4×10^{-3}	8×10^{-3}	5.04×10^{-4}
"	3×10^{-3}	8×10^{-3}	3.84×10^{-4}
"	2×10^{-3}	8×10^{-3}	4.16×10^{-4}
"	1×10^{-3}	8×10^{-3}	3.96×10^{-4}
"	4×10^{-3}	6×10^{-3}	5.55×10^{-4}
"	4×10^{-3}	4×10^{-3}	5.32×10^{-4}
"	4×10^{-3}	2×10^{-3}	5.21×10^{-4}
"	1×10^{-3}	8×10^{-3}	5.12×10^{-4}
3×10^{-5}	1×10^{-3}	8×10^{-3}	5.12×10^{-4}
2×10^{-5}	1×10^{-3}	8×10^{-3}	4.89×10^{-4}
1×10^{-5}	1×10^{-3}	8×10^{-3}	5.26×10^{-4}

Table 3.8

[4-NBZ]/ mol dm^{-3}	[NaOMe]/ mol dm^{-3}	[$C_6F_5CH_2CN$]/ mol dm^{-3}	kobs/s^{-1} at 313nm
4×10^{-5}	1×10^{-3}	8×10^{-3}	3.02×10^{-4}
3×10^{-5}	1×10^{-3}	8×10^{-3}	3.04×10^{-4}
2×10^{-5}	1×10^{-3}	8×10^{-3}	2.95×10^{-4}
1×10^{-5}	1×10^{-3}	8×10^{-3}	2.63×10^{-4}

Figure 3.3

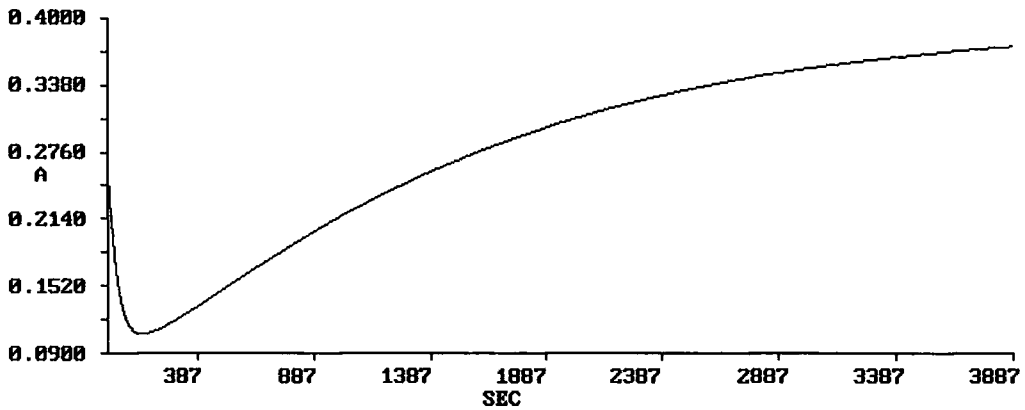

Absorbance against time plot with $[C_6F_5CH_2CN] = 8\times10^{-3}M$,[NaOMe] = $1\times10^{-3}M$ and [4-NBF] = $4\times10^{-5}M$ at 313nm.

From the results it can be seen that there is little variation in rate constant with varying concentration of either the nitroaromatic, sodium methoxide or carbon nucleophile. Thus the second slow reaction must have a rate determining step not involving any of these species. It has been suggested however, that due to the spectral shapes of the absorbance versus time plots (figure 3.3) that we are in fact observing an A→B→C type of reaction which would involve more complex data manipulation to obtain the rate constants.

It is thought that the coloured species formed by this slow reaction may be unstable in the presence of acid and since this species is possibly an anion the effect of acid may produce a neutral product. The nitroaromatic, and carbanion were reacted and the slow reaction allowed to occur before addition of acid to 2ml of the coloured species formed. Results are shown in tables 3.9 and 3.10.

Table3.9

RCH_2CN	[4-NBF]/ mol dm^{-3}	[NaOMe] / mol dm^{-3}	[RCH_2CN]/ mol dm^{-3}	Volume of acid added (0.1M HCl)	λ_{max}/ nm
$CH_2(CN)_2$	4×10^{-5}	1×10^{-3}	1×10^{-2}	none	579
	"	"	"	0.02ml	579
	"	"	"	further 0.02ml	579
	"	"	"	further 0.04ml	579
$4\text{-}NO_2C_6H_4CH_2CN$	4×10^{-5}	1×10^{-3}	1×10^{-2}	none	494
	"	"	"	0.02ml	476
	"	"	"	further 0.02ml	439
	"	"	"	further 0.04ml	429
$C_6F_5CH_2CN$	4×10^{-5}	1×10^{-3}	1×10^{-2}	none	339
	"	"	"	0.02ml	394
	"	"	"	further 0.02ml	402
	"	"	"	further 0.04ml	397

Table 3.10

RCH_2CN	[4-NBZ]/ mol dm^{-3}	[NaOMe]/ mol dm^{-3}	[RCH_2CN]/ mol dm^{-3}	Volume of acid added (0.1M HCl)	λ_{max}/ nm
$CH_2(CN)_2$	4×10^{-5}	1×10^{-3}	1×10^{-2}	none	533
	"	"	"	0.02ml	532
	"	"	"	further 0.02ml	539
	"	"	"	further 0.04ml	526
$4\text{-}NO_2C_6H_4CH_2CN$	4×10^{-5}	1×10^{-3}	1×10^{-2}	none	526
	"	"	"	0.02ml	546
	"	"	"	further 0.02ml	545
	"	"	"	further 0.04ml	546
$C_6F_5CH_2CN$	4×10^{-5}	1×10^{-3}	1×10^{-2}	none	336
	"	"	"	0.02ml	317
	"	"	"	further 0.02ml	318
	"	"	"	further 0.04ml	318

From these results it can be seen that acid has no siginificant effect on the coloured species formed in the slow reaction, except in the case of the pentafluorophenylacetonitrile. Here there is a small change in λ_{max}, however this may be due to destruction of the reactant species.

To confirm that the species formed using the more concentrated solutions required for NMR studies are the same as those produced under the more dilute conditions used for spectrophotometric studies, concentrated species were produces and then diluted. The spectra obtained from these solutions was then compared with those obtained form previous spectrophotometric studies. Results are shown in tables 3.11 and 3.12 below.

Table 3.11

All concentrations are shown before dilution.

[4-NBF]/ mol dm^{-3}	$[CH_2(CN)_2]$/ mol dm^{-3}	[NaOMe]/ mol dm^{-3}	Dilution factor
1×10^{-3}	1×10^{-2}	2×10^{-3}	1:20
5×10^{-3}	"	1×10^{-2}	1:100
"	8×10^{-3}	"	"
"	6×10^{-3}	"	"
"	1×10^{-2}	8×10^{-3}	"
"	"	6×10^{-3}	"
"	"	5×10^{-3}	"
"	"	3×10^{-3}	"
"	5×10^{-3}	5×10^{-3}	"
7.5×10^{-3}	7.5×10^{-3}	7.5×10^{-3}	1:200

Table 3.12

All concentrations are shown after dilution

[4-NBF]/ mol dm^{-3}	$[CH_2(CN)_2]$/ mol dm^{-3}	[NaOMe]/ mol dm^{-3}	Absorbance at 579nm
5×10^{-5}	5×10^{-4}	1×10^{-4}	0.823
"	1×10^{-4}	"	1.384
"	8×10^{-5}	"	1.370
"	6×10^{-5}	"	1.550
"	1×10^{-4}	8×10^{-5}	1.884
"	"	6×10^{-5}	2.093
"	"	5×10^{-5}	1.710
"	"	3×10^{-5}	0.978
"	5×10^{-5}	5×10^{-5}	1.703
3.75×10^{-5}	3.75×10^{-5}	3.75×10^{-5}	1.953

Standard dilute solution for comparison

[4-NBF]/ mol dm^{-3}	$[CH_2(CN)_2]$/ mol dm^{-3}	[NaOMe]/ mol dm^{-3}	Absorbance at 579nm
4×10^{-5}	4×10^{-2}	4×10^{-3}	1.540

There is no change in spectral shape in the diluted solutions compared to the standard solution, thus dilution does not affect the colour forming process. The projected absorbance for the diluted solutions calculated from the standard solution is 1.93 and almost all the diluted solutions give absorbances close to this value. Thus NMR studies using more concentrated solutions may be used in the further investigation of the product of the slow reaction.

3.2 Size exclusion chromatography and h.p.l.c.

In a further attempt to identify the products of the second slow reaction the techniques of size exclusion chromatography and h.p.l.c. were employed.

Size exclusion chromatography discriminates by molecular size, larger molecules having a shorter retention time as smaller ones are held in cavities on the column. This is a good method for identification of large species such as the σ-complexes produced in this reaction. The following solutions were prepared and run at 410nm and 240nm.

Table 3.13

Sample	Solution	Solvent
A	0.05%, w/v, 4-NBF, NaOMe + $4\text{-}NO_2C_6H_4CH_2CN$	50/50, v/v THF/MeOH
B	0.05%, w/v 4-NBF + MeOH	"
C	0.05%, w/v, $4\text{-}NO_2C_6H_4CH_2CN$	"
D	0.05%, w/v, 4-NBF, NaOMe + $CH_2(CN)_2$	"
E	0.05%, w/v, $CH_2(CN)_2$	"

Solutions B, C, and E are standards to test for parent peaks in the product spectra, however there was no evidence of species from solution B in either product spectra. Peaks due to solutions A and E were seen, but the product spectra were too complex to gain any meaningful information.
Thus h.p.l.c. was utilised to analyse the product solutions.

Standard h.p.l.c. methods were used, the wavelengths used were again 410nm and 240nm and measurements were made at 40°C. The eluent profile used is show in figure 3.4. The solutions used are shown in table 3.14.

Figure 3.4

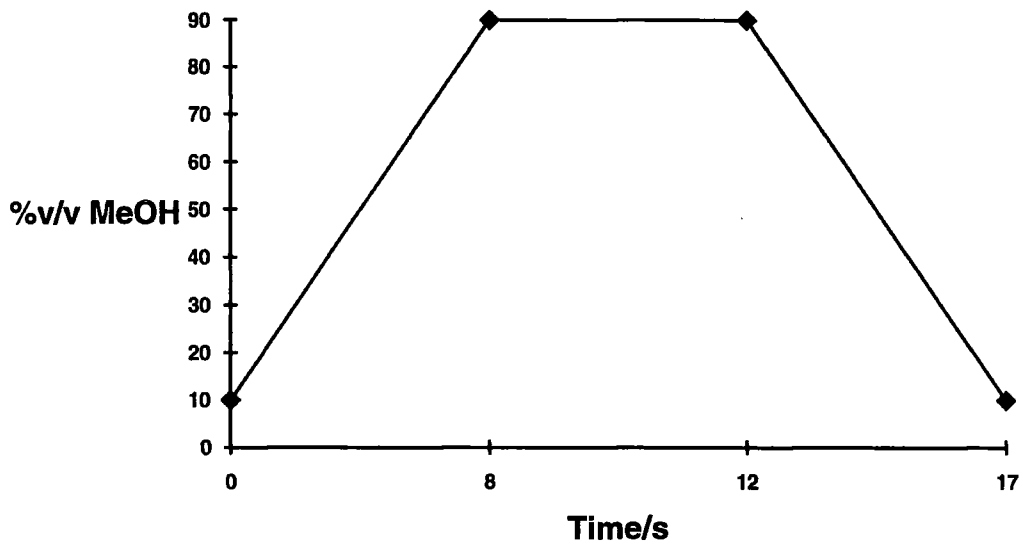

Table 3.14

Sample	Solution	Solvent
1	0.05%, w/v, 4-NBF, NaOMe + 4-$NO_2C_6H_4CH_2CN$	50/50, v/v MeOH/H_2O
2	0.05%, w/v 4-NBF + NaOMe	"
3	0.05%, w/v, 4-$NO_2C_6H_4CH_2CN$	"
4	0.05%, w/v, 4-NBF, NaOMe + $CH_2(CN)_2$	"
5	0.05%, w/v, $CH_2(CN)_2$+ NaOMe	
6	0.05%, w/v, 4-NBF	"

Sample 1

A very complex spectrum is obtained with no indication of any residual 4-NBF or 4-4-$NO_2C_6H_4CH_2CN$ present, there are however peaks due to species from solution 2. Four main product peaks are observed at both wavelengths, occuring at around 8 and 10 seconds, respectively, and all absorb strongly in the aromatic region, at 240nm.

Sample 2

Again a very complex product spectra was obtained, and peaks due to species from solution 2 were again observed.

From these results it is impossible to draw any definite conclusions as to the identity of any of the product species thus other techniques must be investigated.

3.3 ESR studies

Another possibility for the slow reaction is that a radical mechanism is operating. To investigate this theory ESR studies were made to ascertain if any radical species are present in the reaction mixtures.

The following solutions were made up to produce the purple coloured species and were then tested for radical species.

[4-NBF]/ mol dm^{-3}	[NaOMe]/ mol dm^{-3}	$[CH_2(CN)_2]$/ mol dm^{-3}	Scan time after mixing	Result
4×10^{-5}	1×10^{-3}	1×10^{-2}	10-90mins	No ESR spectrum
1.2×10^{-4}	2.5×10^{-3}	3×10^{-2}	5 mins	No ESR spectrum
4×10^{-5}	4×10^{-3}	8×10^{-3}	15 mins	No ESR spectrum

[4-NBZ]/ mol dm^{-3}	[NaOMe]/ mol dm^{-3}	$[CH_2(CN)_2]$/ mol dm^{-3}	Scan time after mixing	Result
8×10^{-5}	4×10^{-3}	4×10^{-2}	10-30mins	No ESR spectrum

Thus it may be concluded that no radicals are present in the subsequent slow reaction. Representative spectra are shown in figure 3.5.

Figure 3.5

Spectrum 1

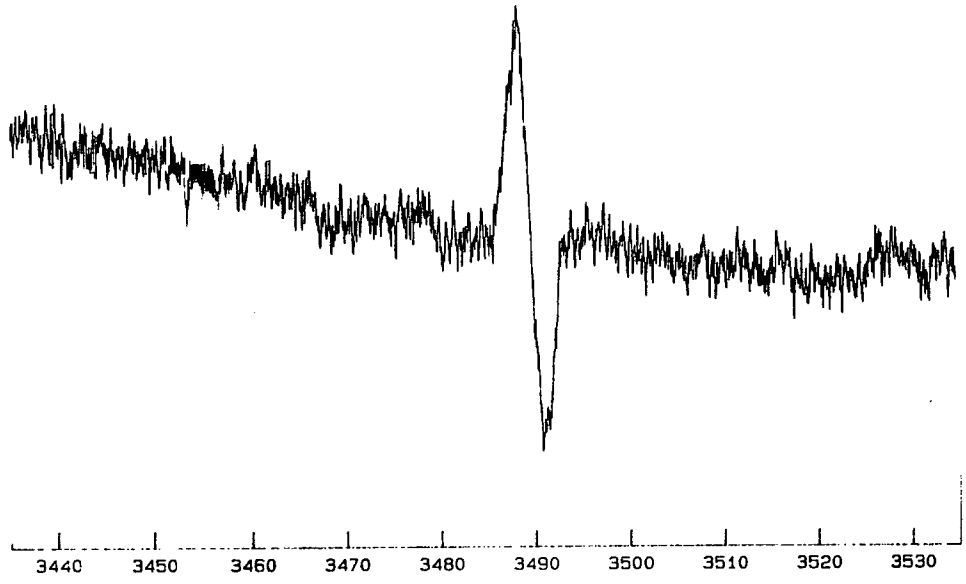

ESR spectrum of 1.2×10^{-4}M 4-NBF, 2.5×10^{-3}M NaOMe and 3×10^{-2}M $CH_2(CN)_2$ after 5 minutes

Spectrum 2

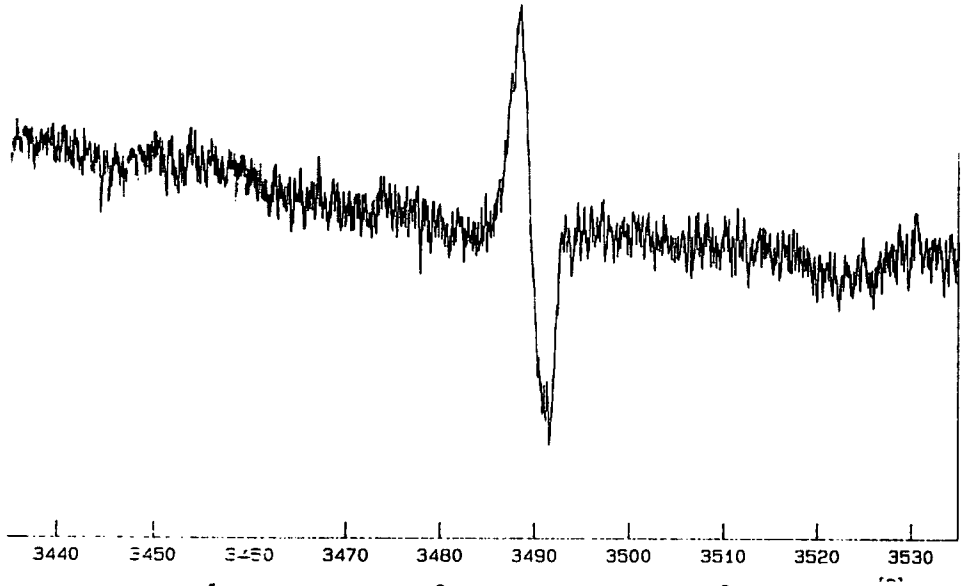

ESR spectrum of 8×10^{-5}M 4-NBZ, 4×10^{-3}M NaOMe and 4×10^{-2}M $CH_2(CN)_2$ after 15 minutes.

3.4 NMR studies

Several attempts were made to study the products of the slow reaction by NMR spectroscopy. Spectra recorded on a 200MHz NMR machine were extremely complex and unable to be resolved, thus spectra were recorded using a 400 MHz machine.
A solution of 0.01M 4-NBF and 0.01M $CH_2(CN)_2$ was produced in CD_3OD and an initial spectrum taken. This spectrum showed bands at δ = 8.53, 7.95 and 7.47 ppm due to the ring hydrogens of the 4-NBF. A band was observed at δ = 3.35 ppm due to hydrogen in residual CHD_2 in the solvent. A strong band was observed at δ = 4.90 ppm due to hydroxyl protons from adventitious water and residual CD_3OH. Interestingly no separate band was observed due to $CH_2(CN)_2$ indicating that the hydrogen had suffered exchange with deuterons in the solvent. CD_3ONa was then added, the solution turned purple immediately, and further spectra were taken at 5, 30 and 60 minutes after this addition. Spectra are shown in figure 3.6.

Figure 3.6

Spectrum 1

5mins

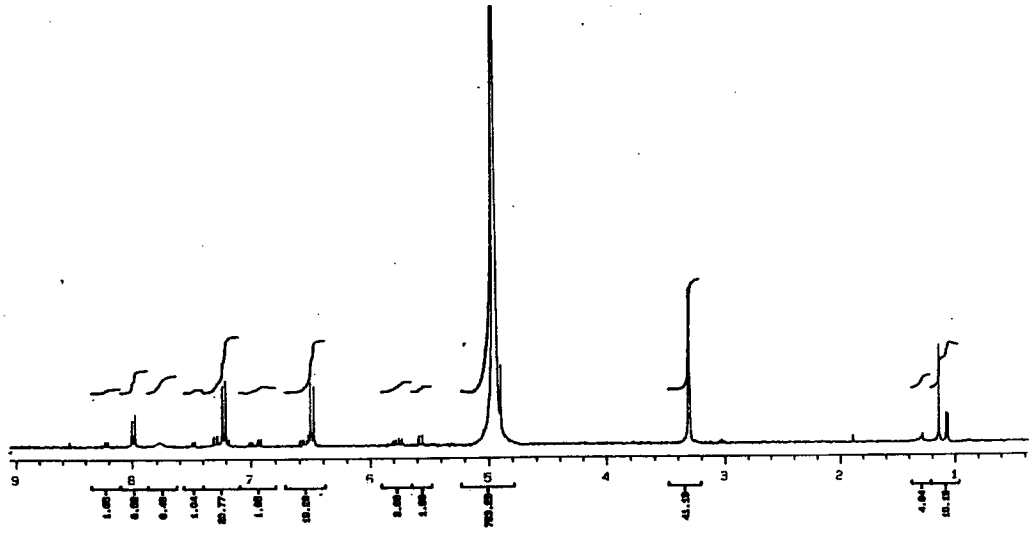

Spectrum 2

30mins

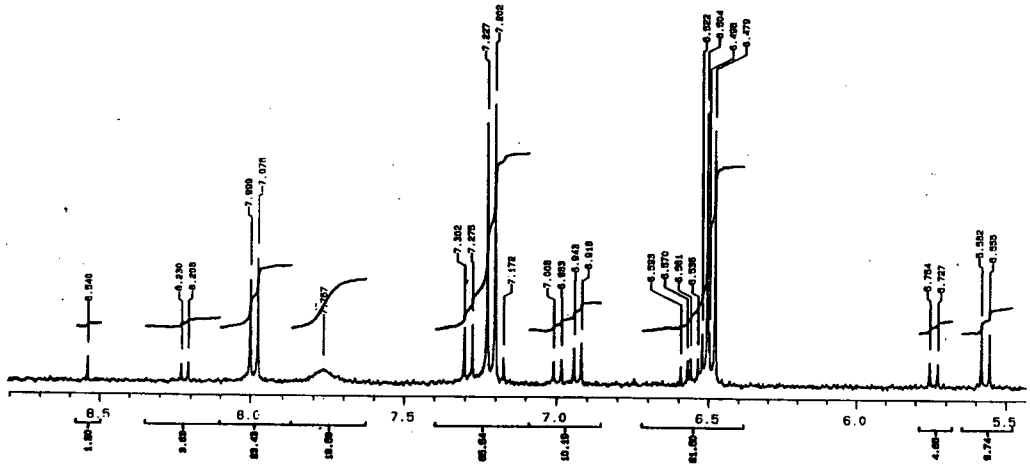

From kinetic studies the half life of the purple species is expected to be approximately 90 seconds, thus we do not expect to see the initial σ-adducts. NMR studies of the σ-adducts formed from reaction of nitromethane anions with 4-NBF indicate peaks at the quoted positions. Bands at very similar positions would be expected from the σ-adducts formed from the reactions of the malononitrile anion.

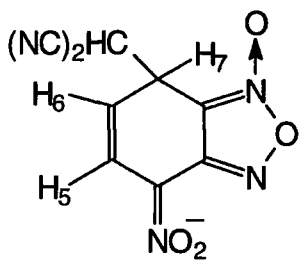

7-adduct

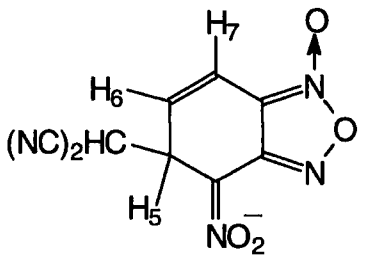

5-adduct

7-adduct

H_5	7.05ppm	J_{56} = 10.40Hz	J_{57} = 2.00Hz
H_6	5.30ppm	J_{56} = 10.40Hz	J_{67} = 3.96Hz
H_7	4.30ppm	J_{57} n/a	J_{67} n/a

5-adduct

H_5	4.60ppm	J_{56} = 4.60Hz	J_{57} n/a
H_6	6.30ppm	J_{56} = 4.60Hz	J_{67} = 10.0Hz
H_7	6.46ppm	J_{57} = 1.70Hz	J_{67} = 10.0Hz

There are no peaks observed in the 4-5ppm region thus it is unlikely that the initial σ-adducts are observed. There are however peaks seen at δ = 7.47ppm and δ = 5.79ppm with J = 8Hz in spectrum 1 which are not present in spectrum 2 and it possible that these may be due to the initial σ-adducts.

Spectrum 2 shows the major product peaks at $\delta = 7.20$ppm and $\delta = 6.50$ppm with $J = 10$Hz. These two spin coupled bands are not coupled to any other peaks, thus the product has only two and not three adjacent ring hydrogens as is the σ-adduct. It is possible that the product is similar to that shown below. Note that no band would be expected from the side chain hydrogen since this will have been exchanged with deuterium.

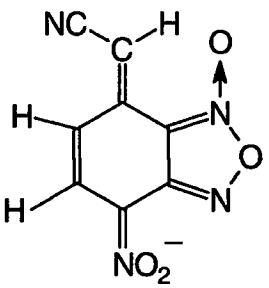

It has been shown that such species exist for reaction of 4,6-DNBF with nitroalkane anions[40].

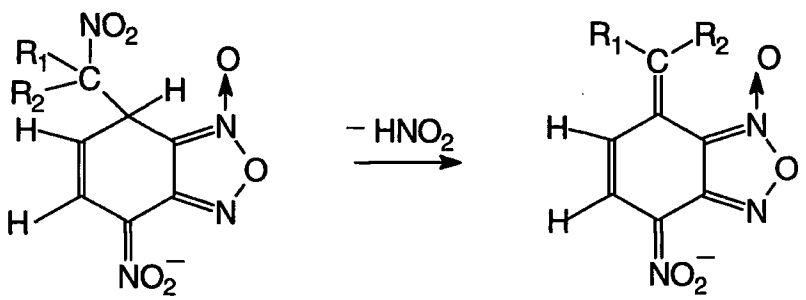

A second pair of doublets, may be present with $\delta = 7.77$ and $\delta = 8.21$, the doublet at 7.77ppm being observed as a broad band, possibly due to hydrogen/deuterium exchange. This possibly corresponds to the other σ-adduct.

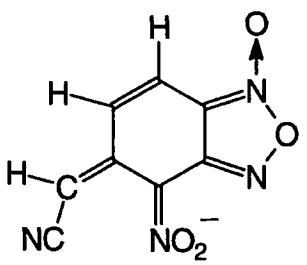

Chapter 4

Synthesis of products from carbanions and nitroaromatics

One of the aims of this work was to examine the possibility of oxidising σ-adducts to yield substituted products. As a first step it was thought to be useful to try and isolate the anionic σ-adducts themselves. In this chapter experiments are described in which solid salts have been prepared, and also experiments where the formation of adducts in solution was followed using NMR spectroscopy. NMR is particularly diagnostic in these studies[41] since nucleophilic attack at a ring-carbon results in a large upfield shift of hydrogen atoms at the site of attack.

It has been shown that Meisenheimer complexes can be synthesised and isolated under certain conditions. Using the carbon nucleophile as a solvent, addition of a base and a nitroaromatic affords the σ-complex. Addition of this complex to dry ether results in precipitation of a solid product. This may then be obtained by filtration. This method has been tried for several nitroaromatics and carbon nucleophiles with varying degrees of success.

4.1 Syntheses

4.1.1 Reaction products of 1,3,5-TNB, nitroalkanes and triethylamine

1,3,5-TNB (0.1g, 4.7×10^{-4} mol) was dissolved in the relevant nitroalkane ($2cm^3$) and triethylamine 0.196 cm^3 (1.4×10^{-3} mol, 3 equivalents) was added. In all cases this resulted in formation of a dark red solution, aliquots of which were added at intervals to 10ml of dry ether.The ether was removed after 24 hours and the solid was dissolved in d_6-DMSO to obtain NMR spectra. The results are shown below.

CH_3NO_2

Reaction time	Product
30 mins	Black tar formed on addition to ether.
60mins	"
180mins	"

$CH_3CH_2NO_2$

Reaction time	Product
30 mins	Red crystals formed on addition to ether.
60mins	"
180mins	"

$CH_3(CH_2)_2NO_2$

Reaction time	Product
30 mins	Red solution formed on addition to ether, no .
60mins	solid was produced.
180mins	"

NMR spectra of the solids from nitromethane and nitroethane showed some residual 1,3,5-TNB and triethylamine and very little product. Samples taken at 30 minutes and 180 minutes gave the same spectra, unfortunately none of which could be assigned.

4.1.2 Reaction products of 1,3,5-TNB, phenylacetonitrile and triethylamine

1,3,5-TNB (0.1g, 4.7×10^{-4} mol) was dissolved in phenylacetonitrile ($2cm^3$) and triethylamine was added. Either 0.196 (1.4×10^{-4} mol, 3 equivalents) or 0.098 (7×10^{-4} mol, 1.5 equivalents) was added. In both cases this resulted in formation of a cloudy blood red solution, aliquots of which were added at intervals to 10ml of dry ether. The ether was removed after 24 hours and the solid was dissolved in d_6-DMSO to obtain NMR spectra. The results are shown below.

1:3 TNB:NEt_3

Reaction time	Product
30 mins	Blood red crystals formed on addition to ether.
60mins	"
120mins	"

1:1.5 TNB:NEt_3

Reaction time	Product
30 mins	Blood red crystals formed on addition to ether.
60mins	"
120mins	"

In both cases the NMR spectra indicated reaction to give the σ-complex in which attack has occurred at an unsubstituted ring position and all peaks in the NMR spectra have been assigned, as shown in figure 4.1.

Figure 4.1

NMR spectrum of 1,3,5-TNB, 3 equivalents of NEt_3 and $PhCH_2CN$.

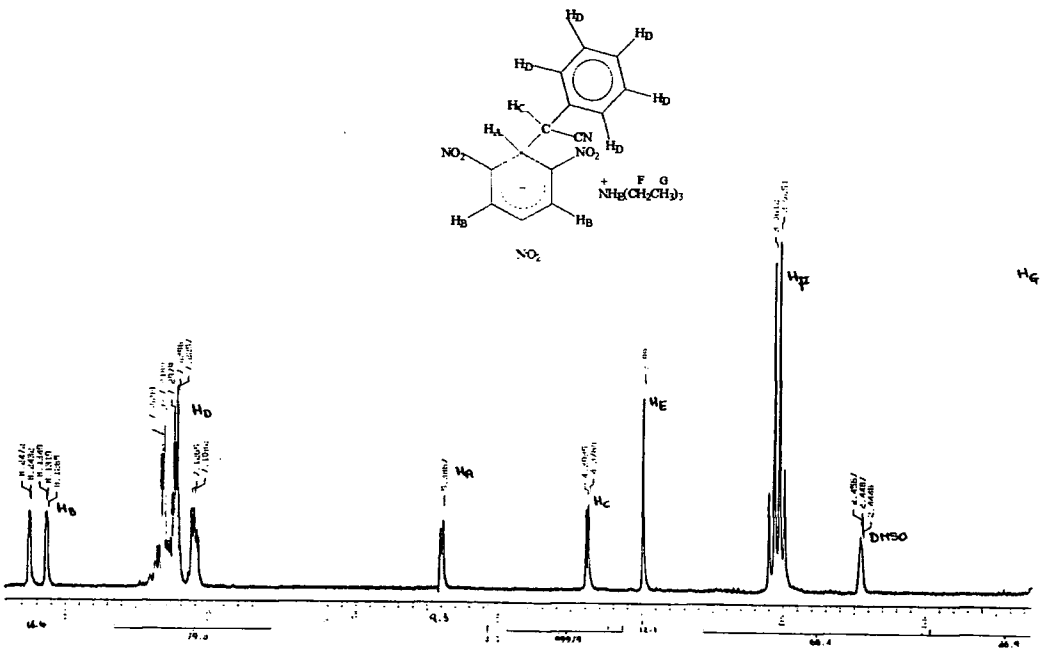

4.1.3 Reaction products of 4-NBF, phenylacetonitrile and triethylamine

4-NBF (0.1g, 5.5×10^{-4} mol) was dissolved in phenylacetonitrile ($5cm^3$) and triethylamine $0.231cm^3$ (1.65×10^{-3} mol, 3 equivalents) or $0.077cm^3$ (5.5×10^{-4} mol, 1 equivalent) was added. In both cases this resulted in formation of a cloudy blood red solution, aliquots of which were added at intervals to 10ml of dry ether. The ether was removed after 24 hours and the solid was dissolved in d_6-DMSO to obtain NMR spectra. The results are shown below.

1:3 4-NBF:NEt_3

Reaction time	Product
30 mins	A black solid formed on addition to ether.
60mins	"
120mins	"

1:1 4-NBF:NEt_3

Reaction time	Product
30 mins	A black solid formed on addition to ether.
60mins	"
120mins	"

In the first case, where triethylamine is in excess, no detectable product was observed in the NMR spectrum even though peaks due to 4-NBF were not observed. Peaks due to phenylacetonitrile and triethylamine were seen and due to the large excess of these species the product peaks may be obscured, figure 4.2. Repeating the reaction using equimolar quantities of 4-NBF and triethylamine gives exactly the same spectrum, however which leads to the conclusion that no product is formed in this reaction.

Figure 4.2

NMR spectrum of 4-NBF, 3 equivalents of NEt_3 and $PhCH_2CN$.

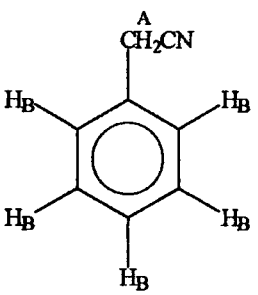

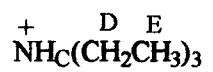

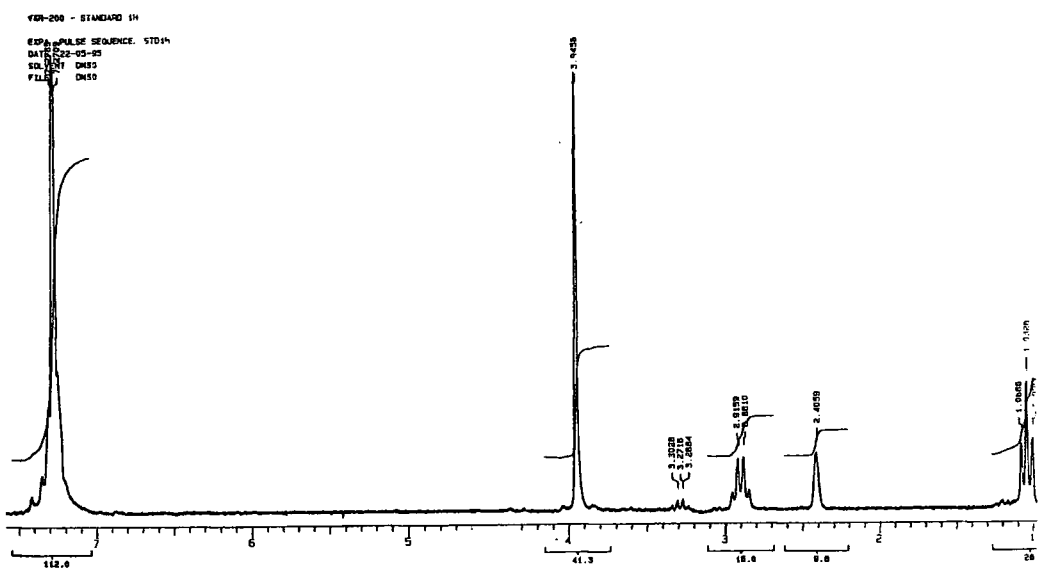

4.1.4 Reaction products of 1,3,5-TNB, 3,5-$(CF_3)_2C_6H_3CH_2CN$ and NEt_3

1,3,5-TNB (0.1g, 4.7×10^{-4} mol) was dissolved in 3,5-$(CF_3)_2C_6H_3CH_2CN$ ($2cm^3$) and triethylamine 0.0625 cm^3 (4.7×10^{-4} mol, 1 equivalent) was added. The reaction was repeated several times and in all cases this resulted in formation of a cloudy blood red solution, aliquots of which were added at intervals of 30, 60 and 120 minutes to 10ml of dry ether.Unfortunately, no solids were precipitated and no NMR spectra could thus be obtained.

4.1.5 Reaction products of 1,3,5-TNB, 3,4- and 2,4-$C_6H_3F_2CH_2CN$ and NEt_3

Separate aliquots of 1,3,5-TNB (0.1g, 4.7×10^{-4} mol) were dissolved in 2,4-$C_6H_3F_2CH_2CN$ ($2cm^3$) and 3,4-$C_6H_3F_2CH_2CN$ ($2cm^3$) and triethylamine 0.0625 cm^3 (4.7×10^{-4} mol, 1 equivalent) was added to each solution. In both cases, aliquots were added at intervals of 30, 60 and 120 minutes to 10ml of dry ether.Unfortunately, in both cases an orange solution was formed but with no precipitation of solid product and no NMR spectra could thus be obtained.

4.1.6 Reaction products of 4-NBZ, CH_3NO_2 and NEt_3

4-NBZ (0.1g, 6.1×10^{-4} mol) was dissolved in CH_3NO_2 ($3cm^3$) to produce a yellow solution. On addition of two equivalents of triethylamine, 0.168 cm^3 (5.5×10^{-4} mol) the solution became purple. Addition of this solution to 5ml of dry ether produced a sticky black tar, which after filtration to remove the residual ether, decomposed on exposure to the atmostphere.

4.2 In situ NMR studies of formation of products from nitroaromatics, and carbanions

These studies enable NMR to be used to follow the reaction closely, as it occurs. Spectra may be taken at regular intervals and concentrations are precisely known, unlike the previous experiments.

4.2.1 Study of 1,3,5-TNB, CD_3NO_2 and NEt_3

1,3,5-TNB (0.05g, 2.35×10^{-4} mol) was dissolved in deuterated nitromethane (1 cm^3) and an initial spectrum was obtained. Triethylamine (0.033 cm^3, 2.35×10^{-4} mol) was then added and spectra were taken at regular intervals. Since nitromethane was the solvent it was necessary to use the dueterated compound in order to avoid massive NMR absorbance.

Initial formation of the σ-complex is observed with some residual 1,3,5-TNB, figure 4.3. The excess 1,3,5-TNB then undergoes unknown decomposition reactions after approximately 15 minutes reaction time.

Figure 4.3

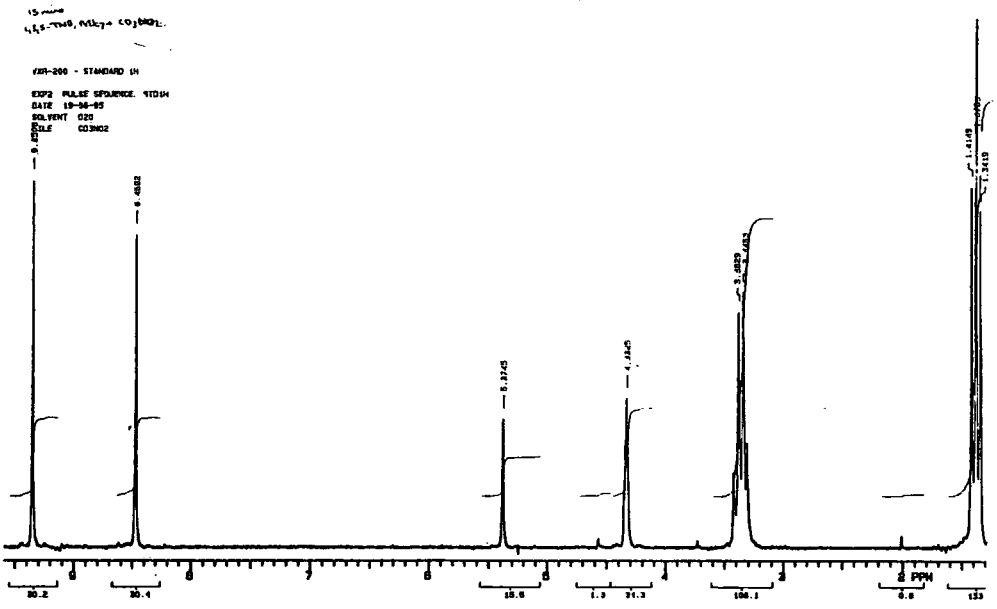

NMR spectrum of $[CD_2NO_2.TNB^-]$ $[ND(CH_2CH_3)_3^+]$.

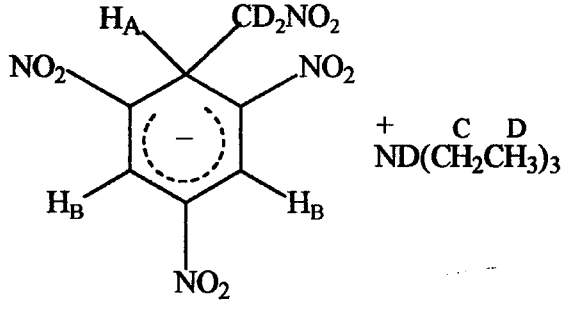

TNB	9.35ppm	singlet
CD_3NO_2	4.33ppm	singlet
H_A	5.37ppm	singlet
H_B	8.47ppm	singlet
H_C	3.36ppm	quartet
H_D	1.38ppm	triplet

4.2.2 Study of 4-NBF, $PhCH_2CN$, and NEt_3 in d_6-DMSO

4-NBF (0.0181g, 1×10^{-4} mol) and phenylacetonitrile (0.0115cm^3, 1×10^{-4} mol) were dissolved in d_6-DMSO (1cm^3) and an initial spectrum was obtained. Triethylamine 0.0135 cm^3, (1×10^{-4} mol, 1 equivalent) of was added and spectra were taken at regular intervals.

After 5 minutes only peaks due to phenylacetonitrile and triethylamine are observed, however peaks due to the complex and 4-NBF may be present but too small to see. After 5 hours small peaks due to 4-NBF and some at ~5ppm, which may be due to the complex, have appeared, figure 4.4.

Increasing the amount of triethylamine used may facilitate observable peaks for the complex, thus the experiment was repeated using 3 equivalents of triethylamine. Unfortunately the same result was obtained as previously, figure 4.4.

Figure 4.4

Spectrum 1

Initial NMR spectrum of 4-NBF and $PhCH_2CN$ in d_6-DMSO.

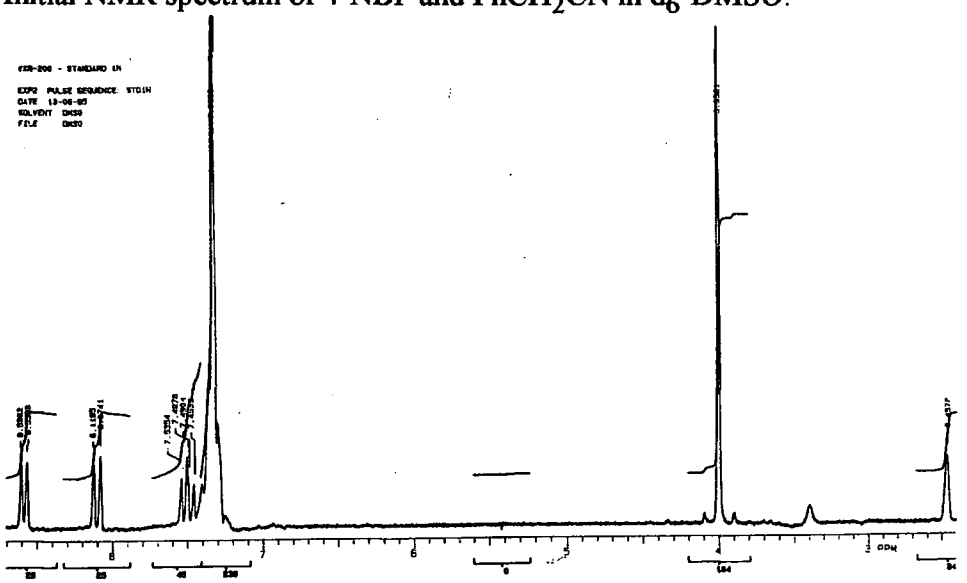

4-NBF	8.60ppm	doublet
	8.11ppm	doublet
	7.53ppm	doublet of doublets
$PhCH_2CN$	7.35ppm	multiplet
	4.02ppm	singlet
d_6-DMSO	2.49ppm	broad singlet

Spectrum 2

NMR spectrum of 4-NBF, $PhCH_2CN$ and NEt_3 (1 equivalent) in d_6-DMSO, after 5 hours.

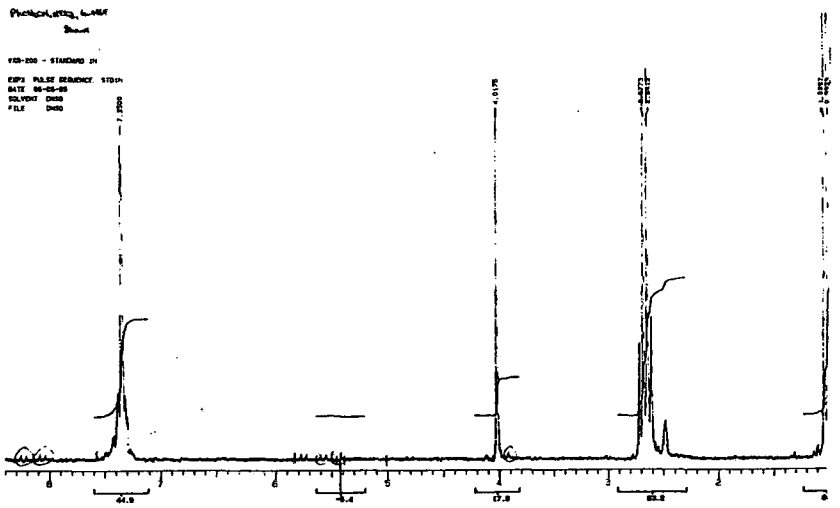

4-NBF	~8ppm	very small triplet and two doublets
complex	~5.5ppm	several doublets
$PhCH_2CN$	7.35ppm	multiplet
	4.02ppm	singlet
NEt_3	2.66ppm	quartet
	0.99ppm	triplet

Spectrum 3

NMR spectrum of 4-NBF, $PhCH_2CN$ and NEt_3 (3 equivalents) in d_6-DMSO, after 24 hours.

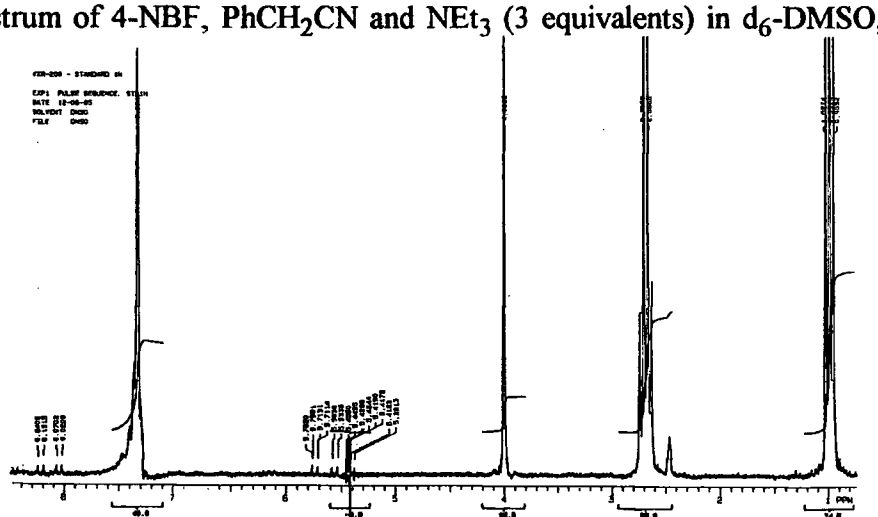

4-NBF	~8ppm	very small triplet and two doublets
complex	~5.5ppm	several doublets
$PhCH_2CN$	7.25ppm	multiplet
	3.92ppm	singlet
NEt_3	2.47ppm	quartet
	0.86ppm	triplet

4.2.3 Study of 4-NBF, $PhCH_2CN$ and $NaOCD_3$

4-NBF (0.0181g, 1×10^{-4} mol) and $PhCH_2CN$ (0.0115cm^3, 1×10^{-4} mol) were dissolved in d_4-methanol (1 cm^3) and $NaOCD_3$ (0.0407 cm^3 of 2.5M, 1×10^{-4} mol) was added. Spectra were taken at regular intervals and peaks due to all the starting materials are observed however no product peaks were seen..This may be due to radicals being produced in this reaction thus obliterating any product peaks.

4.2.4 Study of 4-NBF, NEt_3 and CD_3NO_2

4-NBF (0.0425g, 2.4×10^{-4} mol) was dissolved in CD_3NO_2 (1 cm^3) and an initial spectrum was recorded. On addition of triethylamine (0.0326 cm^3, 1 equivalent) a strong red colour was produced. Spectra were taken at regular intervals.

The spectra clearly show two distinct products are produced as well as residual peaks of the starting materials. The two products are the 5-adduct and 7-adduct of 4-NBF with the carbanion and each has an associated triethylammonium cation, figure 4.5. After approximately 15 minutes all peaks disappear, most probably due to formation of radical species.

The assignment of the observed bands to the 5- and 7- adducts follows from previous work involving methoxy adducts[26] and phenoxy adducts[42]. Details are given in the table below.

	5-Methoxy adduct	7-Methoxy adduct	7-Phenoxy adduct*
H_5	5.52ppm	7.19 ppm	6.89ppm
H_6	6.43ppm	5.23 ppm	5.01ppm
H_7	6.68ppm	5.32 ppm	4.65ppm
J_{56}	4.7Hz	10.3Hz	10.2Hz
J_{67}	9.8Hz	4.4Hz	4.3Hz
J_{57}	<1Hz	<1Hz	1.7Hz

* Bonding occurs via the ring-carbon para to the phenoxy group.

Figure 4.5

Spectrum 1

Initial spectrum of 4-NBF and CD_3NO_2.

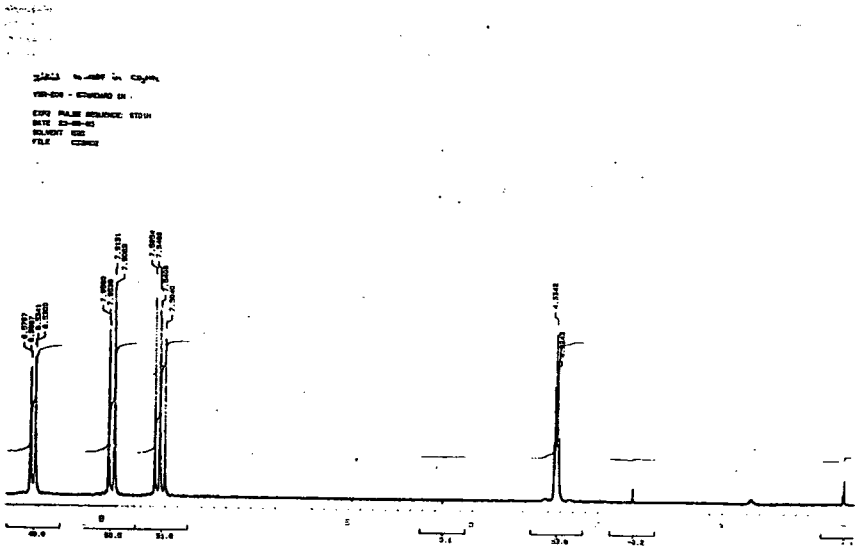

4-NBF	8.55ppm	doublet
	7.93ppm	doublet
	7.54ppm	triplet
CD_3NO_2	4.33ppm	multiplet

Spectrum 2

NMR spectrum of 5-CD_2NO_2.NBF and 7-CD_2NO_2.NBF after 5 minutes.

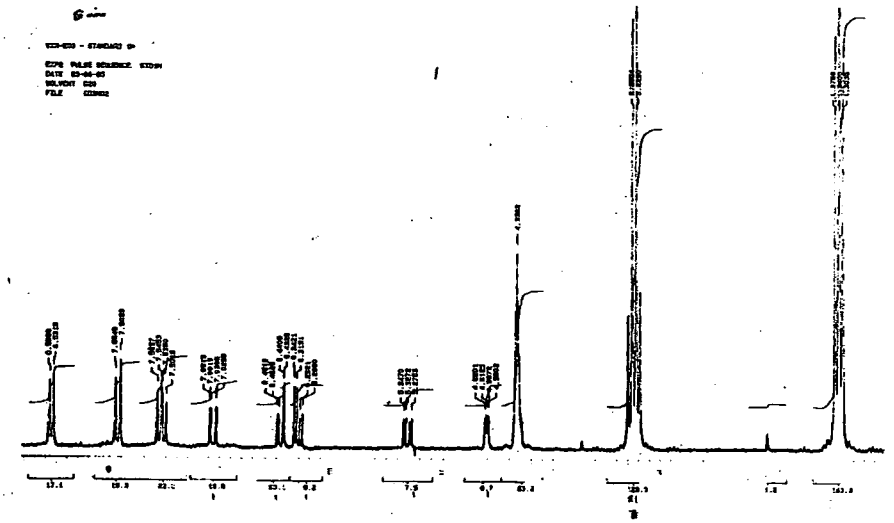

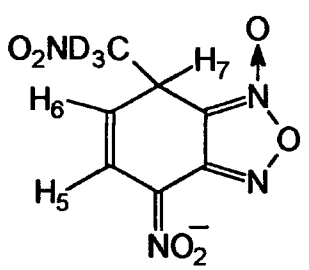

7-adduct

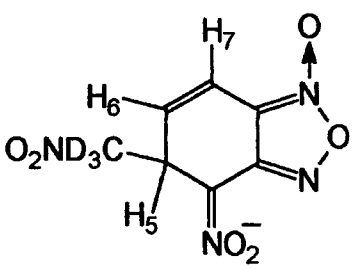

5-adduct

7-adduct

H_5	7.05ppm	J_{56} = 10.40Hz	J_{57} = 2.00Hz
H_6	5.30ppm	J_{56} = 10.40Hz	J_{67} = 3.96Hz
H_7	4.30ppm	J_{57} n/a	J_{67} n/a

5-adduct

H_5	4.60ppm	J_{56} = 4.60Hz	J_{57} n/a
H_6	6.30ppm	J_{56} = 4.60Hz	J_{67} = 10.0Hz
H_7	6.46ppm	J_{57} = 1.70Hz	J_{67} = 10.0Hz

The bands observed for the nitromethane adducts at $\delta = 7.05$, 5.30 and 4.30ppm can be assigned to the 7-adduct. The shift of the proton attached to the carbon where nucleophilic attack occurs is affected by the nature of the attacking nucleophile. With carbon nucleophiles the value is significantly lower than with oxygen nucleophiles. Correspondingly, the bands observed at $\delta = 6.46$, 6.30 and 4.60ppm may be assigned to the 5-adduct formed from nitromethane.

Since the use of one equivalent of triethylamine does not use all the available 4-NBF, the experiment was repeated using three equivalents. Unfortunately this produced collapse of the spectra very quickly, most likely due to production of radical species.

4.2.5 Study of 4-NBZ, NEt_3 and CD_3NO_2

4-NBZ (0.0388g, 2.35×10^{-4} mol) was dissolved in CD_3NO_2 ($1cm^3$) and an initial spectrum was recorded. Triethylamine 0.0326 cm^3 (2.35×10^{-4} mol, 1 equivalent) was added and spectra were recorded at 5, 10 and 40 minutes after this addition. The spectrum indicates formation of the 5-adduct and it is unusual that the 7-adduct is not observed, figure 4.6. Previously reactions of 4-NBF and 4-NBZ with nucleophiles have generally indicated that attack at the 5-position is kinetically preferred while adducts at the 7-position have greater thermodynamic stability. It is possible that the 5-adduct is both kinetically and thermodynamically preferred to its isomer. Alternatively the reversion of the 5-adduct to reactants, which would allow equilibration between the isomers is so slow that other decomposition pathways prevail. The 5-adduct remains stable for approximately one hour before decomposition occurs.

Figure 4.6

NMR spectrum of 4-NBZ, NEt_3 and CD_3NO_2 after 10 minutes.

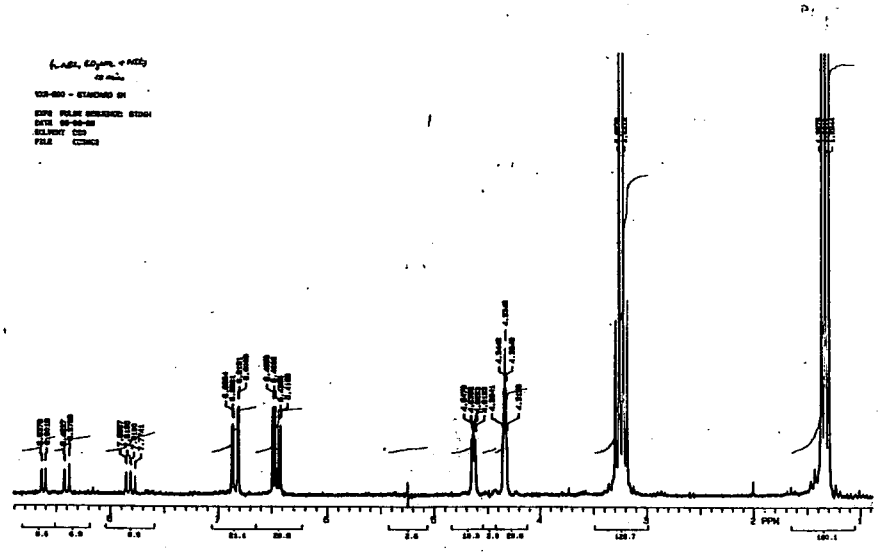

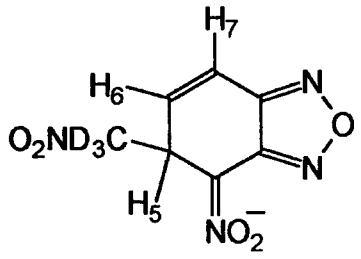

5-adduct

H_5	4.63ppm	J_{56} = 4.58Hz	J_{57} = 1.88Hz
H_6	6.45ppm	J_{56} = 4.58Hz	J_{67} = 10.1Hz
H_7	6.84ppm	J_{57} = 1.88Hz	J_{67} = 10.1Hz

Chapter 5

Oxidation of Meisenheimer complexes

Due to the success of producing the salt from 1,3,5-TNB, phenylacetonitrile and triethylamine as a solid, further spectroscopic analysis of this compound may be undertaken with the ultimate aim being oxidation of this species. Oxidation reactions, due to potential oxidation of the solvent, may not be performed in DMSO thus the stability of the salt in other solvents was investigated. Results are shown in table 5.1.

Table 5.1

Solvent	λ_{max}/nm	Stability
DMSO	458	Stable, absorbance = 0.80
Water	462	Absorbance decreases by 0.4 over 2 hrs
Dioxan	456	Absorbance decreases by 0.25 over 2 hrs
Acetonitrile	454	Absorbance does not decrease over 2 hrs

$[(C_6H_5CHCN.TNB^-)(NHEt_3^+)] = 4\times10^{-5}$mol dm^{-3}

It was therefore decided to use acetonitrile as the solvent for the oxidation reactions.

5.1 Oxidations using chlorine gas and aqueous chlorine solution

Many different oxidants have been used to oxidise σ-adducts including both organic, e.g. chloranil and N-bromosuccinamide and inorganic oxidants, e.g. halogens[43] and $AgNO_3$. Since a supply of chlorine gas was readily available, it was decided to investigate this as a potential oxidant for the σ-adduct formed from 1,3,5-TNB, phenylacetonitrile and triethylamine, the $C_6H_5CHCN.TNB^- NEt_3^+$ salt shown below.

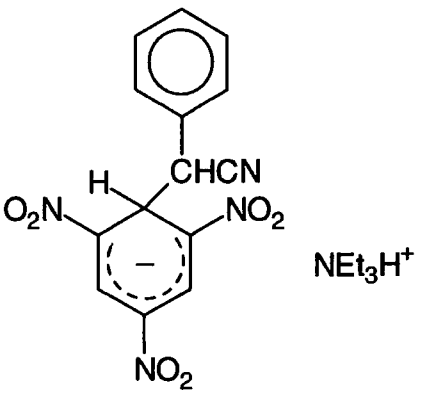

Chlorine gas was passed through a red solution of 1×10^{-4} M salt in acetonitrile in a bubbler, the chlorine gas being scrubbed using 2M sodium hydroxide solution. The solution turned immediately pale yellow, probably due to dissolved chlorine gas, and then turned a deeper yellow colour indicating that reaction had occurred. This was a slightly exothermic reaction. The success of this qualitative test prompted further quantitative investigation.

For spectrophotometric and stopped-flow investigation it is more convenient to have reactants in solution form, thus an aqueous solution of chlorine was produced. The concentration of which was determined by Andrews titrations.

Excess potassium iodide was added to 1ml aliquots of the chlorine solution with approximately 5ml of water. This was then titrated against 0.01M sodium thiosulfate solution, starch indicator being added just before the end point where the solution turns from green to colourless.

$$Cl_2 + 2\,KI \longrightarrow 2\,KCl + I_2$$

$$I_2 + 2\,Na_2S_2O_3 \longrightarrow 2\,NaI + Na_2S_4O_6$$

End point/cm^3	24.00	31.35	38.70
Start/cm^3	16.65	24.00	31.35
Volume $Na_2S_2O_3$ used/cm^3	7.35	7.35	7.35
Molarity of Cl_2 solution/ mol dm^{-3}	0.0368	0.0368	0.0368

Spectrophotometric investigations were made of the effect of chlorine on the salt in solution. Initially a 50/50 volume/volume mixture of DMSO/ water was used, table 5.2. Since the aqueous chlorine solution will absorb in the uv-visible region, blanks containing chlorine solutions were used.

Table 5.2

[Salt]/mol dm^{-3}	**[Cl_2]/ mol dm^{-3}**	**λ_{max}**	**Observations**
4×10^{-5}	_	461nm	Red solution
4×10^{-5}	1.86×10^{-2}	461nm	Red solution, decrease in absorbance faster than without Cl_2.

Since oxidation does not occur in this solution a 50/50 volume/volume acetonitrile/water solvent was then used. Again chlorine blanks were used and results are shown in table 5.3.

Table 5.3

[Salt]/mol dm^{-3}	**[Cl_2]/ mol dm^{-3}**	**λ_{max}**	**Observations**
4×10^{-5}	_	457nm	Red solution
4×10^{-5}	1.86×10^{-2}	228nm	Immediate decolourisation
4×10^{-5}	9.25×10^{-3}	220nm	Immediate decolourisation
4×10^{-5}	4.60×10^{-3}	219nm	Immediate decolourisation

Thus reaction occurs in 50/50 acetonitrile/ water solutions to give decolouration and most probably the oxidised product. In order to obtain rate constants for this fast reaction, stopped-flow investigation was undertaken.
Measurements were made at 461nm, the absorbance maximum of the salt, and all concentrations are quoted after mixing.

Solvent v/v	[Salt]/mol dm^{-3}	$[Cl_2]$/ mol dm^{-3}
50/50 CH_3CN/H_2O	2×10^{-5}	9.25×10^{-3}

Unfortunately the reaction is too fast to observe, thus the observed rate constant must be in excess of 500 s^{-1}. An alternative solvent with a higher proportion of water was then used as this should decrease the observed rate constant.

Solvent v/v	[Salt]/mol dm^{-3}	$[Cl_2]$/ mol dm^{-3}
30/70 CH_3CN/H_2O	4×10^{-5}	9.25×10^{-3}

Again the rate constant was too large to measure.

NMR investigation was undertaken to identify the products of the oxidation reaction and to ascertain if the product is indeed the oxidised neutral species we expect.

The salt was dissolved in CD_3CN and a spectrum was obtained. Chlorine gas was then passed through the solution, resulting in instant decolourisation and a second spectrum taken. We can tentatively assign this spectrum as that of the oxidised neutral product as shown in figure 5.1.

Figure 5.1

Spectrum 1

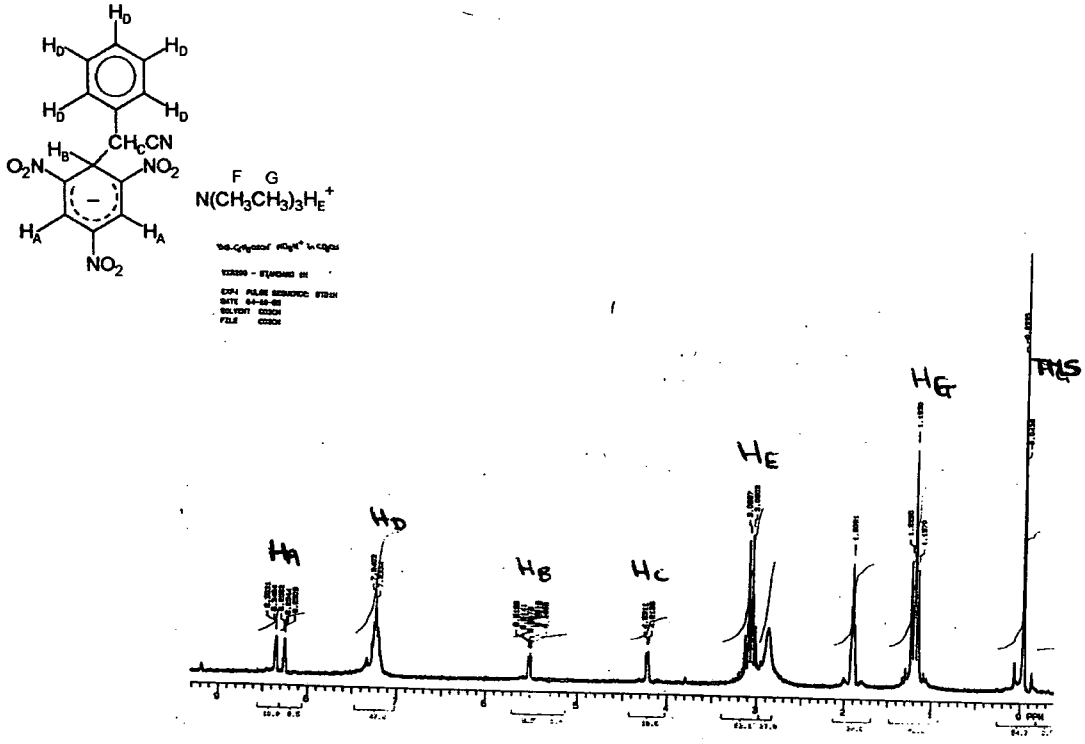

Spectrum 2

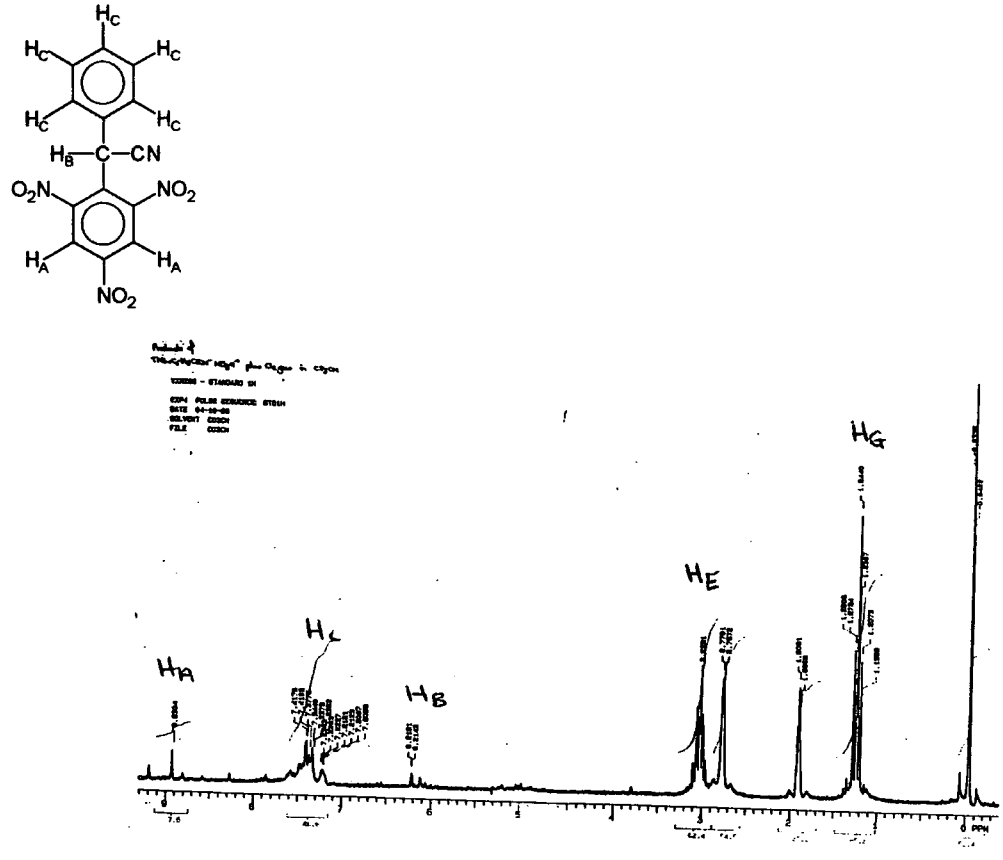

A larger scale synthesis of the oxidised product was attempted to assist in identifying the species and also produce a quantity of the product.

Firstly the salt was produced by dissolving 0.5g of 1,3,5-TNB in 5ml of phenylacetonitrile and adding 0.6ml of triethylamine to produce a blood red solution. After 45 minutes this was added to 10ml of dry ether and blood red crystals were precipitated. These were then filtered, dried and added to to the minimum amout of acetonitrile required to dissolve all the crystals. Chlorine gas was then passed through the solution until it decolourised. The acetonitrile was then allowed to evaporate which left a black residue and white crystals, most likely triethylammonium chloride, which were removed by washing with water. Samples were taken for NMR, however only a large peak due to the triethylammonium chloride could be seen even after further repeated washing.

5.2 Oxidation using triphenylmethyl bromide

In the search for suitable oxidants it was found that on addition of 0.0324g of triphenylmethyl bromide to a 4×10^{-5} M solution of the $C_6H_5CHCN.TNB^-NEt_3^+$ salt, immediate decolourisation occurred. Thus further spectrophotometric investigation was undertaken using acetonitrile as the solvent, results are shown in table 5.4 and a representative spectrum is shown in figure 5.2.

Table 5.4

[Salt]/mol dm^{-3}	[Ph_3CBr]/ mol dm^{-3}	λ_{max}	Variation in absorbance
_	1×10^{-2}	401nm	No increase in absorbance
4×10^{-5}	_	454nm	"
"	1×10^{-2}	370nm	Decreasing absorbance
"	5×10^{-3}	369nm	"
"	2.5×10^{-3}	369nm	"
"	1×10^{-3}	369nm	"
"	5×10^{-4}	370nm	"
"	2.5×10^{-4}	454nm	"

Figure 5.2

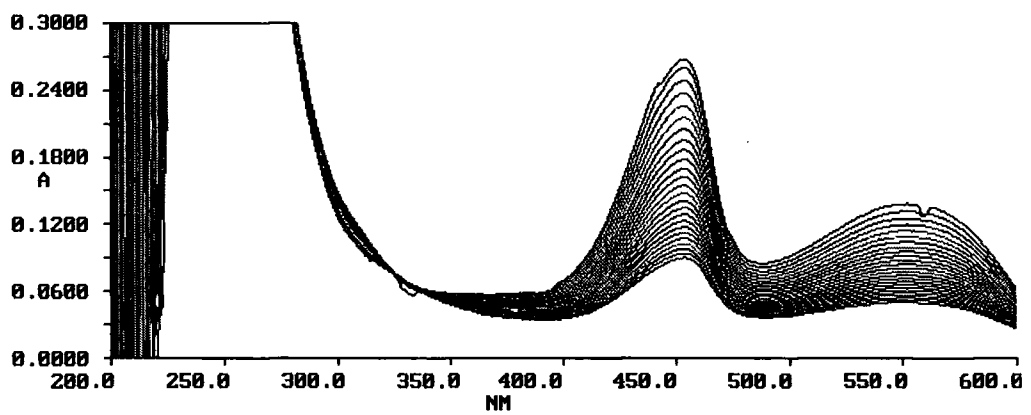

Absorbance spectrum of decay of 4×10^{-5} M salt with 2.5×10^{-3} M Ph_3CBr over 20 minutes.

The results show that as the concentration of triphenylmethyl bromide is increased the absorbance maximum shifts from 454nm to 369nm. With time the absorbance at either wavelength decreases.

From these results it is postulated that at low concentrations of Ph_3CBr decay of the salt is observed, where as at higher concentrations another species is seen to decay, probably the protonated form of the salt, scheme 5.1.

Scheme 5.1

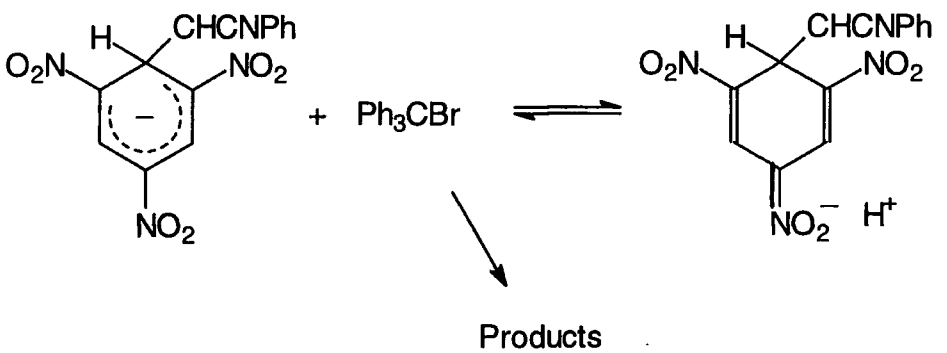

Inhibiting the protonation using a base should produce spectra showing decay of the salt only. Thus spectrophotometric measurements were made with triethylamine added to the system. Results are shown in table 5.5.

Table 5.5

[Salt]/ mol dm^{-3}	[Ph_3CBr]/ mol dm^{-3}	[NEt_3]/ mol dm^{-3}	λ_{max}	Variation in absorbance
4×10^{-5}	2×10^{-3}	_	371nm	Decrease in absorbance
"	_	2×10^{-3}	453nm	No decrease in absorbance
"	2×10^{-3}	"	454nm	No decrease in absorbance
"	"	1×10^{-2}	455nm	No decrease in absorbance
"	"	5×10^{-4}	453nm	Decrease in absorbance
"	"	1×10^{-3}	454nm	Decrease in absorbance
"	6×10^{-3}	1×10^{-3}	454nm	Decrease in absorbance
"	4×10^{-3}	1×10^{-3}	455nm	Decrease in absorbance

Thus the addition of triethylamine prevents protonation and decay of the salt alone is observed. There are however, two limiting cases.

For $[NEt_3] >> [Ph_3CBr]$, we observe inhibition of salt decomposition and no protonated species.

For $[NEt_3] < [Ph_3CBr]$, we observe dacay of the salt but no protonated species.

Timedrives were then made at 454nm to ascertain the rate of decay of the salt. Results are shown in table 5.6 and all concentrations are quoted after mixing.

Table 5.6

[Salt]/mol dm^{-3}	$[Ph_3CBr]$/ mol dm^{-3}	$[NEt_3]$/ mol dm^{-3}	k_{obs}/s^{-1}
4×10^{-5}	2×10^{-3}	1×10^{-3}	1.75×10^{-3}
"	3×10^{-3}	"	4.32×10^{-3}
"	4×10^{-3}	"	4.21×10^{-3}
"	5×10^{-3}	"	4.23×10^{-3}

From these results the following kinetic scheme may be postulated, where X is the protonated intermediate.

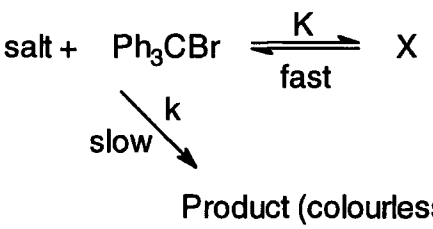

It is assumed initially that there is a direct reaction between the salt and triphenylmethyl bromide which results in oxidation of the salt to yield a colourless product. Protonation to give X presumably occurs due to the equilibrium of Ph_3CBr with traces of water present in the solvent.

$$Ph_3CBr + H_2O \rightleftharpoons Ph_3COH + HBr$$

Hence the acid produced would be expected to depend on the concentration of Ph_3CBr present.

$$[salt] + [product] + [X] = 4 \times 10^{-5}$$

$$\text{Thus } \frac{d[salt]}{dt} + \frac{d[product]}{dt} + \frac{d[X]}{dt} = 0$$

$$\text{Since } K = \frac{[X]}{[salt][Ph_3CBr]} \text{ and } \frac{d[product]}{dt} = k[salt][Ph_3CBr]$$

$$\frac{d[salt]}{dt} + K[Ph_3CBr]\frac{d[salt]}{dt} + k[salt][Ph_3CBr] = 0$$

$$\frac{d[salt]}{dt}(1 + K[Ph_3CBr) + k[salt][Ph_3CBr] = 0$$

$$\text{Since} \frac{-d[salt]}{dt} = k_{obs}[salt]$$

$$-k_{obs}(1 + K[Ph_3CBr]) + k[Ph_3CBr] = 0$$

$$k_{obs} = \frac{k[Ph_3CBr]}{1 + K[Ph_3CBr]}$$

If $1 >> K[Ph_3CBr]$, at low Ph_3CBr, $k_{obs}=k[Ph_3CBr]$

If $K[Ph_3CBr] >> 1$, $k_{obs}=\frac{k}{K}$

Kinetic measurements are now made without triethylamine over a range of concentrations of salt and triphenylmethyl bromide. Results are shown in table 5.7 and a representative trace is shown in figure 5.3. All concentrations are quoted after mixing.

Table 5.7

Item	[Salt]/mol dm^{-3}	[Ph_3CBr]/ mol dm^{-3}	λ/nm	k_{obs}/s^{-1}
1	4×10^{-5}	1×10^{-3}	454	2.48×10^{-3}
2	"	1.5×10^{-3}	"	4.87×10^{-3}
3	"	2×10^{-3}	"	4.49×10^{-3}
4	"	4×10^{-3}	"	5.64×10^{-3}
5	"	6×10^{-3}	"	5.72×10^{-3}
6	2×10^{-5}	1×10^{-3}	"	4.60×10^{-3}
7	"	1.5×10^{-3}	"	4.88×10^{-3}
8	"	6×10^{-3}	"	5.98×10^{-3}
9	4×10^{-5}	1×10^{-3}	371	6.15×10^{-3}
10	"	2×10^{-3}	"	6.11×10^{-3}
11	"	3×10^{-3}	"	6.81×10^{-3}
12	"	4×10^{-3}	"	6.44×10^{-3}
13	"	5×10^{-3}	"	6.35×10^{-3}

Figure 5.3

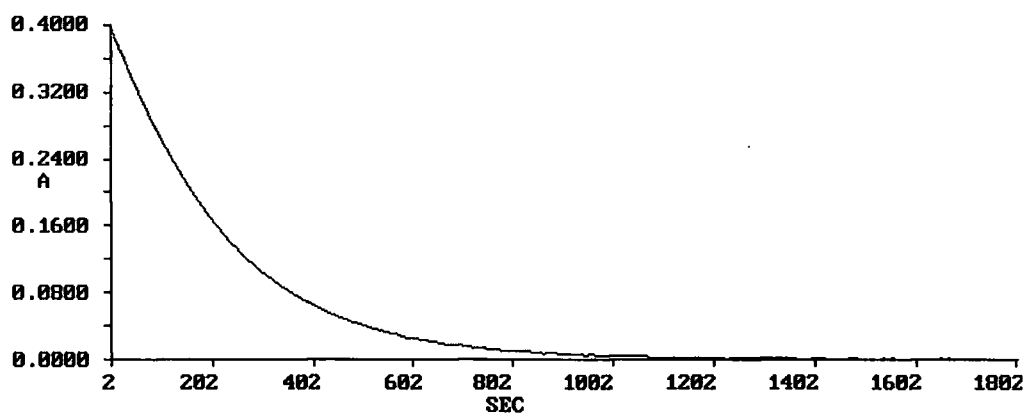

Absorbance *versus* time plot for 4×10^{-5}M salt and 2×10^{-4}M Ph_3CBr at 454nm.

The data are not particularly self consistent. Thus items 1 and 9 report different rate constants for kinetic runs carried out with the same concentrations of reactants. This may be because runs 1-5, 6-8 and 9-13 were carried out on different occasions. It is possible that the solvents used contained different quantities of adventitious water resulting in different acidities. Nevertheless the data show that rate constants increase with increasing concentration of Ph_3CBr and reach a limit of about $6.3\times10^{-3}\ s^{-1}$.

The results are in agreement with the predicted kinetic equation, a graph of k_{obs} *versus* $[Ph_3CBr]$ for items 1-5 gives a curve as shown below in figure 5.4.

Figure 5.4

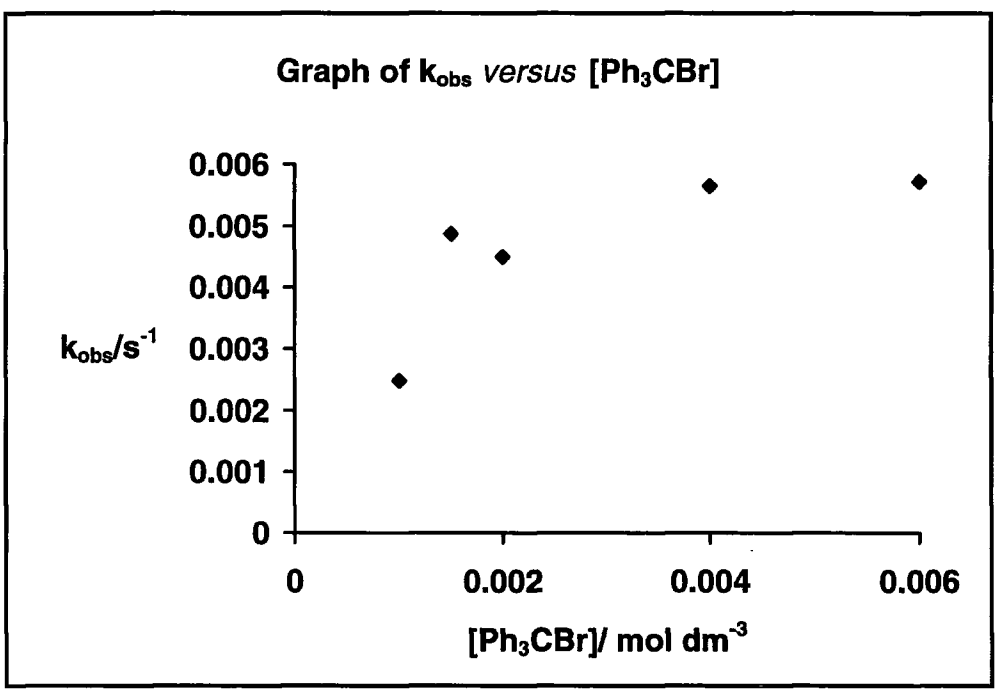

Since $k_{obs} = \dfrac{k[Ph_3CBr]}{1 + K[Ph_3CBr]}$ plotting $\dfrac{1}{k_{obs}}$ against $\dfrac{1}{[Ph_3CBr]}$ gives a straight line graph with gradient $\dfrac{1}{k}$ and intercept $\dfrac{K}{k}$.

However this is not the only possibility for the kinetic scheme. The intermediate X may undergo slow decomposition to the product instead of the salt.

$$\text{salt} + \text{Ph}_3\text{CBr} \underset{\text{fast}}{\overset{K}{\rightleftharpoons}} X \xrightarrow[\text{slow}]{k} \text{Product (colourless)}$$

$$[\text{salt}] + [X] + [\text{Product}] = \text{constant}$$

$$\frac{d[\text{salt}]}{dt} + \frac{d[X]}{dt} + \frac{d[\text{Product}]}{dt} = 0$$

$$K = \frac{[X]}{[\text{salt}][\text{Ph}_3\text{CBr}]}$$

$$\text{Thus } \frac{d[\text{salt}]}{dt} = \frac{d[X]}{dt}\frac{1}{K[\text{Ph}_3\text{CBr}]}$$

$$\frac{d[\text{Product}]}{dt} = k[X]$$

$$\text{Therefore } \frac{d[X]}{dt}\left(1 + \frac{1}{K[\text{Ph}_3\text{CBr}]}\right) + k[X] = 0$$

$$-\frac{d[X]}{dt} = k_{obs}[X]$$

$$\text{Thus } -k_{obs}\left(\frac{1 + K[\text{Ph}_3\text{CBr}]}{K[\text{Ph}_3\text{CBr}]}\right) + k = 0$$

$$k_{obs} = \frac{kK[\text{Ph}_3\text{CBr}]}{1 + K[\text{Ph}_3\text{CBr}]}$$

$$\text{This gives } \frac{1}{k_{obs}} = \frac{1}{kK[\text{Ph}_3\text{CBr}]} + \frac{1}{k}$$

Thus a reciprocal plot as before gives a gradient of $\frac{1}{kK}$ and an intercept of $\frac{1}{k}$.

From kinetic path 1

$k = 42.7\ s^{-1}\ dm^3\ mol^{-1}$

$K = 5.13\times10^3\ dm^3\ mol^{-1}$

From kinetic path 2

$k = 8.38\times10^{-3}\ s^{-1}\ dm^3\ mol^{-1}$

$K = 5.10\times10^3\ dm^3\ mol^{-1}$

It is not possible from the observed kinetics to distinguish between these possibilities. There is the possibility that there is also a reaction between the triphenylmethyl bromide and the triethylamine. To investigate this spectrophotometric measurements were made, results are shown in table 5.8.

Table 5.8

$[Ph_3CBr]$/ mol dm^{-3}	$[NEt_3]$/ mol dm^{-3}	λ_{max}/nm
1.5×10^{-4}	1×10^{-2}	_
"	5×10^{-3}	_
"	1×10^{-3}	shoulder 258nm
"	5×10^{-4}	shoulder 253nm
"	_	265nm

Thus increasing the concentration of triethylamine causes the peak due to triphenylmethyl bromide to disappear indicating some interaction between the species.

Further investigation into the equilibration between the salt and protonated species involved altering the conditions of the reaction and recording spectral and kinetic variations.

Firstly the effect of concentration of triethylamine on the extent of protonated species produced was observed. Different concentrations of triethylamine were added to solutions of salt and Ph_3CBr and the spectral maxima recorded. Results are shown in table 5.9.

Table 5.9

[Salt]/ mol dm^{-3}	$[Ph_3CBr]$/ mol dm^{-3}	$[NEt_3]$/ mol dm^{-3}	λ_{max}/nm
4×10^{-5}	4×10^{-3}	2×10^{-3}	451 (smaller absorbance), 370 (greater absorbance)
"	"	4×10^{-3}	453, 370, even absorbances
"	"	1×10^{-2}	454 (greater absorbance), 370 (smaller absorbance)

As may be expected, increasing the concentration of triethylamine increases the amount of salt produced, λ_{max}= 451nm, however the species still decay over time.

5.3 Effect of solvent composition

The amount of water in the system should, in the same way as triethylamine, also affect the extent of protonation and thus the rate of decay of the species. Results are shown in tables 5.10 and 5.11.

Table 5.10

[Salt]/ mol dm^{-3}	[Ph_3CBr]/ mol dm^{-3}	v/v CH_3CN/H_2O	λ_{max}/nm
4×10^{-5}	2×10^{-3}	100% CH_3CN	454, 370, even absorbances
"	"	99/1	454
"	"	95/5	454

Addition of appreciable amounts of water prevents protonation and more salt is observed thus kinetic rate measurements at 99/1 CH_3CN/ H_2O were thus made at 454nm.

Table 5.11

[Salt]/mol dm^{-3}	[Ph_3CBr]/ mol dm^{-3}	k_{obs}/s^{-1}
4×10^{-5}	2×10^{-3}	1.14×10^{-3}
"	4×10^{-3}	1.28×10^{-3}
"	6×10^{-3}	1.45×10^{-3}
"	8×10^{-3}	1.76×10^{-3}
"	1×10^{-2}	2.07×10^{-3}

These are much slower than the values in 100% CH_3CN. The rate constants in other solvent compositions were then investigated. Results are shown in table 5.12, measurements were made at 454nm.

Table 5.12

[Salt]/mol dm^{-3}	[Ph_3CBr]/ mol dm^{-3}	k_{obs}/s^{-1}	v/v CH_3CN/H_2O
4×10^{-5}	2×10^{-3}	1.24×10^{-3}	99/1
"	"	1.04×10^{-3}	98/2
"	"	4.61×10^{-4}	97/3
"	"	4.67×10^{-4}	96/4
"	"	5.17×10^{-4}	95/5
4×10^{-5}	1×10^{-2}	1.40×10^{-3}	99/1
"	"	6.67×10^{-4}	98/2
"	"	3.85×10^{-4}	97/3
"	"	4.04×10^{-4}	96/4
"	"	3.68×10^{-4}	95/5

As may be expected, the rate of decay of the salt decreases as the percentage of water in the solution increases up to 97/3 CH_3CN/H_2O. After this further increase in the percentage of water do not further decrease the value of the rate constant.

5.4 Effect of acid

The results obtained in the presence of Ph_3CBr indicate that with increasing concentrations of the additive the adduct with λ_{max} = 460nm is converted to a species with λ_{max} = 370nm. It has been attributed to protonation of the adduct to give a nitronic acid.

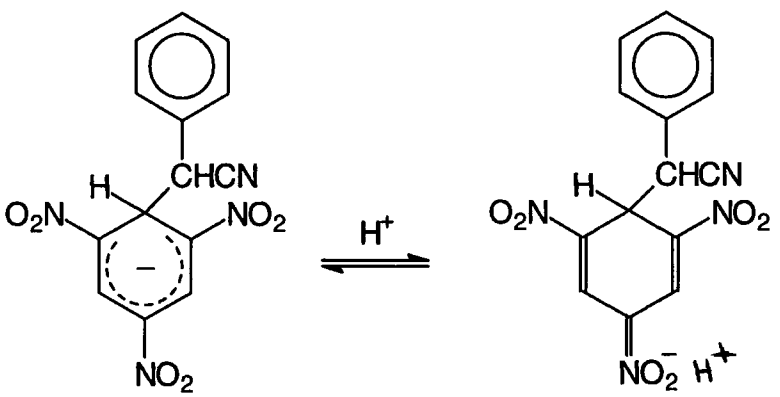

Reaction of σ-adducts formed from oxygen and nitrogen nucleophiles with acid usually results in rapid decomposition to reactants[41i)].

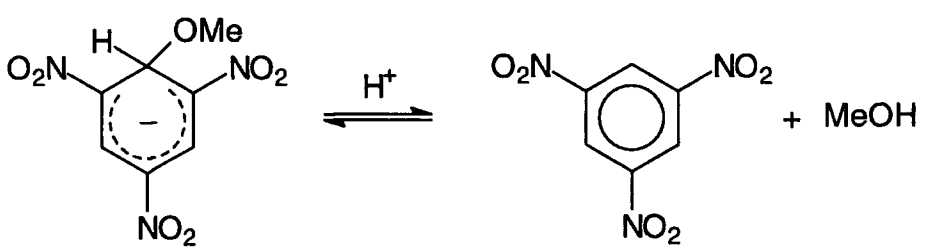

However it is known[41i),44] that addition of acids to hydride adducts of 1,3,5-TNB and to adducts with carbon nucleophiles may result in the observation of relatively stable nitronic acids. It was reported that the nitronic acids from adducts of 1,3,5-TNB absorb at 370nm. Hence there is good evidence that the spectral change seen in the present work is due to reversible formation of the nitronic acid.

In the previous work the acid causing protonation was a by-product of the triphenylmethyl bromide added. It was thought to be worthwhile to examine the direct interaction of the salt with acid. Quantitative measurements should be easier to obtain here, since the concentration of added acid could be directly measured.

Initial measurements were made in a 99/1CH_3CN/H_2O solution. Results are shown in table 5.13.

Table 5.13

[Salt]/mol dm^{-3}	[HCl]/mol dm^{-3}	λ_{max}/nm	Rate of decay
4×10^{-5}	_	454	No decay
"	1×10^{-3}	454	slow decay
"	2×10^{-3}	454	↓
"	5×10^{-3}	454	↓
"	7.5×10^{-3}	454	↓
"	1×10^{-2}	454	faster decay

Since no protonated species are formed, solutions with a lower percentage of water were used. Measurements were made in 99.9/0.1 CH_3CN/H_2O solutions, results are shown in table 5.14 and a typical spectrum is shown in figure 5.5.

Table 5.14

[Salt]/mol dm^{-3}	[HCl]/mol dm^{-3}	λ_{max}/nm
4×10^{-5}	1×10^{-2}	454 large peak, 370nm smaller peak
"	7.5×10^{-3}	454 large peak, 370nm very small peak
"	5×10^{-3}	454 large peak, 370nm very small peak
"	2.5×10^{-3}	_

Figure 5.5

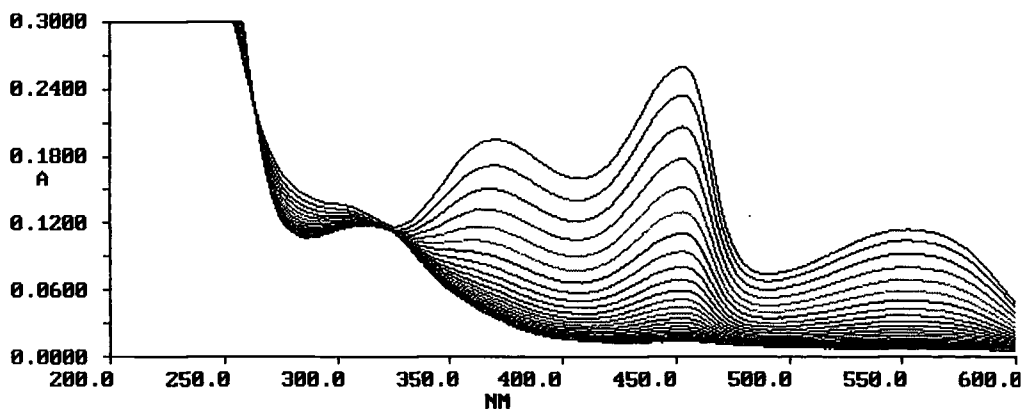

Absorbance spectrum of 4×10^{-5} salt and 1×10^{-2} HCl in 99.9/0.1 CH_3CN/H_2O.

Since the species which absorbs at 370nm is produced by addition of HCl to the salt it is likely to be a protonated form of the salt. However since only a small amount is produced even in concentrated acid, it is possible that ion pair formation is occurring with HCl. However it is known[45] that perchloric acid is fully dissociated in acetonitrile so that protonation of the salt should be favoured. Initial measurements were carried out in 99/1 CH_3CN/H_2O solutions with varying concentrations of $[HClO_4]$, results are shown in table 5.15.

Table 5.15

[Salt]/ mol dm^{-3}	$[HClO_4]$/ mol dm^{-3}	λ_{max}/nm	Rate of decay
4×10^{-5}	5×10^{-3}	454 large peak, 371nm very small peak	slow decay
"	1×10^{-2}	454 large peak, 371nm very small peak	↓
"	2×10^{-2}	454 large peak, 371nm smaller peak	↓
"	3×10^{-2}	454 large peak, 371nm smaller peak	↓
"	4×10^{-2}	454 small peak, 371nm larger peak	↓
"	5×10^{-2}	454 small peak, 371nm larger peak	↓
"	6×10^{-2}	454 very small peak, 371nm large peak	faster decay

Triethylamine was then added to the reaction mixture, after decay of the species and also immediately after acid addition to test for reversibility of the salt- protonated salt equilibrium.

[Salt]/ mol dm^{-3}	$[HClO_4]$/ mol dm^{-3}	$[NEt_3]$/ mol dm^{-3}	λ_{max}/nm
4×10^{-5}	2×10^{-3}	7.2×10^{-3} added after decay	300nm, no change in spectrum
"	5×10^{-3}	7.2×10^{-3} added immediately	454, shifts from 371nm instantaneously

Thus protonation is the driving force for the 454nm to 370nm shift, the form at 370nm being protonated. The equilibrium is also reversible, immediate addition of triethylamine producing a maximum at 454nm. Rates of decay of the species and the equilibrium constant for protonation with this acid will now be investigated in various solvent compositions.

5.5 Rate and equilibrium constants for decay of salt with $HClO_4$

In order to obtain rate constants for decay, measurements were made at the wavelength of the species predominant at the concentration of acid used. For predominantly the salt form measurements were made at 454nm, for predominantly the protonated form measurements were made at 371nm. Absorbances at both 454nm and 371nm were measured for all solutions to obtain values for the equilibrium constants. This is calculated at 454nm as follows.

$$A^- + H^+ \overset{K}{\rightleftharpoons} AH$$

$[A^-] + [AH] = \text{constant} = 4\times10^{-5}$

$\text{Absorbance} = \varepsilon_A [A^-] + \varepsilon_{AH} [AH]$

$\text{Absorbance} = \varepsilon_A (4\times10^{-5} - [AH]) + \varepsilon_{AH} [AH]$

$\text{Absorbance} = \varepsilon_A \times(4\times10^{-5}) - \varepsilon_A [AH]) + \varepsilon_{AH} [AH]$

$$[AH] = \frac{\varepsilon_A \times (4\times10^{-5}) - \text{Abs}}{\varepsilon_A - \varepsilon_{AH}}$$

$$[AH] = \frac{\text{Abs}_0 - \text{Abs}}{\varepsilon_A - \varepsilon_{AH}}$$ where Abs_0 is the absorbance in the presence of salt only.

In a related way it may be shown that $[A^-] = \frac{\text{Abs} - \text{Abs}_\infty}{\varepsilon_A - \varepsilon_{AH}}$ where Abs_∞ is the absorbance corresponding to complete conversion to the protonated form.

Since $K = \frac{[AH]}{[A^-][H^+]}$

$$K = \frac{\text{Abs}_0 - \text{Abs}}{(\text{Abs} - \text{Abs}_\infty)[H^+]}$$

Similarly values of K were calculated from absorbance measurements at 371nm using the relation $K = \frac{\text{Abs} - \text{Abs}_0}{(\text{Abs}_\infty - \text{Abs})[H^+]}$.

Results are shown in tables 5.16 to 5.24, all concentrations are after mixing.

Firstly absorbances at 454nm and 371nm were measured to ascertain Abs_0 and Abs_∞ for total conversion to the salt form and total conversion to the protonated form.

Table 5.16

[Salt]/ mol dm^{-3}	$[HClO_4]$/ mol dm^{-3}	v/v CH_3CN/H_2O	Absorbance at 454nm	Absorbance at 371nm
4×10^{-5}	_	100% CH_3CN	1.0142 = Abs_0	0.0129 = Abs_0
4×10^{-5}	0.186	99.2/0.8	0.0693 = Abs_∞	0.4722 = Abs_∞

Approximately 99/1 v/v CH_3CN/H_2O

Table 5.17

[Salt]/ mol dm^{-3}	$[HClO_4]$/ mol dm^{-3}	v/v CH_3CN/H_2O	k_{obs}/s^{-1}
4×10^{-5}	5×10^{-3}	99.02/0.98	1.42×10^{-3}
"	1×10^{-2}	99.04/0.96	2.41×10^{-3}
"	2×10^{-2}	99.09/0.91	3.83×10^{-3}
"	3×10^{-2}	99.13/0.87	5.32×10^{-3}
"	4×10^{-2}	99.17/0.83	5.70×10^{-3}
"	5×10^{-2}	99.22/0.78	6.65×10^{-3}
"	6×10^{-2}	99.26/0.74	7.00×10^{-3}

Table 5.18

[Salt]/ mol dm^{-3}	$[HClO_4]$/ mol dm^{-3}	v/v CH_3CN/H_2O	Absorbance at 454nm	Absorbance at 371nm	K(454nm) /dm^3 mol^{-1}	K(371nm) /dm^3 mol^{-1}
4×10^{-5}	5×10^{-3}	99.02/0.98	0.730	0.112	86.0	58.0
"	1×10^{-2}	99.04/0.96	0.689	0.138	52.5	20.6
"	2×10^{-2}	99.09/0.91	0.499	0.211	59.9	37.9
"	3×10^{-2}	99.13/0.87	0.444	0.291	50.7	51.2
"	4×10^{-2}	99.17/0.83	0.295	0.348	79.7	67.5
"	5×10^{-2}	99.22/0.78	0.233	0.390	103	91.8
"	6×10^{-2}	99.26/0.74	0.189	0.411	115	108

98/2 v/v CH_3CN/H_2O

Table 5.19

[Salt]/mol dm^{-3}	$[HClO_4]$/mol dm^{-3}	k_{obs}/s^{-1}
4×10^{-5}	5.83×10^{-3}	5.99×10^{-4}
"	1.17×10^{-2}	9.22×10^{-3}
"	2.33×10^{-2}	1.39×10^{-3}
"	4.66×10^{-2}	3.33×10^{-3}
"	6.99×10^{-2}	4.39×10^{-3}
"	0.117	5.84×10^{-3}
"	0.140	6.05×10^{-3}
"	0.163	6.83×10^{-3}
"	0.186	7.08×10^{-3}

Table 5.20

[Salt]/ mol dm^{-3}	$[HClO_4]$/ mol dm^{-3}	Absorbance at 454nm	Absorbance at 371nm	K(454nm) /dm^3 mol^{-1}	K(371nm) /dm^3 mol^{-1}
4×10^{-5}	5.83×10^{-3}	0.889	0.064	27.4	23.5
"	1.17×10^{-2}	0.865	0.058	16.9	10.1
"	2.33×10^{-2}	0.824	0.098	11.3	10.8
"	4.66×10^{-2}	0.648	0.193	14.5	15.7
"	6.99×10^{-2}	0.560	0.252	14.3	18.4
"	0.117	0.359	0.348	22.2	31.9
"	0.140	0.297	0.394	26.8	61.7
"	0.163	0.236	0.426	36.8	_
"	0.186	0.188	0.424	54.3	_

96/4 v/v CH_3CN/H_2O

Table 5.21

[Salt]/mol dm^{-3}	$[HClO_4]$/mol dm^{-3}	k_{obs}/s^{-1}
4×10^{-5}	1.17×10^{-2}	5.75×10^{-4}
"	2.33×10^{-2}	8.43×10^{-4}
"	4.66×10^{-2}	1.85×10^{-3}
"	9.32×10^{-2}	2.64×10^{-3}
"	0.140	3.98×10^{-3}
"	0.186	5.14×10^{-3}
"	0.233	5.40×10^{-3}
"	0.326	5.87×10^{-3}
"	0.373	6.30×10^{-3}

Table 5.22

[Salt]/ mol dm^{-3}	$[HClO_4]$/ mol dm^{-3}	Absorbance at 454nm	Absorbance at 371nm	K(454nm) /dm^3 mol^{-1}	K(371nm) /dm^3 mol^{-1}
4×10^{-5}	1.17×10^{-2}	0.971	0.018	4.11	1.02
"	2.33×10^{-2}	0.921	0.031	4.70	1.77
"	4.66×10^{-2}	0.822	_	5.48	_
"	9.32×10^{-2}	0.756	0.115	4.03	3.05
"	0.140	0.646	0.154	4.57	3.18
"	0.186	0.578	0.233	5.69	5.77
"	0.233	0.406	0.309	7.75	4.93
"	0.326	0.266	0.420	11.7	7.79
"	0.373	0.578	0.233	16.3	23.8

94/6 v/v CH_3CN/H_2O

Table 5.23

[Salt]/mol dm^{-3}	$[HClO_4]$/mol dm^{-3}	k_{obs}/s^{-1}
4×10^{-5}	1.75×10^{-2}	4.51×10^{-4}
"	3.49×10^{-2}	6.21×10^{-4}
"	6.98×10^{-2}	1.26×10^{-3}
"	0.140	2.42×10^{-3}
"	0.209	3.62×10^{-3}
"	0.279	4.78×10^{-3}
"	0.349	5.76×10^{-3}
"	0.489	6.94×10^{-3}
"	0.558	6.39×10^{-3}

Table 5.24

[Salt]/ mol dm^{-3}	$[HClO_4]$/ mol dm^{-3}	Absorbance at 454nm	Absorbance at 371nm	K(454nm) /dm^3 mol^{-1}	K(371nm) /dm^3 mol^{-1}
4×10^{-5}	1.75×10^{-2}	1.004	0.062	0.631	1.65
"	3.49×10^{-2}	1.027	0.091	_	2.95
"	6.98×10^{-2}	0.936	0.064	1.34	0.49
"	0.140	0.924	0.080	0.65	0.52
"	0.209	0.841	0.137	1.13	1.15
"	0.279	0.725	0.188	1.68	1.59
"	0.349	0.589	0.248	2.53	2.24
"	0.489	0.336	0.390	6.07	6.22
"	0.558	0.257	0.452	9.02	14.5

The results given in tables 67 to 74 show that values of K, determined from absorbance measurements, decrease with increasing water content of the solvent. These decreases probably reflect the better solvation of the proton by water than by acetonitrile. The values show some variation at a given water concentration. The most accurate values are likely to be those where conversion of A^- to AH is between 20% to 80%. At the limits values will be less accurate since the calculations involve small differences in absorbance values.

Equilibrium constants may also be calculated from the rate constant measurements, this also allows the calculation of the decay constants. This is defined as follows.

$$A^- + H^+ \underset{}{\overset{K}{\rightleftharpoons}} AH \xrightarrow{k} \text{Products}$$

$$\text{Rate} = k[AH]$$

$$K = \frac{[AH]}{[A^-][H^+]}$$

$$[A]_T = [A^-] + [AH]$$

$$\text{Thus} \qquad [A]_T = \frac{[AH]}{K[H^+]} + [AH]$$

$$\text{Rearranging} \quad [AH] = [A]_T\left(\frac{K[H^+]}{1+K[H^+]}\right)$$

$$\text{Therefore} \quad \text{Rate} = k[A]_T\left(\frac{K[H^+]}{1+K[H^+]}\right)$$

$$\text{However} \quad \text{Rate} = k_{obs}[A]_T$$

$$\text{Thus} \qquad k_{obs} = \frac{kK[H^+]}{1+K[H^+]}$$

$$\text{Thus} \qquad \frac{1}{k_{obs}} = \frac{1}{kK[H^+]} + \frac{1}{k}$$

Plots of $\frac{1}{k_{obs}}$ *versus* $\frac{1}{[HClO_4]}$ were made which gave an intercept of $\frac{1}{k}$ and a gradient of $\frac{1}{kK}$. A representative plot is shown in figure 5.6 and data are collected for the various solvent compositions in table 5.25.

Figure 5.6

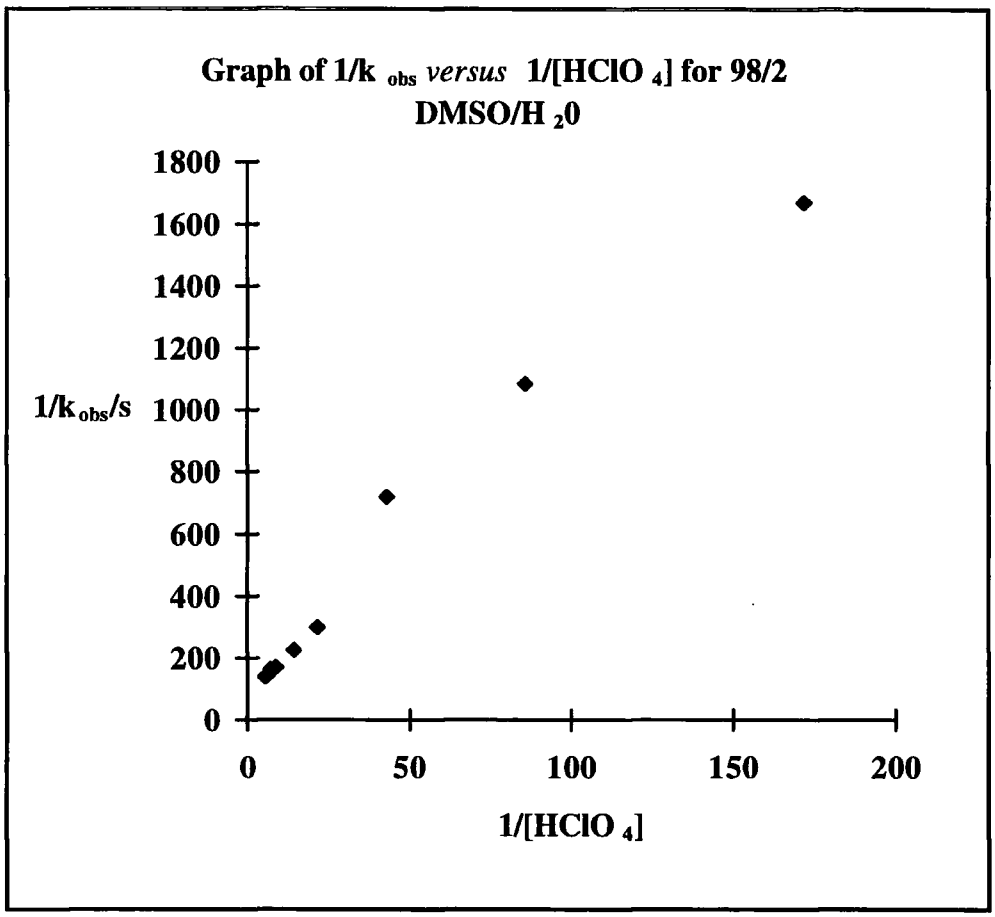

Table 5.25

v/v CH_3CN/H_2O	K/ $dm^3\ mol^{-1}$	k/ $dm^3\ mol^{-1}s^{-1}$
approx 99/1	31.2	1.05×10^{-2}
98/2	13.4	7.80×10^{-3}
96/4	6.43	7.82×10^{-3}
94/6	3.12	8.04×10^{-3}

These values of K are in reasonable agreement with those calculated from the absorbance measurements. These results also show that as the percentage of water in the solvent

increases the value of K decreases. These changes are in accord with the proposed scheme

$$A^- + H^+ \underset{}{\overset{K}{\rightleftharpoons}} AH \xrightarrow{k} \text{Products}$$

The major effect of water will be to solvate the proton resulting in decreases in value of K with increasing water content.

An alternative formulation is

$$A^- + H^+ \overset{K}{\rightleftharpoons} AH$$
$$\searrow^{k}$$
$$\text{Products}$$

Here the decomposition is competitive with formation of AH. This scheme leads to

$$k_{obs} = \frac{k[H^+]}{1 + K[H^+]}$$

$$\frac{1}{k_{obs}} = \frac{1}{k[H^+]} + \frac{K}{k}$$

On this basis the results quoted in Table 5.26 are obtained.

Table 5.26

v/v CH_3CN/H_2O	K/ $dm^3\ mol^{-1}$	k/ $dm^3\ mol^{-1}\ s^{-1}$
approx 99/1	31.2	0.330
98/2	13.4	0.100
96/4	6.43	0.050
94/6	3.12	0.025

Here both values of K and k decrease with increasing water content, attributable to the decrease in activity of the proton as it is better solvated by water.

The data do not allow a distinction to be made between the two possible schemes. It has been established that the species AH is the nitronic acid.

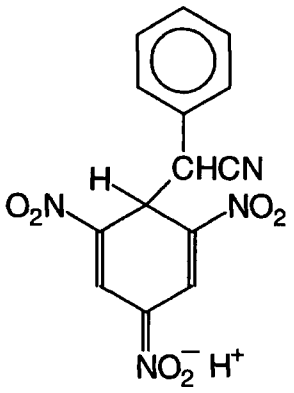

The irreversible decomposition is likely to involve slow reversion to the reactants. A possible pathway (an elaboration of the second scheme given above) is

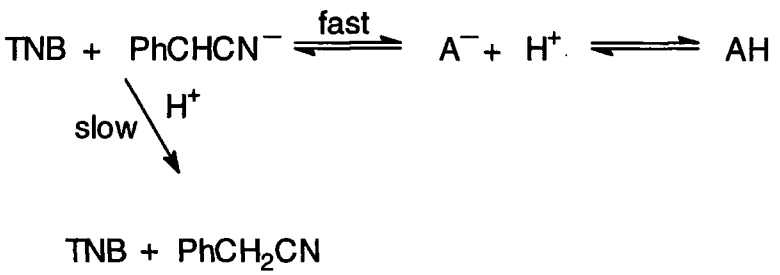

This will give the observed acid dependence only if the equilibrium between 1,3,5-TNB, $PhCHCN^-$ and A^- is a rapid equilibrium. The rate-limiting step would then be protonation of the phenylacetonitrile anion.

It is also possible that the reaction on addition of acid results in loss of hydrogen to yield the reduction product.

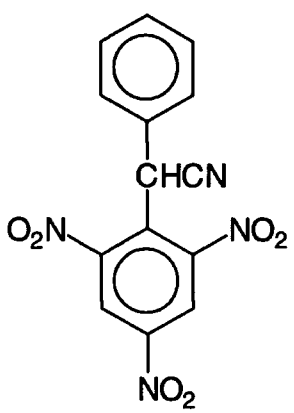

In conclusion the results give interesting information about the reversible protonation of the σ-adduct. Further work to elucidate the products of the slow decomposition would be useful.

Figure 4.6

NMR spectrum of 4-NBZ, NEt_3 and CD_3NO_2 after 10 minutes.

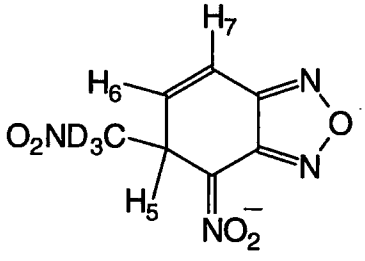

5-adduct

H_5	4.63ppm	J_{56} = 4.58Hz	J_{57} = 1.88Hz
H_6	6.45ppm	J_{56} = 4.58Hz	J_{67} = 10.1Hz
H_7	6.84ppm	J_{57} = 1.88Hz	J_{67} = 10.1Hz

Chapter 6

Experimental

6.1 Measurement techniques

6.1.1 U.V.-Visible spectrophotometry

All U.V.-visible spectra and the kinetics of slow reactions ($t_{1/2} > 20$ s) were obtained on a Perkin - Elmer Lambda 2 instrument with solutions in 1 cm path length quartz cells. Kinetic measurements were made under pseudo first order conditions at 298K. Before reaction the freshly prepared solutions were placed in a water bath and thermostatted at 298K, the cell holder was also maintained at this temperature with water from the water bath, The absorbance/time data were analysed using a computer fitting program PECSS (Perkin - Elmer Computerised Spectroscopy Software), which determined the observed rate constants k_{obs} based on the derivation show below.

For a first order process A $\rightarrow$ B, the rate of formation of product, B, or disappearance of reactant, A, is expressed as

$$-\frac{d[A]}{dt} = \frac{d[B]}{dt} = k_{obs}[A]$$

Integration of this equation gives an expression for the first order rate constant, k_{obs}.

$$-\int_{[A]_0}^{[A]_t} \frac{1}{[A]} d[A] = \int_0^t k_{obs} dt$$

$$\ln[A]_t - \ln[A]_0 = -k_{obs}t$$

$$k_{obs} = \frac{1}{t} \ln \frac{[A]_0}{[A]_t} \qquad \text{equation 6.1}$$

Where $[A]_0$ and $[A]_t$ are the concentrations of A at times t = 0 and t = t respectively.

Using the Beer - Lambert law

$$A = \varepsilon.c.l$$

where A is the absorbance, ε is the molar extinction coefficient and l is the path length and assuming the path length to be 1cm, expressions for the absorbance at times t = 0 and t = t are derived.

$$A_0 = \varepsilon_A[A]_0$$

$$A_t = \varepsilon_A[A]_t + \varepsilon_B[B]_t$$

Ideally a wavelength where reactant A absorbs strongly and Product B has negligible absorbance is chosen.

Since $[B]_t = [A]_0 - [A]_t$, then substituting for $[B]_t$ gives

$$A_t = \varepsilon_A[A]_t + \varepsilon_B[A]_0 - \varepsilon_B[A]_t$$

Now $A_\infty = \varepsilon_B[B]_\infty = \varepsilon_B[A]_0$ since $[B]_\infty = [A]_0$

Thus $(A_t - A_\infty) = \varepsilon_A[A]_t + \varepsilon_B[A]_t$

$$[A]_t = \frac{(A_t - A_\infty)}{(\varepsilon_A - \varepsilon_B)} \qquad \text{equation 6.2}$$

Similarly $A_0 = \varepsilon_A[A]_0$ and $A_\infty = \varepsilon_B[B]_\infty = \varepsilon_B[A]_0$

Thus $(A_0 - A_\infty) = \varepsilon_A A_0 - \varepsilon_B[A]_0$

$$[A]_0 = \frac{(A_0 - A_\infty)}{(\varepsilon_A - \varepsilon_B)} \qquad \text{equation 6.3}$$

Substituting equations 6.2 and 6.3 into equation 6.1 gives,

$$k_{obs} = \frac{1}{t} \ln \frac{(A_0 - A_\infty)}{(A_t - A_\infty)}$$

Rearrangement of this equation gives a graphical y = mx + c form.

$$\ln (A_t - A_\infty) = -k_{obs}t + \ln (A_0 - A_\infty)$$

Thus a plot of ln ($A_t - A_\infty$) against t should be linear with a slope of $-k_{obs}$. The infinity values A_∞, were determined after a period of ten half lives and the decrease in absorbance followed for at least two half lives.

6.1.2 Stopped - flow Spectrometry

For measurement of rapid reactions (2 ms ≤ t½ ≤ 20 s) where rate constants are too fast to measure by conventional methods a High - Tech SF-3 series stopped-flow spectrometer was used. This is shown in figure 6.1 below.

Figure 6.1

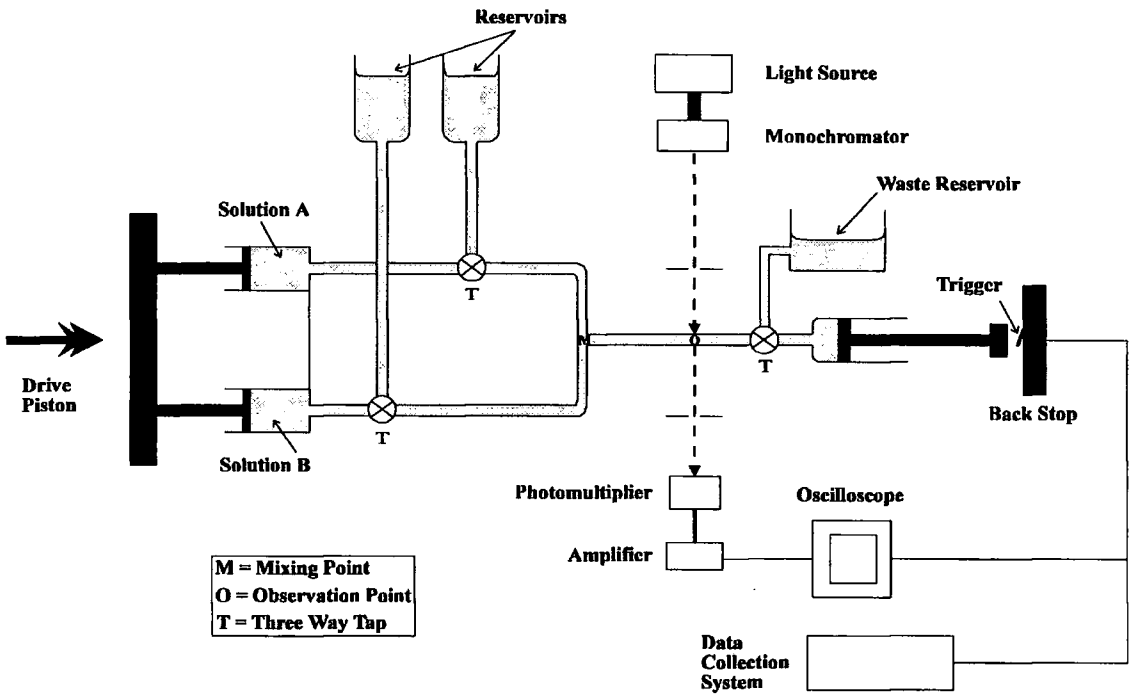

The two solutions to be reacted, A and B, are stored in reservoirs and are drawn into two identical syringes so that equal volumes of each solution are mixed. The syringes are compressed simultaneously by hand and mixing occurs extremely rapidly at point M. The dead time of this spectrometer is approximately 2 ms, thus reactions with half lives smaller than this cannot be measured by stopped-flow techniques. The mixture flows into a thermostatted 2 mm path length cell at point O. The plunger of the third syringe hits a

back stop and the flow of solution is halted. The plunger hitting the back stop also triggers the acquisition of data from the reaction.

To observe the reaction a beam of monochromatic light of the appropriate wavelength is passed through the observation cell by a fibre optic cable. The light is then passed through a photomultiplier and the change in voltage, due to the change in absorbance of the solution, is observed. The software used to run the stopped-flow spectrometer transforms the voltage/time data into absorbance/time data and calculates the observed rate constants. Rate constants are the mean of ten values and are accurate to ±5%.

6.2 Reagents

6.2.1 Solvents

General purpose methanol and high purity water (departmentally produced) were used for washing all apparatus. Solvents for synthetic work were of the highest grades. For UV-visible experiments 99.9+% HPLC grade methanol, 99.9+% DMSO and 99.9+% HPLC grade acetonitrile from Aldrich were used.

For NMR experiments acetonitrile-d_3, 99.5 atom % D, DMSO-d_6, 99.9 atom % D, methanol-d_3, 99.9 atom % D and nitromethane-d_3, 99.9 atom % D obtained from Aldrich were used.

6.2.2 Reagents

All commercially purchased reagents were of the highest grade. Reagents requiring synthesis are described below.

4-Cyanophenylacetonitrile

4-Bromophenylacetonitrile, 5.018g (0.0256 mol), was dissolved in ethanol, 250 cm^3, by heating to 50°C. Potassium cyanide, 1.802g (0.0277 mol), was dissolved in water, 10cm^3, and added to the ethanolic solution. The resultant mixture was heated to 50°C in a water bath for one hour and then allowed to cool. The cooled solution was then added to iced water, 300 cm^3, and a solid was precipitated. The solid was recrystallizes from methanol, 100 cm^3, to produce yellow crystalline 4-cyanophenylacetonitrile, melting point 100°C (lit.[47] 100°C).

4-Nitrobenzofurazan

Benzofuroxan, 10g (0.0741mol), was dissolved in ethanol, 150 cm^3, and hydroxylamine hydrochloride, 15g (0.219 mol) was added. Aqueous 25% sodium hydroxide was added carefully to this mixture until evolution of nitrogen gas had stopped. The ethanol was allowed to evaporate and the resultant benzofurazan was steam distilled.

The benzofurazan was dissolved in six times its weight of 90% sulfuric acid and nitrated at 5-10°C by addition of a 4/1 (w/v) mixture of sulfuric and 100% nitric acid. The resultant solution was added dropwise to iced water, 200 cm^3, to precipitate a yellow

solid. The product was recrystallized from boiling ethanol to produce yellow crystals, melting point 93°C (lit.[48] 93°C).

Sodium methoxide-d_3

Clean sodium, approximately 0.5g (0.217 mol), was slowly added to methanol-d_4, 10g (0.278 mol), under nitrogen to produce a clear viscous solution. The concentration of this solution was determined by titration of 0.1ml aliquots against HCl, 0.0208 mol dm^{-3}, with phenolphthalein as the indicator. A solution of sodium methoxide, concentration 2.45 mol dm^{-3} was produced.

Appendix

A.1 First Year Induction Course (October 1993)

The course consisted of a series of one hour lectures on the services available in the department.

1. Introduction, research resources and practicalities.
2. Safety matters.
3. Electrical appliances and hands on spectroscopic services.
4. Departmental computing.
5. Chromatography and high pressure operations.
6. Elemental analysis.
7. Mass spectroscopy.
8. Nuclear Magnetic Resonance spectroscopy.
9. Glassblowing techniques.

A.2 Colloquia, Lectures and Seminars

1993

September 13 Prof. Dr. A.D. Schlüter, Freie Universität Berlin, Germany
Synthesis and Characterisation of Molecular Rods and Ribbons

October 20 Dr. P. Quayle, University of Manchester
Aspects of Aqueous ROMP Chemistry

October 27 Dr. R.A.L. Jones, Cavendish Laboratory, Cambridge
Perambulating Polymers

December 1 Prof. M.A. McKervey, Queens University, Belfast
Synthesis and Applications of Chemically Modified Calixarenes

1994

February 9 Prof. D. Young, University of Sussex
Chemical and Biological Studies on the Coenzyme Tetrahydrofolic Acid

February 23 Prof. P.M. Maitlis, University of Sheffield
Across the Border: From Homogeneous to Heterogeneous Catalysis

March 2 Dr. C. Hunter, University of Sheffield
Noncovalent interactions between Aromatic Molecules

March 10 Prof. S.V. Ley, University of Cambridge
New Methods for Organic Synthesis

October 5 Prof. N.L. Owen, Brigham Young University, Utah, USA
Determining Molecular Structure-the INADEQUATE NMR way

November 10 Dr. M. Block, Zeneca Pharmaceuticals, Macclesfield
Large-scale Manufacture of ZD 1542, a Thromboxane Antagonist Synthase Inhibitor

November 16 Prof. M. Page, University of Huddersfield
Four-membered Rings and β-Lactamase

December 7 Prof. D. Briggs, ICI and University of Durham
Surface Mass Spectroscopy

1995

January 11 Prof. P. Parsons, University of Reading
Applications of Tandem Reactions in Organic Synthesis

January 25 Dr. D.A. Roberts, Zeneca Pharmaceuticals

The Design and Synthesis of Inhibitors of the Renin-angiotensin System

May 4 Prof. A.J. Kresge, University of Toronto

The Ingold Lecture

Reactive Intermediates: Carboxylic-acid Enols and Other Unstable Species

October 13 Prof. R. Schmultzer, University of Braunschwieg, FRG

Calixarene-Phosphorus Chemistry: A New Dimension in Phosphorus Chemistry

October 25 Dr. D. Martin Davies, University of Northumbria

Chemical Reactions in Organised Systems

November 8 Dr. D. Craig, Imperial College, London

New Strategies for the Assembly of Heterocyclic Systems

November 22 Prof. I. Soutar, Lancaster University

A Water of Glass? Luminescence Studies of Water-Soluble Polymers

1996

January 24 Dr. A. Armstrong, Nottingham University

Alkene Oxidation and Natural Product Synthesis

February 7 Dr. R.B. Moody, Exeter University

Nitrosations, Nitrations and Oxidations with Nitrous Acid

February 28 Prof. E.W. Randall, Queen Mary and Westfield College

New Perspectives in NMR imaging

April 30 Dr. L.D. Pettit, IUPAC Commission of Equilibrium Data

pH-metric Studies using very small quantities of uncertain impurity

A.3 Conferences Attended

International Union of Pure and Applied Chemistry.

12th conference on physical organic chemistry, Padova, Italy, August 28th - September 2nd, 1994.

Poster presented: "Carbanion reactivity: Reactions of phenylacetonitrile anions with aromatic nitro-compounds."

Royal Society of Chemistry Organic Reaction Mechanisms Group.

One day conferences at:

Zeneca, Huddersfield, September 1994.

Merck, Sharpe and Dohme, Harlow, September 1995.

Zeneca Physical Organic Chemistry CASE conference.

Warwick University, March 1994.

Presentation given: "Carbanion reactivity: Reactions of phenylacetonitrile anions with aromatic nitro-compounds."

References

1. R.Taylor "Electrophilic Aromatic Substitution". Wiley Interscience, 1990.

2. B.Gibson and M.R.Crampton, *J.Chem.Soc., Perkin Trans. 2*, 1979, 648.

3. A.H.M.Renfrew, J.A.Taylor, J.M.J.Whitmore and A.Williams, *J.Chem.Soc., Perkin Trans. 2*, 1993, 1703.

4. M.C.A.Lobry de Bruyn, *Recl.Trav.Chim.Pays-Bas*, 1883, **2**, 105.

5. R.B.Chapas, R.D.Knudsen, R.F.Nystrom and H.R.Snyder, *J.Org.Chem.*, 1975, **40**, 3746.

6. M.Hamana, G.Iwasaki and S.Saeki, *Heterocycles*, 1982, **17**, 177.
   G.Iwasaki, S.Saeki, K.Wada and M.Hamana, *Heterocycles*, 1984, **22**, 1811.

7. R.B.Davis and L.C.Pizzini, *J.Org.Chem*, 1961, **25**, 1884.
   E.J.Bara, R.B.Davis and L.C.Pizzini, *J.Org.Chem*, 1961, **26**, 4720.

8. G.B.Stahly, *J.Org.Chem*, 1985, **50**, 3091.

9. L.Testafera, M.Tiecco and M.Tignoli, *J.Chem.Soc., Perkin Trans. 2*, 1979, 469.

10. M.K.Stern, *J.Org.Chem*, 1993, **58**, 6883.

11. G.Bartoli, M.Bosco, A.Melandri and A.C.Boicelli, *J.Org.Chem*, 1979, **44**, 2087.
    G.Bartoli, *Acc.Chem.Res.*, 1984, **17**, 109.

12. G.Bartoli, M.Bosco and R.Dalpozzo, *Tetrahedron Lett.*, 1988 **29**, 2251.

13. G.Bartoli, M.Bosco and G.Baccolini, *J.Org.Chem*, 1980, **45**, 522.

14. N.Armilleta, G.Bartoli, M.Bosco and R.Dalpozzo, *Synthesis*, 1982, 836.

15. T.V.Rajanbabu, G.S.Reddy and T.Fukunaga, *J.Am.Chem.Soc.*, 1985, **107**, 5473.

16. T.V.Rajanbabu, G.S.Reddy and T.Fukunaga, *J.Org.Chem.*, 1986, **51**, 1704.

17. M.Makosza, J.Golinski and J.Baran, *J.Org.Chem.*, 1984, **49**, 1488.

18. C.Bjorklund and M.Nilson, *Acta Chem. Scand.*, 1968, **22**, 2338.

19. i) O.Haglund, A.A.K.M.Hai and M.Nilson, *Synthesis*, 1990, 942.
    ii) O.Haglund, "Copper-Mediated Vicarious Nucleophilic Substitution", PhD. Thesis, Chalmers University of Technology, Gouteborg, 1993.

20. J.Meisenheimer, *Ann.*, 1902, **323**, 205.

21. I.Kolb, V.Machacek and V.Sterba, *Collect.Czech.Chem.Comm.*, 1976, **41**, 1914.

22. J.P.L.Cox, M.R.Crampton and P.J.Wight, *J.Chem.Soc., Perkin Trans. 2*, 1988, 25.

23. M.R.Crampton, T.P.Kee and J.R.Wilcox, *Can.J.Chem.*, 1986, **64**, 1714.

24. F.Terrier, M.P.Simonnin, M.J.Pouet and J.Strauss, *J.Org.Chem.*, 1981, **46**, 3537.

25.F.Terrier, F.Millot, A.P.Chatrousse, M.P.Simonnin and M.J.Pouet, *Org.Magn. Resonance*, 1976, **8**, 56.

26.E.Buncel, N.Chuaqui-Offermanns, B.K.Hunter and A.R.Norris, *Can.J.Chem.*, 1977, **55**, 2852.

27. C.F.Bernasconi, *Pure.Appl.Chem.*, 1982, **54**, 2335.

28. C.F.Bernasconi, *Tetrahedron,* 1985, **41**, 3219.

29. F.Aitken, B.G.Cox, P.E.Sorensen, *J.Chem.Soc., Perkin Trans. 2*, 1993, 783.

30. M.R.Crampton and J.A. Stevens, *J.Chem.Soc., Perkin Trans. 2*, 1991, 1715.

31. C.H.Rochester, "Acidity Functions". Academic Press, 1970.

32. D.J.Kroeger and R.Stewart, *Can.J.Chem.*, 1967, **45**, 2163.

33. J.H.Atherton, M.R.Crampton, G.L.Duffield and J.A.Stevens, *J.Chem.Soc., Perkin Trans. 2*, 1995, 443.

34. B.G.Cox, " Modern Liquid Phase Kinetics ". Oxford, 1994.

35. J.N.Bunting, C.Fu and J.W.Tam, *Can.J.Chem.*, 1990, **68**, 1762.

36. F.Terrier, M-J.Pouet, E.Kizilian, J-C.Halle, F.Outurquin and C.Paulinier, *J.Org.Chem.*, 1993, **58**,4696.

37. C.F.Bernasconi, *Tetrahedron,* 1989, **45**, 4017.

38. A.I.Biggs and R.A.Robinson, *J.Chem.Soc.,* 1961, 388.

39. O.A.Reutov, I.P.Beletskaya and K.P.Butin, " CH-Acids ", Pergamon Press, 1978, pg 57.

40. F.Terrier, R.Goumont, M-J Pouet and J-C.Halle, *J.Chem.Soc., Perkin Trans. 2*, 1995, 1620.

41. i) E.Buncel, M.R.Crampton, M.J.Strauss and F.Terrier, " Electron Deficient Aromatic- and Heteroaromatic- Base Interactions ", Elsevier, 1989.

ii) M.I.Foreman, R.Foster and M.J.Strauss, *J.Chem.Soc.(B),* 1970, 147.

42. E.Buncel and R.A.Manderville, *J.Chem.Soc., Perkin Trans. 2*, 1993, 1887.

43. N.V.Ignatiev, V.N.Boiko and L.M.Yagupoliskii, *Russian J.Org.Chem.*, 1980, **16**, 1292.

44. O.Wennerstrom, *Acta Chem. Scand.*, 1971, **25**, 2341.

O.Wennerstrom and C.Moberg, *Acta Chem. Scand.*, 1971, **25**, 2355.

45. I.M.Kolthoff, S.Bruckerstein and M.K.Chantoori, *J.Am.Chem.Soc.*, 1961, **83**, 3927.
I.M.Kolthoff and M.K.Chantoori, *J.Am.Chem.Soc.*, 1965, **87**, 4428.
46. C.F.Bernasconi, *J.Am.Chem.Soc.*, 1970, **92**, 4682.
47. N.Mellinghof, *Berichte*, 1889, **22**, 3209.
48. J.P.Picard and J.V.R.Kaufman, *J.Am.Chem.Soc.*, 1954, **76**, 2233.